Characterization of Various Pyrene-Labelled Macromolecules in Solution by Fluorescence

by

Jamie Yip

A thesis

presented to the University of Waterloo

in fulfilment of the

thesis requirement for the degree of

Master of Science

in

Chemistry

Waterloo, Ontario, Canada, 2010

Author's Declaration

I hereby declare that I am the sole author of this thesis. This is a true copy of the thesis, including any required final versions, as accepted by my examiners

I understand that my thesis may be made electronically available to the public.

Abstract

Time-resolved fluorescence was applied to linear and branched pyrene-labelled macromolecules to study their internal dynamics. The linear macromolecules consisted of two series of pyrene-labelled poly(*N*-isopropylacrylamide)s where the polymer was either end-labelled (Py_2-PNIPAM-Y where Y represents the molecular weight of the polymer and equals 6, 8, 14, 25, and 45 kDa) or randomly labelled (Py-PNIPAM-X% where X represents the pyrene content and is equal to 0.1, 2, 3, 4, 5, and 6 mol%) with pyrene. Four dendrimer generations based on a bis(hydroxymethyl)propionic acid backbone represented the branched macromolecules where the terminal sites were labelled with pyrene (Py_X-GY-COOH where X represents the number of pyrene units incorporated into the Y`th generation dendrimer). A polystyrene-dendrimer hybrid was also synthesized (Py_X-GY-PS). The fluorescence decays of the Py_2-PNIPAM-Y and Py-PNIPAM-X% samples were acquired in solvents of varying viscosity and were analyzed with the Birks Scheme and the Fluorescence Blob Model (FBM) to yield the excimer formation rate constants k_{cy} and $< k_{blob} \times N_{blob} >$, respectively. The two parameters showed the same trends with varying viscosity, implying that the same information concerning chain dynamics is obtained from the randomly and end-labelled PNIPAM samples. The fluorescence decays of the Py_2-PNIPAM-Y samples were acquired in ethanol and in water to determine how pyrene solubility affects the behavior of the polymers in solution, as probed by time-resolved fluorescence. It was found that the decreased pyrene solubility in water led to large amounts of intra- and intermolecular pyrene aggregation. Finally, the pyrene-labelled dendrimers were studied in tetrahydrofuran (THF) to probe the mobility of the chain ends as a function of generation number. The average rate of excimer formation, $< k >$, obtained from the Model-Free analysis of the fluorescence decays in THF,

increased linearly with generation number. This finding, combined with molecular mechanics optimizations, led to the conclusion that excimer formation was greatly enhanced due to the branched nature of the dendrimer molecule. Together, these studies illustrate three different applications of the use of time-resolved fluorescence to characterize the internal dynamics of pyrene-labelled macromolecules.

Acknowledgements

First, I would like to thank my supervisor Prof. Jean Duhamel for taking me on as a graduate student and giving me the opportunity to perform research in his lab. His continued guidance, support, advice, and friendship have kept me going over the past two years and have made this thesis possible.

I am very grateful to the University of Waterloo and to the GWC^2 for accepting me as a Masters student and for their financial support. In addition, I must also acknowledge NSERC for their additional funding of these projects.

I would also like to acknowledge Prof. Françoise Winnik and Xing Ping Qiu of the Université de Montréal for providing the PNIPAM samples studied in this thesis, as well as Prof. Alex Adronov and Greg J. Bahun of McMaster University for providing the pyrene-labelled dendrimers studied in this thesis.

Next, I must thank all of the Duhamel and Gauthier lab members, especially Howard "Uncle" Siu and Christine "Keyes-Baig-Ah" Keyes-Baig. Your constant picking on me kept me going throughout those long days and the last two years would not have been nearly as much fun without you. For you guys, and only you guys, I will be 100%. Yes, that includes you too, Wang.

Finally, I would like to thank all of my family, especially my big sister Sandra, my beautiful niece Jada, my loving parents, and my ever-nagging grandparents whose constant love, support, and super-high expectations motivated me to achieve to my fullest potential throughout my life. I love you guys.

Table of Contents

List of Figures

List of Tables

List of Schemes

List of Abbreviations

AIBN: Azobisisobutyronitrile

DEGDIM: Diethylene glycol di(2-(1-isobutyl)sulfanylthiocarbonylsulfanyl-2-methylpropionate)

DMF: *N*,*N*-dimethylformamide

DMSO: Dimethylsulfoxide

DNA: Deoxyribonucleic acid

EEC: End-to-end cyclization

FBM: Fluorescence Blob Model

FRET: Fluorescence resonance energy transfer

GPC: Gel permeation chromatography

HPLC: High pressure liquid chromatography

HS_2-PNIPAM: α,ω-dimercapto poly(*N*-isopropylacrylamide)

iBS: Isobutylsulfanylthiocarbonylsulfanyl

iBS_2-PNIPAM: *i*sobutylsulfanylthiocarbonylsulfanyl end-capped poly(*N*-isopropylacrylamide)

LED: Light-emitting diode

MF: Model-Free

MD: Molecular dynamics

NASI: *N*-acryloxysuccinimide

NIPAM: *N*-isopropylacrylamide

NMR: Nuclear Magnetic Resonance

PTI: Photon Technology International

PDI: Polydispersity Index

PDMA: Poly(*N*,*N*-dimethylacrylamide)

PEO: Poly(ethylene oxide)

PGA: Poly(L-glutamic acid)

PNIPAM: Poly(*N*-isopropylacrylamide)

PS: Polystyrene

PyBuOH: 1-pyrenebutanol

Py_2-PEO: Pyrene end-labelled poly(ethylene oxide)

Py_2-PNIPAM-Y: Pyrene end-labelled poly(*N*-isopropylacrylamide)

Py-PNIPAM-X%: Randomly labelled poly(*N*-isopropylacrylamide)

Py_2-PS: Pyrene end-labelled polystyrene

Py_X-GY-COOH: Pyrene-labelled dendrimers

Py_X-GY-PS: pyrene-labelled dendrimer-polystyrene hybrid

RAFT: Reversible addition-fragmentation chain transfer polymerization

SEC: Size exclusion chromatography

SPC: Single photon counting

SS: Steady state

TC-SPC: Time-correlated single photon counting

THF: Tetrahydrofuran

TPP: Triphenylphosphine

UV: Ultraviolet

List of Symbols

a_i	The i'th pre-exponential factor obtained from fitting a fluorescence decay with a sum of exponentials
A_{E-} / A_{E+}	Sum of the negative pre-exponential factors divided by the sum of the positive pre-exponential factors obtained from fitting an excimer decay with a sum of exponentials
$\ln A$	Scaling factor used in Equations 2.42 and 2.44
α	Exponent on the viscosity term used in Equations 2.42 and 2.44
$[blob]$	The concentration of blobs within a polymer
β	Exponent on the molecular weight term used in Equations 2.42 ad 2.44
C_∞	The characteristic ratio of a polymer.
$E0^*$	The properly stacked excimer species.
EL^*	The improperly stacked excimer species.
ε_{342}	The molar extinction coefficient of 1-pyrenebutanol at 342 nm.
f_{Mdiff}	Fraction of pyrene species in a monomer decay which form excimer by diffusion.
f_{Mk_2}	Fraction of pyrene species in a monomer decay which form excimer with a rapid rate constant k_2.
f_{Mfree}	Fraction of pyrene species in a monomer decay which do not form excimer.
f_{Ediff}	Fraction of excimers from an excimer decay which were formed by diffusion.
f_{Ek_2}	Fraction of excimers from an excimer decay which formed excimer with a rapid rate constant k_2.
f_{EE0}	Fraction of excimers from an excimer decay which are properly stacked.
f_{EEL}	Fraction of excimers from an excimer decay which are improperly stacked.

f_{diff}	Fraction of overall pyrene species which form excimer by diffusion.
f_{k_2}	Fraction of overall pyrene species which form excimer with a rapid rate constant k_2.
f_{free}	Fraction of overall pyrene species which are isolated and do not for excimer.
f_{E0}	Fraction of overall pyrene species which have formed excimer and are properly stacked.
f_{EL}	Fraction of overall pyrene species which have formed excimer and are improperly stacked.
$f(t)$	Function representing the time-dependence of the excimer formation rate constant.
$h\nu_{em}$	Energy of a photon of emitted light of wavelength λ_{em}.
$h\nu_{ex}$	Energy of a photon of excitation light of wavelength λ_{ex}.
η	Solvent viscosity.
$[\eta]$	Intrinsic viscosity of a polymer in a given solvent.
I_1	Intensity of the first peak of the fluorescence spectrum of pyrene.
I_3	Intensity of the third peak of the fluorescence spectrum of pyrene.
I_1 / I_3	Ratio of the intensities of the first to the third peak of the fluorescence spectrum of pyrene.
I_E	Steady-state excimer fluorescence emission intensity.
I_M	Steady-state monomer fluorescence emission intensity.
I_E / I_M	Ratio of the excimer to monomer fluorescence emission intensities calculated from the steady-state fluorescence spectra.
$(I_E / I_M)^{SPC}$	Ratio of the excimer to monomer fluorescence emission intensities calculated from the time-resolved fluorescence decay.
k_1	Bimolecular diffusional encounter rate constant of an excited and a ground-state pyrene.
k_2	Rapid excimer formation rate constant.
k_{-2}	Rate of excimer dissociation.

k_{blob} Excimer formation rate constant inside a blob containing one excited and one ground-state pyrene.

k_{cy} Cyclization rate constant.

k_{-cy} Decyclization rate constant.

k_e Rate constant of exchange of ground-state pyrenes between blobs.

k_q Pyrene quenching rate constant.

$< k >$ Average rate constant of excimer formation.

κ Instrument-dependent constant used to relate the I_E / I_M ratio with the excimer formation rate constant, according to Equation ***.

λ_{em} Wavelength of light emitted by fluorescence.

λ_{ex} Wavelength of excitation light.

λ_{Py} Pyrene content of a pyrene-labelled polymer, measured in μmol/g.

m Mass.

M_1 Molecular weight of the labelled NIPAM monomer, equal to 326 g·mol^{-1}.

M_2 Molecular weight of the labelled unlabelled NIPAM monomer, equal to 113 g·mol^{-1}.

$\overline{M}_n$ Number-average molecular weight of a polymer sample.

N Degree of polymerization of a polymer sample.

n The number of exponentials used in a sum of exponentials analysis.

N_{blob} The size of a blob measured in number of monomer units.

$< n >$ The average number of ground-state pyrenes per blob.

P_A Peak-to-valley ratio of the (0,0) peak for the S_1 to S_0 transition observed in the absorption spectrum of a pyrene-labelled macromolecule.

Py^*_{diff}	The pyrene species which forms excimer by diffusion.
$Py^*_{k_2}$	The pyrene species which forms excimer with a rapid rate constant k_2.
Py^*_{free}	The pyrene species which is isolated and does not form excimer.
Py^*_S	A short-lived pyrene species.
$[Py]_{loc}$	Local concentration of ground-state pyrenes within a pyrene-labelled polymer.
R	The ideal gas constant.
ρ	Density.
S_0	Ground-state electronic level of an electron.
S_1	First excited-state electronic level of an electron.
T	Temperature in Kelvins.
τ_i	Lifetime of the i'th exponential obtained from a sum of exponentials analysis of a fluoroscence decay.
τ_E	Excimer lifetime.
τ_{E0}	Lifetime of a properly stacked excimer.
τ_{EL}	Lifetime of an improperly stacked excimer.
τ_M	Lifetime of the pyrene monomer.
τ_S	Short pyrene lifetime.
$<\tau>$	Weighted average lifetime of the lifetimes obtained from a sum of exponentials analysis of the monomer or excimer fluorescence decays.
V	Volume.
φ^0_E	Excimer fluorescence quantum yield.
φ^0_M	Monomer fluorescence quantum yield.

Chapter 1: Introduction

1.1 Fluorescence and Fluorescence Quenching

Fluorescence is the process whereby an excited electron in the singlet state returns to the singlet ground state, releasing its energy via the emission of a photon of light.[1a] Fluorescence is well-described by the Jablonski diagram, shown in Figure 1.1. First, an electron in the lowest vibrational energy level of the S_0 electronic state absorbs a photon of light of energy $h\nu_{ex}$ corresponding to a wavelength λ_{ex}. Absorption typically occurs on a time-scale of approximately 10^{-15} second. This time-scale is much too short for any significant movement of atoms or nuclei to occur. Depending on the excitation wavelength, the electron gets promoted to one of the vibrational energy levels of the S_1 or higher electronic state. Immediately following excitation, a quick, non-emissive internal conversion occurs where the electron releases some energy, usually in the form of heat, and drops from its excited state to the lowest vibrational level of the S_1 electronic state. This process occurs within 10^{-12} second. Finally, the excited electron in the ground vibrational energy level of the S_1 electronic state drops back to one of the vibrational levels of the S_0 electronic state, in the process emitting a photon of light with an energy $h\nu_{em}$. The wavelength of light emitted depends upon which vibrational level the electron falls to. The combined energy losses between excitation and emission results in a red-shift in the fluorescence emission, commonly referred to as Stokes' Shift, and implies that the emission wavelength will usually be longer than the excitation wavelength. Fluorescence typically occurs on the nanosecond time-scale which happens to be a suitable window for monitoring the internal dynamics of macromolecules, the topic of this thesis.

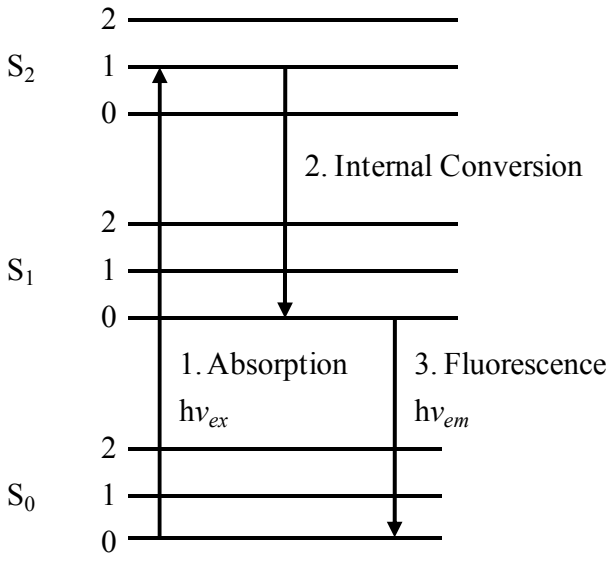

Figure 1.1: Jablonski Diagram depicting the energy transitions of an excited state relaxing to the ground state by releasing this excess energy under the form of fluorescence.

Fluorescence quenching, on the other hand, is the process whereby the intensity of the fluorescence emission of an excited fluorophore decreases due to the presence of an external quencher.[1b] Oxygen is a well-known quencher. Quenching can be monitored either by steady-state or time-resolved fluorescence. Quenching always results in a decrease of the steady-state fluorescence intensity, and, depending on the nature of the quenching process, a decrease in the fluorophore lifetime may be observed. Fluorescence quenching can occur over a distance, a feature which is taken advantage of when conducting an experiment based on Fluorescence Resonance Energy Transfer (FRET),[1c] or it can occur through a physical encounter between the fluorophore and quencher.[2] The latter form, called collisional quenching, will be used in this study in order to gain information concerning the dynamics of fluorescently labelled macromolecules.

1.2 Pyrene

The general structure of pyrene is shown in Figure 1.2. Pyrene has been long used as a fluorescent probe in order to gain information about the internal dynamics of macromolecules.[2,3] The key photophysical properties of pyrene fluorescence that make it such a useful probe are its relatively high quantum yield (0.32 for pyrene in cyclohexane),[4] its long lifetime in organic solvents (200 – 300 ns),[5] and the fact that it self-quenches.[5] The high quantum yield of pyrene allows the experimentalist to work at dilute concentrations. This ensures that unwanted artifacts such as the inner filter effect can be avoided. The relatively long lifetime of pyrene provides a temporal window that is suitable to monitor the fluorescence quenching of pyrene covalently attached onto a macromolecule. Finally, the ability of pyrene to self-quench is its most useful property for a number of reasons which are provided hereafter. First, quenching studies using pyrene involve only one molecule, whereas other fluorophores require the presence of a second molecule that acts as the quencher. This feature simplifies the experimental procedure, especially when fluorophore and quencher need to be covalently attached to the macromolecule. Second, excimer formation occurs via collisional quenching.[5] The production of excimer thus implies that two pyrene units came into direct physical contact. Third, in the process of quenching, an excited dimer, or excimer, is formed.[5] The excimer fluoresces at a wavelength distinguishable from that of the monomer, allowing the experimentalist to acquire an excimer decay in addition to a monomer decay.[2,3] Finally, since the kinetics of monomer disappearance due to collisional quenching are coupled with the kinetics of excimer formation, global analysis of the monomer and excimer decays becomes possible, increasing the accuracy of the parameters retrieved from the analysis.

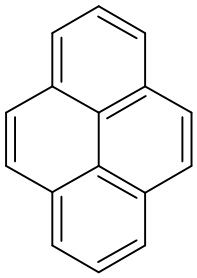

Figure 1.2: The pyrene molecule

1.3 Intramolecular Collisional Quenching

The reaction of two far-flung units within a macromolecule can be monitored via intramolecular collisional quenching of pyrene covalently attached to a macromolecule.[2] Intramolecular collisional quenching studies have applications in areas where the dynamics of intramolecular interactions between well-separated points within a macromolecule are of interest. These areas include the study of protein folding,[6] coil-to-globule transitions,[7] and the conformational rearrangement of associative polymers under shear stress.[8] Provided that solutions of the pyrene-labelled macromolecule are adequately dilute, excimer formation is due to a pyrene-pyrene encounter that occurs intra- and not intermolecularly. Excimer formation indicates that the two positions of the macromolecule that were labelled with pyrene have come into physical contact. In turn, the experimental determination of the time scale over which excimer formation takes place provides information about the internal dynamics of the macromolecule. Intramolecular excimer formation was used in this thesis to study the internal dynamics of linear polymers that were either end-labelled or randomly labelled with pyrene and a series of dendrimers whose ends were labelled with pyrene. In addition, excimer formation was used to monitor pyrene aggregation in aqueous solution, both intra- and intermolecularly. For each labelling scheme, the time-resolved fluorescence

decays acquired must be analyzed using an appropriate model in order to extract quantitative information from these complex decays. The three different labelling schemes, as well as the models used to analyze their fluorescence decays, are described in the next few sections.

1.3.1 Intramolecular Collisional Quenching in End-Labelled Polymers

Numerous aromatic compounds are known to form excimers. J. B. Birks introduced a reaction scheme that describes accurately the kinetics of excimer formation.[5] In recognition of this seminal contribution, this scheme is often referred to as the Birks Scheme and it has been applied numerous times to describe the kinetics of excimer formation when the fluorophore pyrene is covalently attached onto the end of a polymer chain.

According to the Birks Scheme,[5] a ground-state pyrene at one end of a polymer gets excited upon absorption of a photon of light. This excited pyrene can then either fluoresce with its natural lifetime, τ_M, or it can encounter the ground-state pyrene at the opposite end of the polymer and form an excimer with a rate constant, k_{cy}. The subscript *cy* reflects the fact that excimer formation represents the cyclization of the polymer chain. The excimer can then either dissociate back into an excited and a ground-state pyrene with a rate constant k_{-cy}, or it can fluoresce with its natural lifetime, τ_E. By applying the Birks Scheme to the fluorescence decays of pyrene end-labelled polymers, information concerning the flexibility of the polymer backbone is obtained since a more flexible backbone cyclizes more easily than a stiffer one, resulting in a larger k_{cy} value.

The Birks Scheme relies on the fundamental assumption that end-to-end cyclization (EEC) can be described via a single k_{cy} value.[5] Since studies have shown that the rate

constant of cyclization is dependent on chain length,[9] EEC experiments must be conducted with monodisperse polymers which usually requires more advanced polymerization techniques such as anionic or living-radical polymerization. The strong decrease of the rate constant of cyclization with increasing chain length also means that EEC studies are restricted to short chains (shorter than 10,000 g·mol^{-1} for polystyrene) as longer chains undergo too few EEC events to be probed. Furthermore, k_{cy} is inversely proportional to solvent viscosity. As a result, the study of end-labelled polymers is also limited to solvents having relatively low viscosity. Nevertheless, despite these limitations, many experiments on EEC were carried out in the early 1980s and they have provided a wealth of information on the EEC of polymer chains.[9-17]

1.3.2 Intramolecular Collisional Quenching in Randomly Labelled Polymers

In 1999, the Fluorescence Blob Model (FBM) was introduced as an analytical tool used to extract information from the complex fluorescence decays obtained from polymers randomly labelled with pyrene.[18] The model assumes that, during the natural lifetime of an excited pyrene, this pyrene molecule can probe a finite volume in space, and that this space is defined as a blob. The polymer backbone is then arbitrarily divided into a cluster of blobs. Making an analogy between blobs and surfactant micelles, the equations derived by Tachiya which were originally used to describe micellar quenching[19] can then be extended to study quenching inside a blob. A typical experiment consists of synthesizing a series of polymers randomly labelled with pyrene, where the pyrene labelling content is varied. One polymer is labelled with a very small amount of pyrene, typically on the order 0.1 to 0.2 mol%, and is used to measure the natural lifetime of the pyrene label in the monomeric form as the low level of labelling precludes intramolecular excimer formation. The other polymers, with

pyrene contents usually ranging from 2 to 10 mol%, are used for the FBM analysis. After acquiring the fluorescence decays of the polymers in a given solvent, their analysis yields the FBM parameters which are used to describe the internal dynamics of the polymer in solution.

The FBM parameters are k_{blob}, $< n >$, $k_e[blob]$, and N_{blob}, whose definitions are given hereafter. k_{blob} represents the quenching rate constant inside a blob containing one excited pyrene and one ground-state pyrene. $< n >$ represents the average number of ground-state pyrene units located inside a blob.[18] The exchange rate constant, k_e, describes the rate at which ground-state pyrene units diffuse between blobs.[18] N_{blob} represents the size of a blob in terms of the number of monomer units found inside a blob.[18] Finally, the product of k_{blob} and N_{blob}, namely $k_{blob} \times N_{blob}$, has been shown to remain constant with pyrene content. When its value is averaged, $< k_{blob} \times N_{blob} >$ provides a measure of the internal dynamics of the polymer in that solvent.[20]

The FBM has been applied to numerous polymer backbones. The first polymers studied using the FBM were a series of pyrene-labelled polystyrenes (PS).[18] Since then, the validity of the FBM has been demonstrated through three different methods. First, the product $< k_{blob} \times N_{blob} >$ obtained through the FBM analysis of the fluorescence decays acquired for a series of randomly labelled PS was compared with k_{cy} obtained from the Birks Scheme analysis of the fluorescence decays acquired for a series of end-labelled PS.[21] The two analyses were shown to provide the same trends for $< k_{blob} \times N_{blob} >$ and k_{cy} with varying viscosity. Second, the blob size, N_{blob}, of a randomly labelled poly(L-glutamic acid) (PGA) determined experimentally by the FBM was found to be similar to that theoretically

predicted by using molecular mechanics optimizations.[22] This study represented the first time that the FBM was applied to a polymer that did not take on a random coil conformation, but rather adopted a rigid, α-helical conformation. The study on pyrene-labelled PGA was extended in 2008 to determine how changing the linker length attaching pyrene to the PGA α-helix would affect excimer formation.[23] Finally, the results of the FBM were compared for two different polymers of known relative flexibilities, namely for the more flexible cis-polyisoprene (PI) and the stiffer PS.[24] The product $< k_{blob} \times N_{blob} >$ was found to be much greater for pyrene-labelled PI than for pyrene-labelled PS, reflecting the expected differences in backbone flexibility. Using pyrene labelled poly(*N*,*N*-dimethylacrylamide) (PDMA), the FBM has also been applied to investigate the effect of solvent quality and polymer concentration on polymer chain dynamics.[25,26]

1.3.3 Intramolecular Collisional Quenching for Other Pyrene Labelling Schemes

The last model to be considered is the Model-Free (MF) model.[27] This model is used to analyze the fluorescence decays of pyrene-labelled macromolecules where the macromolecule is neither a randomly nor an end-labelled polymer. This model is the most basic of the three models used because it does not make any assumption about the mathematical form of the rate of excimer formation. Instead, it relies on a simple sum of exponentials to describe the quenching that occurs between two pyrene-labelled units of a macromolecule. However simple, it still provides information about the internal dynamics of the macromolecule under study.

The MF analysis of the fluorescence decays acquired for the pyrene-labelled macromolecule yields the decay times and pre-exponential factors used to globally fit the monomer and excimer decays with a sum of exponentials.[27] Since the disappearance of

monomer due to quenching results in the formation of excimer, the monomer and excimer decays are coupled. This allows for the global analysis of the monomer and excimer decays, which greatly improves the accuracy of the decaytimes and pre-exponential factors obtained. One quantity that can be measured using the MF model is the average rate constant of excimer formation, $< k >$, given by Equation 1.1,[28]

$$< k > = \frac{1}{< \tau >} - \frac{1}{\tau_M} \tag{1.1}$$

where τ_M and $< \tau >$ represent the natural lifetime of pyrene and the number-average lifetime of the pyrene species in solution, respectively. $< \tau >$ is given by Equation 1.2,

$$< \tau > = \frac{\sum_{i=1}^{n} a_i \tau_i}{\sum_{i=1}^{n} a_i} \tag{1.2}$$

where n represents the number of exponentials used and a_i and τ_i represent the amplitude and decaytime of the i^{th} exponential, respectively.

The MF model also allows the determination of the molar fractions of each pyrene species in solution.[27] This feature is of tremendous interest to an experimentalist as it can be used to infer the amount of mono-labelled chains in a pyrene end-labelled sample or the

amount of unreacted pyrene derivatives left after the synthesis of a pyrene-labelled macromolecule. Another important feature is the ability to calculate the absolute monomer (I_M) and excimer (I_E) fluorescence intensities based on the MF analysis of the time-resolved fluorescence decays. The ratio of I_E over I_M yields the $(I_E/I_M)^{SPC}$ ratio, where the superscript *SPC* acts as a reminder that this ratio was calculated using parameters retrieved from the analysis of fluorescence decays acquired by the single-photon counting technique. One clear advantage of using the $(I_E/I_M)^{SPC}$ ratio is that it is an absolute quantity which allows measurements from different laboratories to be compared directly.

1.4 Other Features of Pyrene Fluorescence

The experiments presented thus far describe some of the more complex studies that can be performed with pyrene labelled macromolecules. However, the fluorescence of pyrene exhibits other, simpler features which still provide useful information about the properties of a pyrene-labelled macromolecule. The experiments that take advantage of these simpler features will be described in the following sections.

1.4.1 The I_E/I_M Ratio

The I_E / I_M ratio serves as the most basic measure of the total amount of excimer formed relative to monomer.[3] It is calculated based on the steady-state fluorescence spectrum of the pyrene-labelled macromolecule, and a sample spectrum is shown in Figure 1.3. The fluorescence spectrum in Figure 1.3 shows the typical features of a pyrene-labelled macromolecule. Monomer peaks are observed in the 375 – 395 nm region, while the excimer emission is seen as a broad, structureless emission centered at around 480 nm.[3] In this thesis,

the I_E / I_M ratio is taken as the ratio of the area under the steady-state emission spectrum from 500-530 nm divided by the area under the spectrum from 373-378 nm. However, calculation of the I_E / I_M ratio can be done using any number of different methods. Consequently, care must be taken when comparing results from different laboratories. The I_E / I_M ratio represents a good starting point in the study of excimer formation, but it does not provide information on whether the excimer is formed by diffusion or by the direct excitation of a ground-state pyrene aggregate. In order to distinguish between these two modes of excimer formation, other experiments must be performed and they will be described at a later stage.

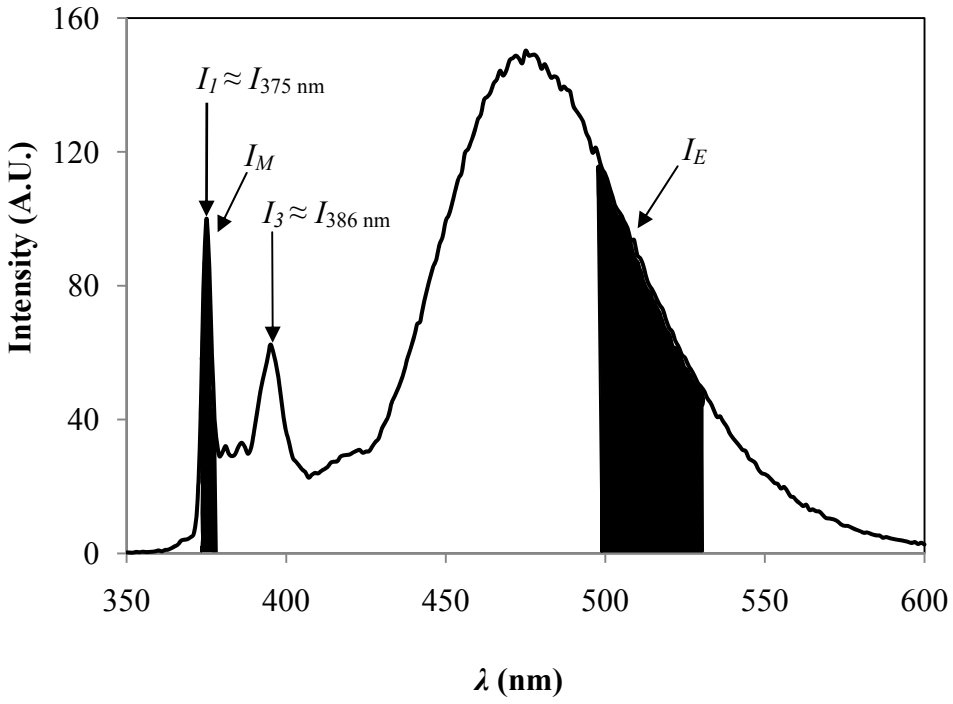

Figure 1.3: Sample steady-state emission spectrum of an excimer-forming pyrene-labelled macromolecule.

Theoretical work done by Cuniberti and Perico showed that the I_E / I_M ratio for a pyrene-labelled macromolecule is given by Equation 1.3,[9]

$$\frac{I_E}{I_M} = \kappa \frac{\varphi_E^0}{\varphi_M^0} \tau_M k_1 [Py]_{loc} \tag{1.3}$$

where κ is a constant that depends on the geometry and sensitivity of the spectrofluorometer used, k_1 is the bimolecular encounter rate constant which for free pyrene units would equal $2RT/(3\eta)$ with R, T, and η being respectively the ideal gas constant, the absolute temperature in K, and the solvent viscosity, φ_M^0 and φ_E^0 are the fluorescence quantum yields of, respectively, the pyrene monomer and excimer, τ_M is the natural lifetime of the monomer, and $[Py]_{loc}$ represents the local concentration of ground-state pyrene units bound to the macromolecule. According to Equation 1.3, the I_E / I_M ratio is proportional to the product $k_1[Py]_{loc}$, and as such, it represents a measure of the rate constant of excimer formation. Thus, the I_E / I_M ratio should also be proportional to the various rate constants of excimer formation described in Section 1.2, as found in a number of instances.[12,14-16,21,27]

1.4.2 The I_1/I_3 Ratio

The I_1 / I_3 ratio is another quantity that is calculated from the fluorescence spectrum. A sample spectrum is shown in Figure 1.3. The I_1 / I_3 ratio has been shown to provide information about the polarity of the medium surrounding pyrene.[29,30] This ratio is calculated as the ratio of the intensities of the first (I_1) to third (I_3) monomer peaks of the fine vibronic

structure of the steady-state emission spectrum. Experimentally, I_1 is taken as the intensity of the first monomer peak, usually centered at 375 nm, while I_3 is taken as the intensity of the third monomer peak, usually centered at around 386 nm (See Figure 1.3).

It has been found that the I_1 / I_3 ratio increases with increasing solvent polarity and vice versa.[29,30] The I_3 peak is insensitive to polarity, while the I_1 peak represents a symmetry forbidden transition that becomes more allowed with increasing polarity.[31] This transition is observed for molecular pyrene, and the effect is eliminated once a substituent such as a methyl group is attached.[32] Attachment of a methyl group breaks the symmetry of the pyrene molecule and removes the sensitivity of the I_1 peak to solvent polarity. Interestingly, upon hydroxylation or amination of the methyl group to form 1-pyrenemethanol or 1-pyrenemethylamine, the effect is partially restored and the I_1 peak once again shows sensitivity to solvent polarity.[33] In the present studies, butyl linkers were used to link pyrene to the macromolecule and the I_1 / I_3 ratio did not change as a function of solvent polarity.

1.4.3 The A_{E-}/A_{E+} Ratio and the P_A Value

By acquiring an excimer fluorescence decay and fitting the decay to a sum-of-exponentials, the sum of the negative pre-exponential factors divided by the sum of the positive pre-exponential factors, or the A_{E-} / A_{E+} ratio, can be calculated.[34] The A_{E-} / A_{E+} ratio is a measure of the level of pyrene aggregation within the macromolecule if no intermolecular associations are taking place. A negative pre-exponential factor corresponds to a risetime in the fluorescence decay and indicates that excimer formation is delayed as

expected for the diffusion-controlled encounters of two pyrene moieties. A positive pre-exponential factor describes the disappearance of excimer. If the sum of the negative pre-exponential factors equals the sum of the positive pre-exponential factors, then the formation of the excimer is exactly matched by its disappearance, the excimer is formed purely by diffusion and no aggregation is present. In this case, an A_{E-} / A_{E+} ratio of -1 is obtained. If pyrene aggregates are present, the relative fraction of excimer being formed by diffusion decreases, and the sum of the negative pre-exponential factors decreases relative to the sum of the positive pre-exponential factors. The result is that the A_{E-} / A_{E+} ratio becomes more positive. Thus, as the A_{E-} / A_{E+} ratio becomes more positive, increasing amounts of pyrene aggregates are present.

The P_A value represents another measure of the level of aggregation of the pyrene pendants of a labelled macromolecule.[2] The P_A value is calculated based on the UV-vis absorption spectrum of the pyrene-labelled macromolecule and a sample spectrum is shown in Figure 1.4. It is taken as the peak-to-valley ratio of the (0,0) transition of the ^1L_a band. It has been found that a P_A value greater than or equal to 3 indicates that no pyrene aggregation is present, while a P_A value smaller than 3 indicates that pyrene aggregation is taking place. Thus, the determination of the A_{E-} / A_{E+} ratio and the P_A value serve as a complementary method for detecting the presence of pyrene aggregation in a pyrene labelled macromolecule.

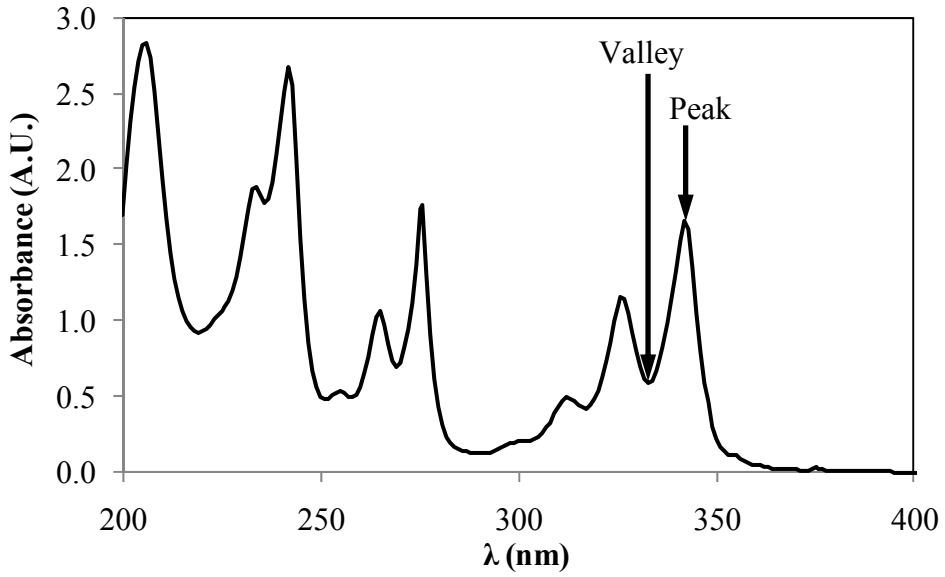

Figure 1.4: Sample UV-Vis absorption spectrum of a pyrene-labelled macromolecule showing the location of the peak and valley used to calculate the P_A value.

1.5 Outline of the Thesis

This thesis is organized in the following manner. Chapter 2 compares the study of polymers randomly and end-labelled with pyrene in solvents of varying viscosity. Two series of pyrene-labelled poly(*N*-isopropylacrylamide)s (PNIPAM) were synthesized. The first series consisted of six PNIPAM samples randomly labelled with pyrene, where the pyrene contents were 0.1, 2, 3, 4, 5, and 6 mol%. The second series consisted of five monodisperse PNIPAM samples end-capped with pyrene whose molecular weights were 6, 8, 14, 25, and 45 kDa. The FBM and the Birks Scheme were applied to analyze the fluorescence decays of the randomly and end-labelled polymers, respectively, and the results were compared. Chapter 3 studies the same five end-labelled PNIPAM samples as in Chapter 2, but their behavior is compared in ethanol and in aqueous solution. These two solvents have similar viscosity and solvent quality towards PNIPAM. Thus, differences in fluorescence can be

attributed to differences in pyrene solubility between the two solvents. Chapter 3 has been accepted for publication as an article in a special issue for Prof. J. C. Scaiano in the *Canadian Journal of Chemistry*. Finally, Chapter 4 details the study of four dendrimer generations with a bis(hydroxymethyl)propionic acid backbone where the terminal sites were labelled with pyrene. The MF analysis was applied to the monomer and excimer fluorescence decays of the pyrene-labelled dendrimers, and the average rate constant of excimer formation was calculated. The trends observed for $< k >$ were then used to determine how the volume probed by the pyrene-labelled ends varies with generation number. Chapter 4 has been published in the *Journal of Physical Chemistry B*. Finally, Chapter 5 summarizes the main results of Chapters 2 to 4 and provides some concluding remarks.

Chapter 2: Studying the Effect of Solvent Viscosity on Long-Range Polymer Chain Dynamics of Pyrene-Labelled Poly(*N*-isopropylacrylamide) by Fluorescence

2.1 Introduction

Since the 1980's, fluorescence dynamic quenching has been used extensively to study polymer chain dynamics in solution.[1-9] The early experiments were conducted by covalently attaching a luminophore and its quencher to the opposite ends of a monodisperse polymer chain. Steady-state and time-resolved fluorescence measurements were then carried out on dilute solutions of the end-labelled polymer to obtain k_q, the rate constant at which the excited luminophore is quenched.[1-10] Since a fluorescence quenching event indicates that the labelled ends of a same chain have encountered, k_q is equivalent to the end-to-end cyclization rate constant, k_{cy}, and reflects the flexibility of the polymer chain.[3-9]

Traditionally, pyrene has been the luminophore of choice used for end-to-end cyclization experiments.[6,11] Pyrene and its derivatives used to label polymers have a relatively high quantum yield (0.32 for pyrene in cyclohexane)[12] and a long lifetime (200-300 ns)[1,10] in most organic solvents. Not only does it self-quench, but in the process of quenching an excited monomer, the encounter of a ground-state and excited monomer results in the formation of an excited dimer, or excimer.[10] The excimer fluoresces at a wavelength distinguishable from that of the monomer,[10] allowing the experimentalist to monitor both the excited monomer (reactant) and dimer (product) in the solution. Comparison of the steady-state fluorescence spectra obtained with different pyrene-labelled polymers can be done quantitatively by determining the ratio of the fluorescence intensity of the excimer, I_E, over

that of the monomer, I_M, or the I_E/I_M ratio.[11] The I_E/I_M ratio represents the most basic measure of the efficiency of excimer formation for a pyrene-labelled polymer. The time-scale over which excimer formation occurs can be determined by acquiring a monomer and an excimer decay at two distinct emission wavelengths. Since the kinetics of the two are coupled, global analysis of the monomer and excimer decays greatly improves the accuracy of the kinetic parameters obtained from the analysis of the fluorescence decays.

The study of pyrene end-labelled polymers has been instrumental in developing our understanding of the process of end-to-end cyclization (EEC). However, this method does not come without limitations. First, the study of EEC has been shown to be limited to short chains and small solution viscosity.[15] Second, a study of the EEC of a chain describes the encounters of the chain ends only. No information is gained concerning the chain itself. Third, the strength of this procedure is rooted in the fact that the EEC process is well described by a single rate constant, namely k_{cy}. The strong dependence of k_{cy} on chain length means that monodisperse, end-labelled polymer samples must be synthesized, a task that is often difficult to accomplish.

An alternative method which circumvents the problems associated with the study of end-labelled polymers is to study polymers randomly labelled with pyrene. Since excimer formation is a local phenomenon, an increase in chain length does not result in a decrease in fluorescence quenching since for a randomly labelled polymer, the local concentration of ground-state pyrene experienced by an excited pyrene remains on average constant along the chain. A decrease in excimer formation due to an increase in viscosity or chain stiffness can be easily overcome by increasing the pyrene content of the polymer. In addition, random

labelling of the chain provides information on the internal dynamics of the entire polymer chain, which is no longer inferred from the behavior of its chain ends. The polymer can also be polydisperse since excimer formation, being a local phenomenon, occurs in a subvolume of the polymer coil. Synthesizing a polydisperse, randomly labelled polymer is usually much simpler than synthesizing a monodisperse, end-labelled polymer. However, the problem with random labelling is that the random distribution of distances between pyrene moeities results in a random distribution of rate constants. This distribution of rate constants complicates the analysis and interpretation of the fluorescence decays.

In 1999, the Fluorescence Blob Model (FBM) was introduced as a mathematical tool to handle the complex fluorescence decays acquired when studying randomly labelled polymers.[13] According to the FBM, a blob is defined as the volume probed by an excited luminophore during its natural lifetime. The polymer backbone is then divided into a cluster of blobs and quenching is monitored at the blob level. After applying the FBM equations to the fluorescence decays of the monomer and excimer, the parameter $k_{blob} \times N_{blob}$ can be obtained[14] where k_{blob} represents the quenching rate constant inside a blob containing one excited and one ground-state luminophore and N_{blob} represents the blob size expressed in number of monomer units.[13] Averaging $k_{blob} \times N_{blob}$ over a series of pyrene-labelled polymers yields $< k_{blob} \times N_{blob} >$ which gives a measure of the rate constant of excimer formation and has been shown to be analogous to k_{cy} found for end-labelled polymers.[14]

Since its introduction in 1999, the FBM has been applied to measure the internal dynamics of several polymeric backbones such as polystyrene,[13-15] poly(*N*,*N*-dimethylacrylamide),[16,17] polyisoprene,[18] and poly(L-glutamic acid).[19,20] The goal of the

present study is to extend the application of the FBM to a completely different polymer, poly(*N*-isopropylacrylamide) (PNIPAM). PNIPAM is a polymer of great interest since it undergoes a coil-to-globule transition at 32 °C in aqueous solution, making its pyrene-labelled analog an excellent candidate for studying this phenomenon.[21]

In this project, six randomly labelled PNIPAM samples (Py-PNIPAM-X% where X represents the pyrene content in mole percent and equals 0.1, 2, 3, 4, 5, and 6%) as well as five end-labelled PNIPAM samples (Py_2-PNIPAM-Y where Y represents the molecular weight of the PNIPAM chain and equals 6, 8, 14, 25, and 45K) were synthesized in the laboratory of Prof. F. M. Winnik at the Université de Montréal. At Waterloo, steady-state emission spectra and time-resolved fluorescence decays of all samples were acquired in organic solvents of varying viscosity. Decays of the Py-PNIPAM-X% and Py_2-PNIPAM-Y samples were analyzed with the FBM and the Birks Scheme yielding $< k_{blob} \times N_{blob} >$ and k_{cy}, respectively. The trends obtained with $< k_{blob} \times N_{blob} >$ and k_{cy} were compared to further demonstrate that the kinetics of excimer formation describe long-range polymer chain dynamics regardless of whether the polymer is labelled randomly or at its ends.

2.2 Experimental Section

2.2.1 Materials

Distilled in glass tetrahydrofuran, high-performance liquid chromatography (HPLC) grade methanol, and HPLC grade acetonitrile were purchased from Caledon Laboratories. HPLC grade ethanol and hexanol were purchased from Fisher-Scientific. Unlabelled PNIPAM ($\overline{M}_n$ = 95 kDa, *PDI* = 1.2) used for intrinsic viscosity measurements was purchased from Sigma-Aldrich. All materials were used as received.

2.2.2 Randomly Labelled Py-PNIPAM-X%

The general structure of the randomly labelled polymers studied in this project is given in Figure 2.1. Their synthesis was conducted in the laboratory of Prof. Françoise Winnik and has been described earlier.[22] The six Py-PNIPAM-X% samples were prepared through radical chain copolymerization of *N*-isopropylacrylamide (NIPAM) and *N*-(acryloxy)succinimide (NASI) in *tert*-butyl alcohol, initiated by azobisisobutyronitrile (AIBN). Copolymerization of NIPAM and NASI yields a random distribution of the two monomers within the polymer and was conducted up to a conversion of 30%. Replacement of the oxysuccinimide group of NASI with [4-(1-pyrenyl)butyl]amine in tetrahydrofuran (THF) via nucleophilic acyl substitution at the carbonyl carbon of NASI results in a random distribution of pyrene labels along the polymer backbone. Any excess NASI is subsequently converted to NIPAM via nucleophilic acyl substitution of NASI with *N*-isopropylamine. The pyrene content is then controlled through the amount of [4-(1-pyrenyl)butyl]amine added.

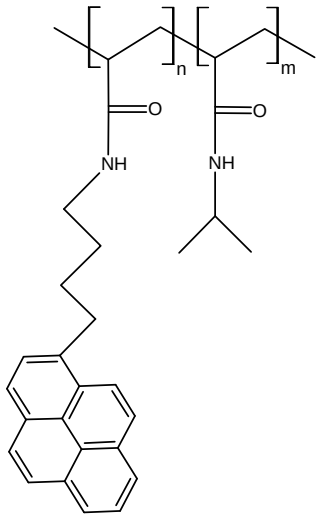

Figure 2.1: General structure of the randomly labelled Py-PNIPAM-X% samples.

In total, six Py-PNIPAM-X% samples were prepared. Their pyrene contents, number-average molecular weights ($\overline{M}_n$), and polydispersity indices (PDI) are listed in Table 2.1.

Table 2.1: Pyrene contents, molecular weights, and polydispersity indices of the Py-PNIPAM-X% samples.

Sample	Py Content (mol%)	$\overline{M}_n$ (kDa)	*PDI*
Py-PNIPAM-0.1%	0.12	104.0	1.75
Py-PNIPAM-2%	2.7	92.4	1.57
Py-PNIPAM-3%	3.6	71.0	1.63
Py-PNIPAM-4%	4.2	81.4	1.37
Py-PNIPAM-5%	5.1	70.5	1.70
Py-PNIPAM-6%	6.3	73.3	1.55

2.2.3 End-Labelled Py_2-PNIPAM-Y

The structure of the end-labelled Py_2-PNIPAM-Y samples is shown in Figure 2.2. Their synthesis, conducted in the laboratory of Dr. Françoise Winnik, has been described earlier.[23,24] The Py_2-PNIPAM-Y polymers were synthesized through a Reversible Addition-Fragmentation Chain Transfer (RAFT) polymerization of *N*-isopropylacrylamide. The initiator used was 2,2-azobisisobutyronitrile (AIBN) and the reversible chain transfer agent used was diethylene glycol di(2-(1-isobutyl)sulfanylthiocarbonylsulfanyl-2-methylpropionate) (DEGDIM). The RAFT polymerization results in the formation of an α,ω-isobutyldithiocarbonylthio end-capped PNIPAM polymer. Aminolysis of the isobutyldithiocarbonylthio end groups using *n*-butylamine results in the formation of an α,ω-dimercapto end-capped PNIPAM polymer. Finally, reaction of the mercapto end groups

with 4-(1-pyrenyl)butyliodide yields a PNIPAM polymer end-labelled with pyrene, as illustrated in Figure 2.2.

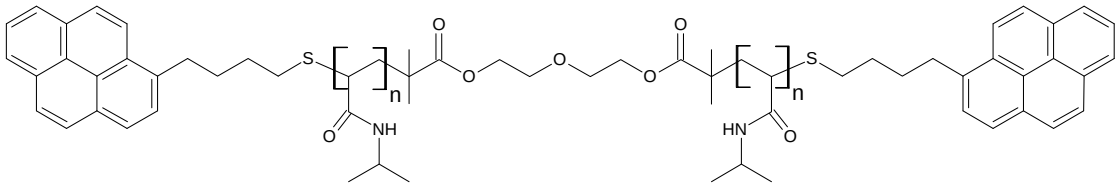

Figure 2.2: General structure of the pyrene end-labelled Py2-PNIPAM-Y polymers.

In total, five pyrene end-labelled samples and one monolabelled sample (Py-PNIPAM-25K) were synthesized. The monolabelled sample was used as a model compound to determine the natural lifetime of pyrene attached to the PNIPAM chain. Their pyrene functionalities, $\overline{M}_n$, and PDI values are listed in Table 2.2. All end-labelled samples were monodisperse, with PDI values less than or equal to 1.10.

Table 2.2: Pyrene functionalities, molecular weights, and polydispersity indices of the end-labelled Py_2-PNIPAM-Y samples.

Sample	Pyrene Functionality (%)	$\overline{M}_n$ (kDa)	PDI
Py_2-PNIPAM-6K	85.4	5.9	1.05
Py_2-PNIPAM-8K	82.6	7.6	1.08
Py_2-PNIPAM-14K	87.4	13.7	1.10
Py_2-PNIPAM-25K	75.5	25.4	1.07
Py_2-PNIPAM-45K	74.8	44.5	1.10
Py-PNIPAM-25K	--	23.5	1.09

2.2.4 Intrinsic Viscosity Measurements

A sample of unlabelled PNIPAM ($\overline{M}_n$ = 95 kDa, PDI = 1.2) was purchased from Sigma-Aldrich and used as a model compound for the pyrene labelled PNIPAM samples to gauge the quality of different organic solvents towards PNIPAM. Solvent quality toward PNIPAM was estimated by conducting intrinsic viscosity measurements. Five concentrations ranging from 2 to 10 g/L were used in order to measure the intrinsic viscosity of PNIPAM in each solvent and solvent mixture. Measurements were done using an Übbelohde viscometer placed in an ethylene glycol/water bath maintained at a constant temperature of 25 ± 0.5 ºC. Intrinsic viscosities of PNIPAM in each solvent are given in Table 2.3.

Table 2.3: Viscosities and densities of, as well as intrinsic viscosities of the unlabelled PNIPAM sample in the solvents used in this study.

Solvent	η(mPa·s)	ρ (g/mL)	$[\eta]$ (dL·g^{-1})
Acetonitrile	0.37	0.78	2.09 ± 0.02
2-Butanone	0.41	0.81	
Ethyl Acetate	0.42	0.90	
Tetrahydrofuran	0.46	0.88	2.8 ± 0.2
Methanol	0.54	0.79	4.3 ± 0.2
80% Methanol/Hexanol	0.71	0.79	
60% Methanol/Hexanol	0.97	0.80	
Ethanol	1.1	0.79	4.85 ± 0.05
30% Methanol/Hexanol	1.7	0.81	
15% Methanol/Hexanol	2.6	0.81	
6% Methanol/Hexanol	3.6	0.81	
Hexanol	4.6	0.82	6.0 ± 0.2

2.2.5 Viscosities of Binary Mixtures of Methanol and Hexanol

A calibration curve for the viscosities of binary mixtures of methanol and hexanol as a function of methanol content was created using an Übbelohde viscometer. First, the time taken by a series of solvents of known viscosity to pass through the Übbelohde viscometer was measured. A viscometer constant (in $cSt \cdot s^{-1}$) was then calculated by dividing the viscosity of the solvent by the time taken to pass through the viscometer. Two viscometers were used, a number 25 and a number 75, whose measurable viscosity ranges were 0.5 – 2 cSt and 1.6 – 8 cSt and which had viscometer constants of 18.2 ± 0.8 $\mu St \cdot s^{-1}$ and 79.1 ± 0.6 $\mu St \cdot s^{-1}$, respectively. Viscosity measurements were conducted on five different solvents which yielded five viscometer constants whose average is regarded as the viscometer constant.

Once the viscometer constants were known, the viscosities of the binary mixtures could be measured. This was done by measuring the time for a mixture to pass through the viscometer and then multiplying this time by the appropriate viscometer constant. Solutions were allowed to sit in the water bath for 30 minutes prior to data acquisition in order for the temperature to equilibrate. Three trials were done per mixture to improve accuracy. Once the viscosities were measured, a calibration curve was generated as shown in Figure 2.3. The point at 40% methanol content represents the transition point between viscometer 25 to viscometer 75. A good agreement was obtained between the viscosities determined with both viscometers at that point. The dynamic viscosities of the solvents and binary solvent mixtures used in this project are given in Table 2.3.

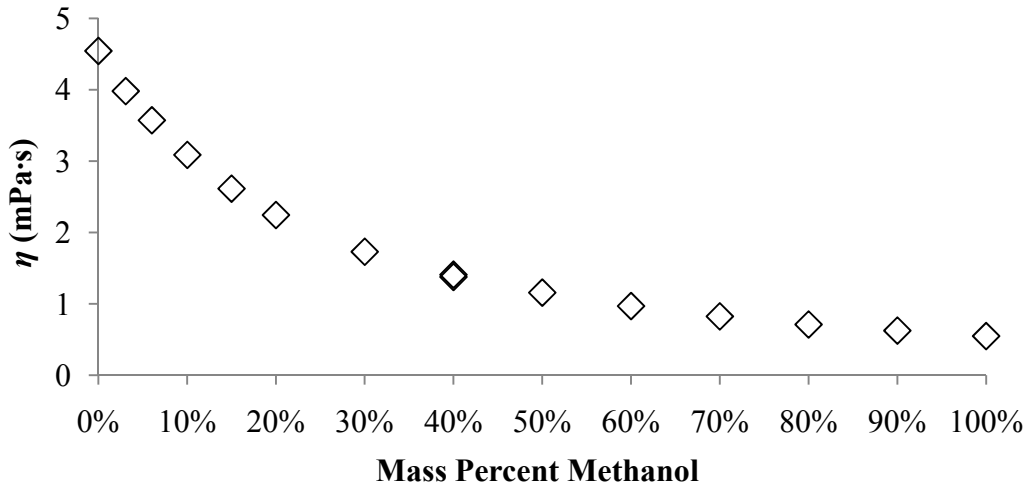

Figure 2.3: Plot of viscosity as a function of methanol content for binary mixtures of methanol and hexanol.

2.2.6 UV-Visible Absorbance Measurements

UV-Visible absorbances were measured on a Cary 100 UV-Visible spectrophotometer with a UV cell having a 1 cm path length. Absorbances were measured in the 200 – 600 nm wavelength range. All PNIPAM solutions used for fluorescence measurements had an absorbance at 344 nm of less than 0.1, corresponding to a pyrene concentration smaller than 2.5 μM. This pyrene concentration ensures that any excimer formation observed is the result of intra- and not intermolecular interactions between pyrene pendants.

The pyrene contents of the Py-PNIPAM-X% samples were also measured using UV-visible spectrophotometry. The molar extinction coefficient of 1-pyrenebutanol was first measured in ethanol and was found to equal 43,000 $M^{-1} \cdot cm^{-1}$ at 344 nm. The absorbance of a known mass concentration of a Py-PNIPAM-X% sample was then measured. The pyrene concentration was calculated using the Beer-Lambert law and the known molar extinction

coefficient of 1-pyrenebutanol in ethanol at 344 nm. The pyrene content, λ_{Py} in μmol/g, can be calculated using Equation 2.1

$$\lambda_{Py} = \frac{[Py]}{m/V} \tag{2.1}$$

where m and V represent the mass of polymer and volume of solvent, respectively. The pyrene content in mol% can then be calculated using Equation 2.2

$$mol\% = \frac{M_1}{M_1 - M_2 + \frac{1}{\lambda_{Py}}} \tag{2.2}$$

where M_1 and M_2 represent the molecular weight of the labelled and unlabelled NIPAM monomer equal to 326 and 113 g·mol^{-1}, respectively.

2.2.7 Steady-State Fluorescence Measurements

Steady-state fluorescence spectra of the pyrene-labelled PNIPAM samples were acquired on a Photon Technology International (PTI) LS-100 steady-state fluorometer. The fluorometer is equipped with an Ushio UXL-75Xe Xenon arc lamp and a PTI 814 photomultiplier detection system. The solutions were excited at 344 nm and their emission was monitored from 350 to 600 nm. All solutions were degassed under a steady stream of

nitrogen for 30 minutes and had a pyrene concentration smaller than 2.5 μM. The monomer fluorescence intensity (I_M) was obtained by taking the integral under the fluorescence spectrum from 372 to 378 nm. The fluorescence intensity of the excimer (I_E) was determined by first acquiring the steady-state fluorescence spectrum of the monolabelled Py-PNIPAM-25K sample. Next, the spectrum of the Py-PNIPAM-25K compound was subtracted from the spectrum of the randomly or end-labelled PNIPAM sample. Finally, the excimer intensity, I_E, was calculated by taking the integral of the subtracted spectrum from 500 to 530 nm.

2.2.8 Time-Resolved Fluorescence Measurements

The fluorescence decays of the pyrene monomer and excimer of the pyrene-labelled PNIPAM solutions were acquired on an IBH time-resolved fluorometer equipped with a nano-LED light source. The solutions were prepared with a pyrene concentration of approximately 2.5 μM, small enough to ensure that no intermolecular excimer formation was being observed. The solutions were excited at a wavelength of 344 nm and emission was monitored at 375 nm and 510 nm for the pyrene monomer and excimer using a cut-off filter at 370 and 495 nm, respectively. A Ludox solution was used at the excitation wavelength to determine the instrument response function which was convoluted with the desired theoretical function for the decay analysis. Fluorescence decays of the Py_2-PNIPAM-Y and Py-PNIPAM-X% samples were analyzed using the Birks Scheme and the FBM, respectively. The equations used for the analysis of the fluorescence decays are described in Section 2.3.

2.3 Fluorescence Decay Analysis Models

2.3.1 The Birks Scheme

The Birks Scheme was first introduced to describe the process of excimer formation between an excited and a ground-state fluorophore molecularly dissolved in solution.[10] This kinetic scheme was then readily extended to study the kinetics of excimer formation for end-labelled polymers as was done in Scheme 2.1.

In Scheme 2.1, an excited pyrene fluoresces with its natural lifetime, τ_M. While excited, it can encounter a ground-state pyrene to form an excimer at a rate governed by the rate constant k_{cy}. This newly formed excimer can then either fluoresce with a lifetime given by τ_{E0} or it can dissociate with a rate constant k_{-cy}. An extra species is added to the scheme to account for the fraction of monolabelled chains in solution which fluoresce with the monomer lifetime, τ_M.

Scheme 2.1: The Birks Scheme illustrating diffusional excimer formation for a pyrene end-labelled polymer.

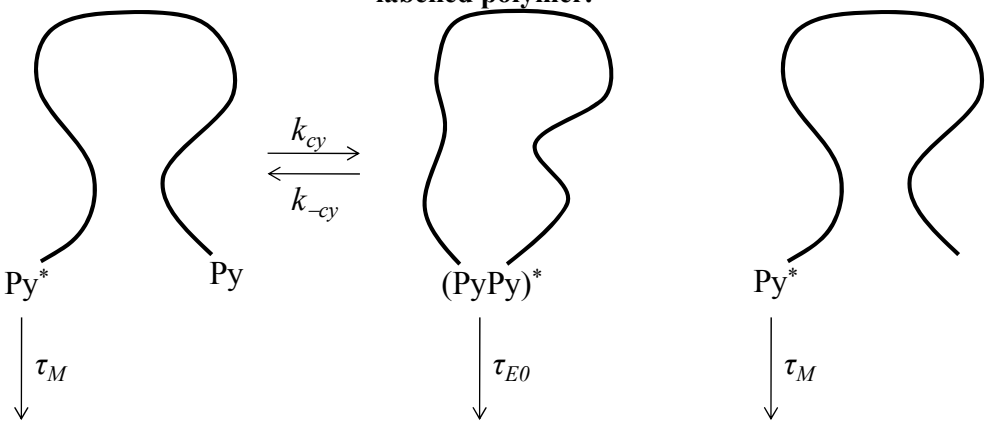

Based on Scheme 2.1, three different pyrene species are assumed to be present in solution at any given time. The species Py^*_{diff} represents the excited pyrene units that form excimer by diffusion, whereas the pyrene units that are attached at the end of mono-labelled chains are referred to as Py^*_{free}. When an excited and a ground-state pyrene stack properly, their interaction yields an excimer ($E0^*$ = (PyPy)* in Scheme 2.1) which can be formed either via collisional encounter between two pyrenyl moieties, or via direct excitation of a pyrene dimer. Analysis of the fluorescence decays acquired with the pyrene-labelled PNIPAMs required that an extra exponential be added in order to account for the presence of a short-lived species. The origin of this species is debatable and could be due to residual light scattering leaking through the detection system or a fluorescent impurity covalently bound to the polymer. This species, referred to as Py^*_S, fluoresces with a short lifetime τ_S and is observed in both the monomer and excimer decays although its contribution is stongest in the excimer decay under conditions that disfavor excimer formation, namely long polymers and high viscosity solvents. Based on the above, the following differential equations describe the time-dependent concentration of the excited monomer and excimer species.

$$\frac{d[Py^*_{diff}]_{(t)}}{dt} = -X[Py^*_{diff}]_{(t)} + k_{-cy}[E0^*]_{(t)} \tag{2.3}$$

$$\frac{d[Py^*_{free}]_{(t)}}{dt} = -\frac{1}{\tau_M}[Py^*_{free}]_{(t)} \tag{2.4}$$

$$\frac{d[Py_S^*]_{(t)}}{dt} = -\frac{1}{\tau_S}[Py_S^*]_{(t)} \tag{2.5}$$

$$\frac{d[E0^*]_{(t)}}{dt} = -Y[E0^*]_{(t)} + k_{cy}[Py][Py_{diff}^*]_{(t)} \tag{2.6}$$

where the definition of X and Y according to the Birks Scheme[10] is given hereafter.

$$X = k_{cy} + \frac{1}{\tau_M} \tag{2.7}$$

$$Y = k_{-cy} + \frac{1}{\tau_{E0}} \tag{2.8}$$

After integration of Equations 2.3 – 2.6, the following expressions are obtained which give the time profile of each pyrene species in solution.

$$[Py_{diff}^*]_{(t)} = \frac{[Py_{diff}^*]_{(t=0)}\left(\frac{1}{\tau_2} - X\right)}{\frac{1}{\tau_2} - \frac{1}{\tau_1}}\left(\exp\left(-\frac{t}{\tau_1}\right) + A\exp\left(-\frac{t}{\tau_2}\right)\right) \tag{2.9}$$

$$[Py^{*}_{free}]_{(t)} = [Py^{*}_{free}]_{(t=0)} \exp\left(-\frac{t}{\tau_M}\right) \tag{2.10}$$

$$[Py^{*}_{S}]_{(t)} = [Py^{*}_{S}]_{(t=0)} \exp\left(-\frac{t}{\tau_S}\right) \tag{2.11}$$

$$[E0^{*}]_{(t)} = \frac{k_{cy}[Py^{*}_{diff}]_{(t=0)}}{\frac{1}{\tau_2} - \frac{1}{\tau_1}} \left(\exp\left(-\frac{t}{\tau_1}\right) - \exp\left(-\frac{t}{\tau_2}\right)\right) \tag{2.12}$$

The expression of A, τ_1, and τ_2 are given in Equations 2.13 – 2.15.

$$A = \frac{\left(X - \frac{1}{\tau_1}\right)}{\left(\frac{1}{\tau_2} - X\right)} \tag{2.13}$$

$$\tau_1 = \left[\frac{1}{2}\left(X + Y + \sqrt{(Y-X)^2 + 4k_{cy}k_{-cy}}\right)\right]^{-1} \tag{2.14}$$

$$\tau_2 = \left[\frac{1}{2}\left(X + Y - \sqrt{(Y-X)^2 + 4k_{cy}k_{-cy}}\right)\right]^{-1} \tag{2.15}$$

Equations 2.9 – 2.11 and 2.11 – 2.12 can be summed to give Equations 2.16 and 2.17, the time-dependent profiles of the overall excited pyrene monomer and excimer species in solution, respectively.

$$[Py^*]_{(t)} = \frac{[Py^*_{diff}]_{(t=0)}\left(\frac{1}{\tau_2} - X\right)}{\frac{1}{\tau_2} - \frac{1}{\tau_1}}\left(\exp\left(-\frac{t}{\tau_1}\right) + A\exp\left(-\frac{t}{\tau_2}\right)\right)$$

$$+ [Py^*_{free}]_{(t=0)}\exp\left(-\frac{t}{\tau_M}\right) + [Py^*_S]_{(t=0)}\exp\left(-\frac{t}{\tau_S}\right) \quad (2.16)$$

$$[E^*]_{(t)} = \frac{k_{cy}[Py^*_{diff}]_{(t=0)}}{\frac{1}{\tau_2} - \frac{1}{\tau_1}}\left(-\exp\left(-\frac{t}{\tau_1}\right) + \exp\left(-\frac{t}{\tau_2}\right)\right)$$

$$+ [Py^*_S]_{(t=0)}\exp\left(-\frac{t}{\tau_S}\right) \quad (2.17)$$

2.3.2 Issues and Limitations Associated with the Use of End-Labelled Polymers to Study Long-Range Polymer Chain Dynamics

The Birks Scheme has proven to be a powerful analytical tool to study the cyclization kinetics of end-labelled polymers. However, the study of end-labelled polymers does not come without its limitations. First, the rate constant of cyclization, k_{cy}, depends strongly on the polymer chain length. It has been shown to scale as $N^{-1.62}$ for a series of pyrene end-labelled polystyrenes (Py_2-PS) in cyclohexane at 34.5 ºC, a theta solvent for PS, where N

represents the number of monomer units.[3] This scaling law translates into a 97.5% decrease for k_{cy} with a 10-fold increase in chain length. From this example, it is quite obvious that as chain length increases and k_{cy} becomes vanishingly small, the excimer signal decreases drastically to the point where no excimer decay can be acquired. A similar effect can be seen with viscosity. Although the polymer under study may be short enough to provide a good excimer signal in a low viscosity solvent such as tetrahydrofuran (η = 0.46 mPa·s), excimer formation will be strongly reduced in a more viscous solvent such as benzyl alcohol (η = 5.5 mPa·s), as was observed for Py_2-PS.[15] Under conditions where the solvent viscosity is high or the polymer chain is long, the excimer signal is too weak to acquire an excimer decay, and the Birks Scheme cannot be used.

Second, it must be pointed out that in an end-to-end cyclization (EEC) experiment, only the ends are probed. For a polymer with a degree of polymerization of 100 monomer units labelled at its two ends, it implies that 98% of the chain remains invisible. Thus, the analysis provides information on the ends of the polymer, and obviously, not the polymer as a whole which is, in principle, the object of a study on polymer chain dynamics, as EEC experiments are often used for.

Third, the synthesis of end-labelled polymers is not always trivial. In many cases, synthesizing a monodisperse polymer labelled at the ends only can be quite challenging. In the present study, this point is exemplified by the fact that the Py_2-PNIPAM-Y polymers were synthesized using the Reversible Addition-Fragmentation Chain Transfer (RAFT) polymerization technique,[23,24] whereas the Py-PNIPAM-X% polymers were synthesized using a relatively more simple radical polymerization.[22]

2.3.3 The Fluorescence Blob Model

Working with randomly labelled polymers solves many of the aforementioned issues and limitations dealt with when studying end-labelled polymers. In this case, the entire polymer is being probed and problems associated with chain length become irrelevant. Excimer formation occurs locally along the chain and increasing the chain length does not affect this process as has been shown in a number of instances.[13,17] Decreased excimer formation due to increased viscosity can be overcome by increasing the pyrene content of the randomly labelled polymer, which reduces the average distance between any two pyrene moeities and enhances excimer formation. The polymers also need not be monodisperse, simplifying the polymerization reaction considerably. However, working with randomly labelled polymers introduces a new problem in that random labelling results in a distribution of distances between pyrene pendants. This distribution of distances results in a distribution of excimer formation rate constants which is difficult to handle.

The Fluorescence Blob Model (FBM) is a mathematical tool that was developed to handle the complicated distribution of rate constants when analyzing the fluorescence decays of a polymer randomly labelled with pyrene.[13] According to the FBM, excimer formation in a polymer randomly labelled with pyrene can be described by Scheme 2.2. According to Scheme 2.2, excimer formation is a two-step process. First, two polymer segments diffuse to a nearby distance such that the pyrene labels are within proximity of each other and can rearrange to form excimer. This diffusive motion of the polymer segments is described by the rate constant k_1. Next, the two pyrene labels rearrange on a faster time scale and form an excimer, $E0^*$. This process is described by the rate constant k_2. The rate constant k_1 depends on the chain length spanning two pyrene labels. Since the pyrene moeities are

attached at random, the chain lengths spanning any two pyrene pendants are also random, resulting in a distribution of rate constants, k_1. This distribution of rate constants results in a complex rate of polymer segment encounters described by a time-dependent function, $f(t)$, which is unknown. The FBM, however, models this time-dependent function $f(t)$ by adapting the equations derived by Tachiya originally to describe micellar quenching.[25]

Scheme 2.2: Excimer formation in randomly labelled polymers.

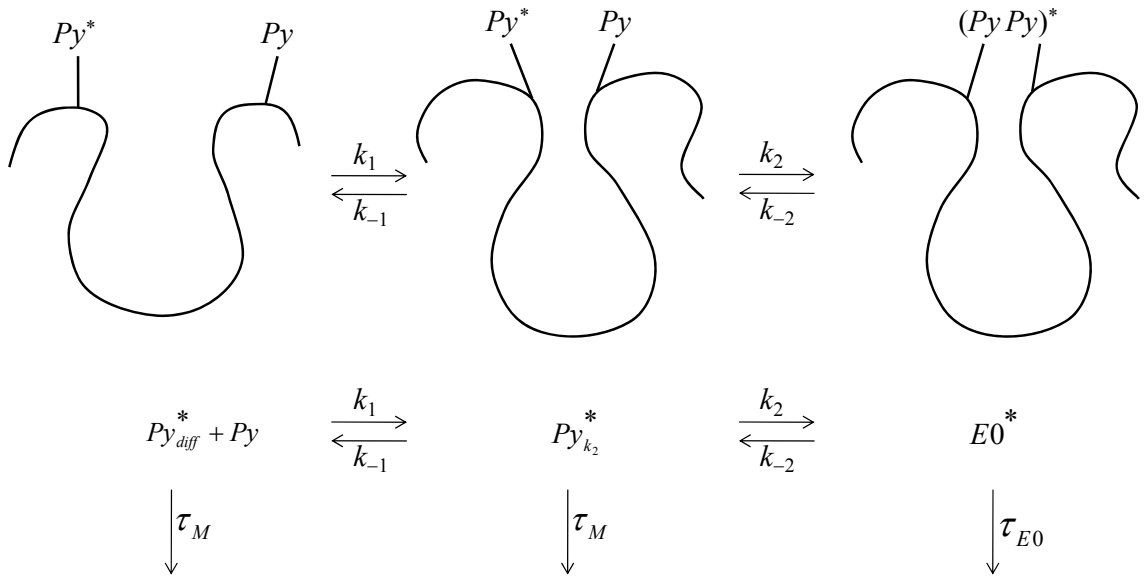

Based on Scheme 2.2, five pyrene species are expected to be present in solution. These species include the excited pyrene units which are isolated (Py^*_{free}) and do not form excimer and fluoresce with the natural lifetime of the monomer, τ_M, the excited pyrene units which diffuse to within range of a ground-state pyrene, are able to form excimers after rearrangement with a rate constant k_2, and fluoresce with the lifetime τ_M (Py^*_{diff}), those excited pyrene units which are already within range of a ground-state pyrene, can rearrange

to form excimers with a rate constant k_2, and fluoresce with the lifetime τ_M ($Py^*_{k_2}$), properly stacked excimers which fluoresce with the natural lifetime of the excimer, τ_{E0} ($E0^*$), and improperly stacked excimers which fluoresce with a long lifetime, τ_{EL} (EL^*). Differential equations can then be derived which give the time-dependence of the concentration of each pyrene species in solution. However, a few simplifications can be made beforehand. First, excimer dissociation is typically negligible at room temperature, eliminating k_{-2}. Second, k_2 is very fast, much faster than k_{-1}. Thus, the process described by k_{-1} can also be ignored. Using these assumptions, Equations 2.18 – 2.22 give the differential equations used to describe each pyrene species present in solution.

$$\frac{d[Py^*_{free}]_{(t)}}{dt} = -\frac{1}{\tau_M}[Py^*_{free}]_{(t)} \tag{2.18}$$

$$\frac{d[Py^*_{diff}]_{(t)}}{dt} = -f(t) - \frac{1}{\tau_M}[Py^*_{diff}]_{(t)} \tag{2.19}$$

$$\frac{d[Py^*_{k_2}]_{(t)}}{dt} = f(t) - \left(k_2 + \frac{1}{\tau_M}\right)[Py^*_{k_2}]_{(t)} \tag{2.20}$$

$$\frac{d[E0^*]_{(t)}}{dt} = k_2[Py^*_{k_2}]_{(t)} - \frac{1}{\tau_{E0}}[E0^*]_{(t)} \tag{2.21}$$

$$\frac{d[EL^*]_{(t)}}{dt} = -\frac{1}{\tau_{EL}}[EL^*]_{(t)} \tag{2.22}$$

According to the model, the FBM assumes that an excited pyrene probes a finite volume in space during its natural lifetime and that this volume defines a blob. Since pyrene moeities are labelled at random along the polymer backbone, the backbone is then arbitrarily divided into a cluster of blobs, according to a Poisson distribution. Three parameters are then defined in terms of this system. The first is k_{blob}, the quenching rate constant inside a blob containing one excited-state and one ground-state pyrene. The second parameter, the exchange rate constant, k_e, describes the process of exchange of ground-state pyrene units between blobs. Finally, $<n>$ gives the average number of ground-state pyrene units per blob. The equations that were derived by Tachiya to describe micellar quenching[25] can then be adapted to describe quenching at the blob level, where the blobs are synonymous with Tachiya's micelles.[13] The following expression is then obtained which describes the concentration of the Py^*_{diff} species as a function of time,

$$[Py^*_{diff}]_{(t)} = [Py^*_{diff}]_{(t=0)} \exp\left[-\left(A_2 + \frac{1}{\tau_M}\right) \times t - A_3\left(1 - \exp(-A_4 t)\right)\right] \tag{2.23}$$

where,

$$A_2 =< n > \frac{k_{blob} k_e [blob]}{k_{blob} + k_e [blob]} \tag{2.24}$$

$$A_3 =< n > \frac{(k_{blob})^2}{(k_{blob} + k_e [blob])^2} \tag{2.25}$$

$$A_4 = k_{blob} + k_e [blob] \tag{2.26}$$

Equation 2.23 provides an expression for $[Py^*_{diff}]_{(t)}$. In turn, this expression can be used to solve Equation 2.19 to obtain $f(t)$, which is given in Equation 2.27.

$$f(t) = [Py^*_{diff}]_{(t)} e^{-A_3} \sum_{i=0}^{\infty} \frac{A_3^i}{i!} \exp\left(-\left(A_2 + iA_4 + \frac{1}{\tau_M} \right) \times t \right) \tag{2.27}$$

This expression for $f(t)$ can be used to solve Equation 2.20, giving an expression for $[Py^*_{k_2}]_{(t)}$. The expression for $[Py^*_{k_2}]_{(t)}$ enables the integration of Equation 2.21, which yields an expression for $[E0^*]_{(t)}$. Finally, the solutions to Equations 2.18 and 2.22 are

trivial, providing expressions for $[Py^{*}_{free}]_{(t)}$ and $[EL^{*}]_{(t)}$, respectively. The expressions for $[Py^{*}_{k_2}]_{(t)}$, $[E0^{*}]_{(t)}$, $[Py^{*}_{free}]_{(t)}$ and $[EL^{*}]_{(t)}$ are given in Equations 2.28 – 2.31.

$$[Py^{*}_{k_2}]_{(t)} = \left([Py^{*}_{k_2}]_{(t=0)} + [Py^{*}_{diff}]_{(t=0)} e^{-A_3} \sum_{i=0}^{\infty} \frac{A_3^i}{i!} \frac{A_2 + iA_4}{A_2 + iA_4 - k_2} \right) \exp\left(-\left(k_2 + \frac{1}{\tau_M} \right) \times t \right)$$

$$- [Py^{*}_{diff}]_{(t=0)} e^{-A_3} \sum_{i=0}^{\infty} \frac{A_3^i}{i!} \frac{A_2 + iA_4}{A_2 + iA_4 - k_2} \exp\left(-\left(A_2 + iA_4 + \frac{1}{\tau_M} \right) \times t \right) \tag{2.28}$$

$$[Py^{*}_{free}]_{(t)} = [Py^{*}_{free}]_{(t=0)} \exp\left(-\frac{t}{\tau_M} \right) \tag{2.29}$$

$$[E0^{*}]_{(t)} = k_2 \left(\left([Py^{*}_{k_2}]_{(t=0)} + [Py^{*}_{diff}]_{(t=0)} e^{-A_3} \sum_{i=0}^{\infty} \frac{A_3^i}{i!} \frac{A_2 + iA_4}{A_2 + iA_4 - k_2} \right) \right.$$
$$\left. \times \frac{\exp\left(-\frac{t}{\tau_{E0}} \right) - \exp\left(-\left(k_2 + \frac{1}{\tau_M} \right) \times t \right)}{k_2 + \frac{1}{\tau_M} - \frac{1}{\tau_{E0}}} + [E0^{*}]_{(t=0)} \exp\left(-\frac{t}{\tau_{E0}} \right) \right.$$

$$+ [Py^{*}_{diff}]_{(t=0)} e^{-A_3} \sum_{i=0}^{\infty} \frac{A_3^i}{i!} \frac{A_2 + iA_4}{A_2 + iA_4 - k_2} \frac{\exp\left(-\left(A_2 + iA_4 + \frac{1}{\tau_M} \right) \times t \right) - \exp\left(-\frac{t}{\tau_{E0}} \right)}{A_2 + iA_4 + \frac{1}{\tau_M} - \frac{1}{\tau_{E0}}} \tag{2.30}$$

$$[EL^{*}]_{(t)} = [EL^{*}]_{(t=0)} \exp\left(-\frac{t}{\tau_{EL}} \right) \tag{2.31}$$

Once the time behaviour of each pyrene species is known, expressions for the time-dependence of the overall excited pyrene monomer and excimer can be obtained using Equations 2.32 and 2.33.

$$[Py^*]_{(t)} = [Py^*_{diff}]_{(t)} + [Py^*_{k_2}]_{(t)} + [Py^*_{free}]_{(t)} \tag{2.32}$$

$$[E^*]_{(t)} = [E0^*]_{(t)} + [EL^*]_{(t)} \tag{2.33}$$

After substitution of Equations 2.28 – 2.31 into Equations 2.32 and 2.33, the following expressions are obtained for the time-dependent equations describing the monomer and excimer decays.

$$\begin{aligned}[Py^*]_{(t)} = {} & [Py^*_{diff}]_{(t=0)} \exp\left[-\left(A_2 + \frac{1}{\tau_M}\right)\times t - A_3\left(1-\exp\left(-A_4 t\right)\right)\right] \\ & + \left([Py^*_{k_2}]_{(t=0)} + [Py^*_{diff}]_{(t=0)}\, e^{-A_3} \sum_{i=0}^{\infty} \frac{A_3^i}{i!} \frac{A_2 + iA_4}{A_2 + iA_4 - k_2}\right) \exp\left(-\left(k_2 + \frac{1}{\tau_M}\right)\times t\right) \\ & - [Py^*_{diff}]_{(t=0)}\, e^{-A_3} \sum_{i=0}^{\infty} \frac{A_3^i}{i!} \frac{A_2 + iA_4}{A_2 + iA_4 - k_2} \exp\left(-\left(A_2 + iA_4 + \frac{1}{\tau_M}\right)\times t\right) \\ & + [Py^*_{free}]_{(t=0)} \exp\left(-\frac{t}{\tau_M}\right)\end{aligned} \tag{2.34}$$

$$[E^*]_{(t)} = k_2\left(\left([Py^*_{k_2}]_{(t=0)} + [Py^*_{diff}]_{(t=0)}\, e^{-A_3}\sum_{i=0}^{\infty}\frac{A_3^i}{i!}\frac{A_2+iA_4}{A_2+iA_4-k_2}\right)\right.$$
$$\left.\times\frac{\exp\left(-\frac{t}{\tau_{E0}}\right)-\exp\left(-\left(k_2+\frac{1}{\tau_M}\right)\times t\right)}{k_2+\frac{1}{\tau_M}-\frac{1}{\tau_{E0}}}+[E0^*]_{(t=0)}\exp\left(-\frac{t}{\tau_{E0}}\right)\right.$$
$$+[Py^*_{diff}]_{(t=0)}\, e^{-A_3}\sum_{i=0}^{\infty}\frac{A_3^i}{i!}\frac{A_2+iA_4}{A_2+iA_4-k_2}\frac{\exp\left(-\left(A_2+iA_4+\frac{1}{\tau_M}\right)\times t\right)-\exp\left(-\frac{t}{\tau_{E0}}\right.}{A_2+iA_4+\frac{1}{\tau_M}-\frac{1}{\tau_{E0}}}$$

$$+[EL^*]_{(t=0)}\exp\left(-\frac{t}{\tau_{EL}}\right) \qquad (2.35)$$

Fitting the monomer and excimer decays using Equations 2.34 and 2.35 yields the parameters k_{blob}, $< n >$, and $k_e[blob]$, where $[blob]$ represents the local blob concentration within the polymer coil. Fitting the monomer decays using Equation 2.34 also yields the fractions f_{Mdiff}, f_{Mk_2}, and f_{Mfree} which represent the molar fractions of the Py^*_{diff}, $Py^*_{k_2}$, and Py^*_{free} species contributing to the monomer decays, respectively. In a similar manner, fitting the excimer decays with Equation 2.35 yields the fractions f_{Ediff}, f_{Ek_2}, f_{EE0}, and f_{EEL} which represent the molar fractions of the Py^*_{diff}, $Py^*_{k_2}$, $E0^*$, and EL^* species contributing to the excimer decays, respectively. The fractions f_{Mdiff}, f_{Mk_2}, f_{Mfree}, f_{Ediff}, f_{Ek_2}, f_{EE0}, and f_{EEL} can then be used to determine the overall molar fractions of each pyrene species present in solution f_{diff}, f_{free}, f_{k_2}, f_{E0}, and f_{EL} by applying Equations 2.36 – 2.40.

$$f_{diff} = \frac{1}{1 + \frac{f_{Mfree}}{f_{Mdiff}} + \frac{f_{Mk_2}}{f_{Mdiff}} + \frac{f_{EEL}}{f_{Ediff}} + \frac{f_{EE0}}{f_{Ediff}}} \tag{2.36}$$

$$f_{free} = f_{diff} \frac{f_{Mfree}}{f_{Mdiff}} \tag{2.37}$$

$$f_{k_2} = f_{diff} \frac{f_{Mk_2}}{f_{Mdiff}} = f_{diff} \frac{f_{Ek_2}}{f_{Ediff}} \tag{2.38}$$

$$f_{E0} = f_{diff} \frac{f_{EE0}}{f_{Ediff}} \tag{2.39}$$

$$f_{EL} = f_{diff} \frac{f_{EEL}}{f_{Ediff}} \tag{2.40}$$

Another parameter that can be calculated based on the FBM parameters is N_{blob}. N_{blob} represents the average number of monomer units per blob and is given by Equation 2.41.

$$N_{blob} = \frac{< n >}{\frac{\lambda_{Py}}{\left(1 - f_{Mfree}\right)}\left(M_1 x + M_2\left(1 - x\right)\right)} \tag{2.41}$$

In Equation 2.41, M_1, M_2, x, and λ_{Py} represent the molecular weight of the pyrene labelled NIPAM monomer (326 g·mol^{-1}), the molecular weight of the unlabelled NIPAM monomer (113 g·mol^{-1}), the fraction of NIPAM monomers that are labelled, and the pyrene content in moles of pyrene per gram of polymer listed in Table 2.1, respectively. The fraction $\lambda_{Py}/(1-f_{Mfree})$ represents the corrected pyrene content, or the pyrene content of the pyrene units attached to the polymer that form excimer by diffusion and follow the FBM.[26] Finally, the parameter $k_{blob} \times N_{blob}$ can be calculated for each pyrene content in a given solvent. Averaging $k_{blob} \times N_{blob}$ values for all of the Py-PNIPAM-X% polymers in a given solvent yields $< k_{blob} \times N_{blob} >$, the overall rate constant of excimer formation of PNIPAM in that solvent. In the case of a series of polystyrene randomly labelled with pyrene, $< k_{blob} \times N_{blob} >$ obtained by applying the FBM analysis to the fluorescence decays acquired with randomly labelled polymers has been shown to be equivalent to k_{cy} obtained by applying the Birks Scheme analysis to the fluorescence decays acquired with end-labelled polymers.[15]

2.4 Results and Discussion

The steady-state fluorescence spectra for the Py_2-PNIPAM-Y and Py-PNIPAM-X% samples were acquired in organic solvents of varying viscosity (see Table 2.2). For comparison, the steady-state spectra of the Py_2-PNIPAM-6K and Py-PNIPAM-3% polymers in all solvents, normalized to the peak at 375 nm, are shown in Figure 2.4. Typical monomer emission peaks are observed in the 370 to 425 nm wavelength region, while the excimer emission is seen as a

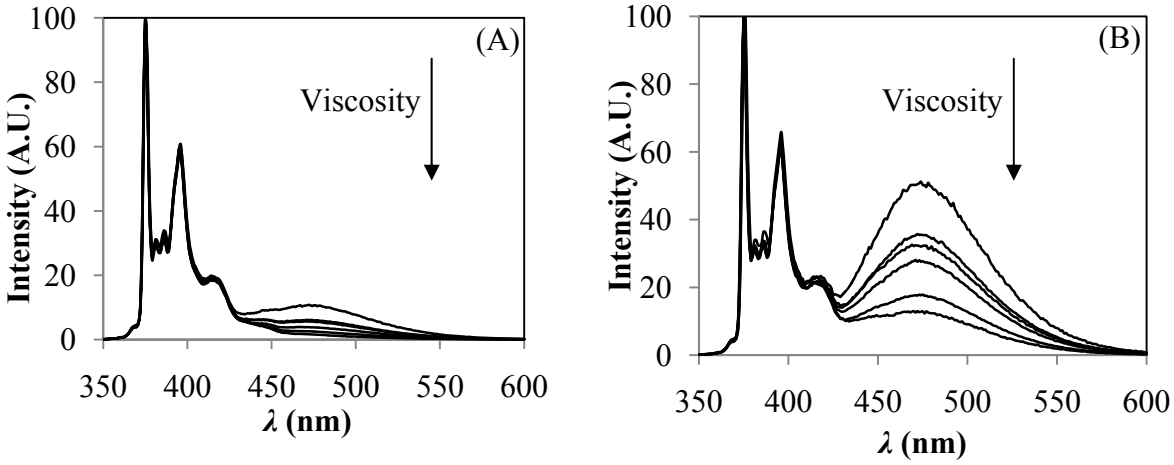

Figure 2.4: Steady-state fluorescence spectra for the (A) Py_2-PNIPAM-6K and (B) Py-PNIPAM-3% samples. λ_{ex} = 344 nm, [*Py*] = 2.5 µM. Top to bottom: Methanol (η = 0.55 mPa·s), 80% methanol/hexanol (η = 0.71 mPa·s), ethanol (η = 1.1 mPa·s), 60% methanol/hexanol (η = 0.97 mPa·s), 30% methanol/hexanol (η = 1.7 mPa·s), hexanol (η = 4.6 mPa·s).

broad, structureless emission centered at around 470 nm. By comparison of Figures 2.4A and 2.4B, it is obvious that the intensity of the excimer emission of the Py-PNIPAM-3% sample is significantly stronger than that of the Py_2-PNIPAM-6K sample, even though the two polymers have similar pyrene contents. This illustrates one of the advantages of studying randomly labelled polymers; for a similar pyrene content and solvent viscosity, the randomly labelled polymers provides a significantly stronger excimer signal.

The analysis of the steady-state fluorescence spectra yields the I_E/I_M ratios for the pyrene-labelled polymers which were calculated using the procedure described in Section 2.2.7. Figure 2.5 displays plots of the I_E/I_M ratio as a function of η^{-1} for the Py-PNIPAM-6K, 8K, and 14K polymers. Figure 2.5 shows that, for the alcohols, I_E/I_M increases

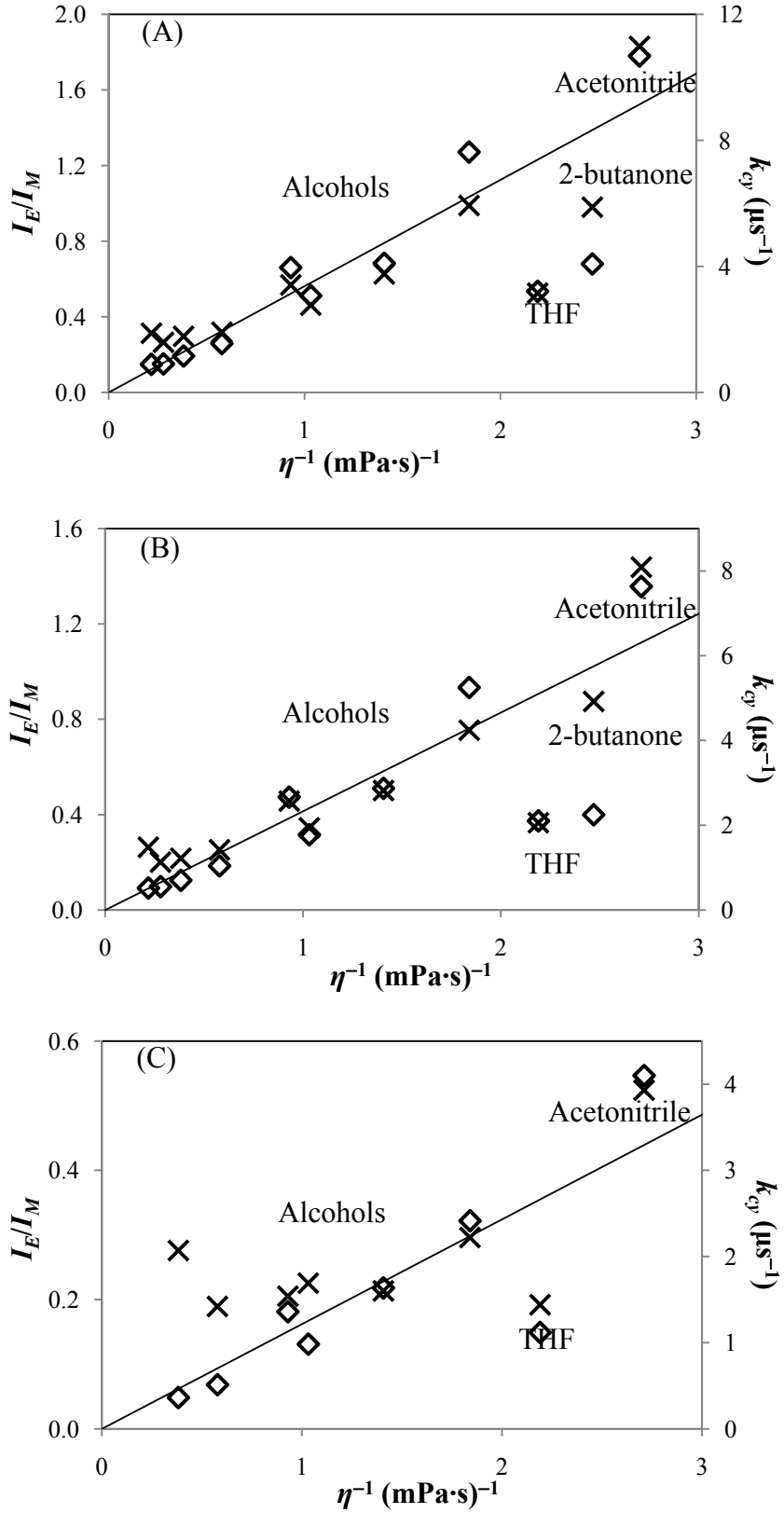

Figure 2.5: Plots of I_E/I_M (◇) and k_{cy} (×) as a function of η^{-1} for the (A) Py_2-PNIPAM-6K, (B) Py_2-PNIPAM-8K, and (C) Py_2-PNIPAM-14K samples.

linearly with decreasing viscosity. A notable difference is observed between the values measured in the alcohols (η^{-1} = 0.22 – 1.84 $mPa^{-1}\cdot s^{-1}$) versus those measured in the aprotic solvents (η^{-1} = 2.2 – 2.7 $mPa^{-1}\cdot s^{-1}$).

Apart from the point in acetonitrile (η^{-1} = 2.7 $mPa^{-1}\cdot s^{-1}$), the two remaining aprotic solvents studied, namely THF and 2-butanone, both give I_E/I_M ratios which are lower than expected. Differences in pyrene fluorescence between alcohols and aprotic solvents is not new and has been observed in the past but the underlying cause of this effect is not known.[27,28]

Previous studies[3,8] have measured the I_E/I_M ratio of end-labelled polymers as functions of viscosity (η) or molecular weight ($\overline{M}_n$). These studies have shown that the I_E/I_M ratio scales as $\eta^{\alpha} M_n^{\beta}$ where α and β have been found to equal –1.0 and –1.6 for poly(bisphenol A-diethylene glycol carbonate),[8] and β has been found to equal 1.62 for polystyrene.[3] According to these findings, $\ln(I_E/I_M)$ should be well described by Equation 2.42

$$\ln\left(\frac{I_E}{I_M}\right) = \ln A + \alpha \ln \eta + \beta \ln \overline{M}_n \tag{2.42}$$

where A represents a proportionality constant. For the Py_2-PNIPAM-Y samples in the alcohols used in this study, $\ln A$, α, and β have been found to equal 12.1 ± 0.5, –1.09 ±

0.06, and -1.72 ± 0.05, respectively, which are in good agreement with previously obtained values.[3,8] The error on the parameters $\ln A$, α, and β were estimated by using the average and standard deviation values for these 30 data points (ignoring the data for the Py_2-PNIPAM-25K sample) to generate 1000 sets of 30 data points that were normally distributed around their average value. Each set out of the 1000 data points was then analyzed to give a 1000 sets of $\ln A$, α, and β values. The standard deviations of these 1000 $\ln A$, α, and β values were taken to be the error for each parameter. Figure 2.6 represents a plot of $\ln(I_E/I_M)$ as a function of viscosity and chain length for the Py_2-PNIPAM-Y samples in the alcoholic solvents and mixtures listed in Table 2.3, according to Equation 2.42. In Figure 2.6, the I_E/I_M ratios for the Py_2-PNIPAM-25K sample were not used in the optimization since these values deviate somewhat from the remaining samples. The reason for this discrepancy is presently unknown.

Figure 2.6 shows a good agreement between the experimentally determined scaling factors and the measured I_E/I_M ratios. Two trends can be observed. First, as viscosity increases, I_E/I_M decreases. Increasing the solvent viscosity hinders the diffusional motion of the polymer. Decreased diffusional motion leads to fewer cyclization events, reducing excimer formation and consequently, the I_E/I_M ratio. Second, as chain length increases, I_E/I_M decreases. A longer chain means that the pyrene units are situated further from each other, resulting in reduced excimer formation.

The I_E/I_M ratios for the Py-PNIPAM-X% samples were also measured and they are plotted as a function of the uncorrected pyrene content in Figure 2.7. Interestingly, Figure 2.7 seems to show an onset pyrene content of around 2 mol%. Below this pyrene content, no

excimer is formed. Only once the onset content of 2 mol% is reached does excimer start to be formed and I_E/I_M increases linearly with increasing pyrene content.

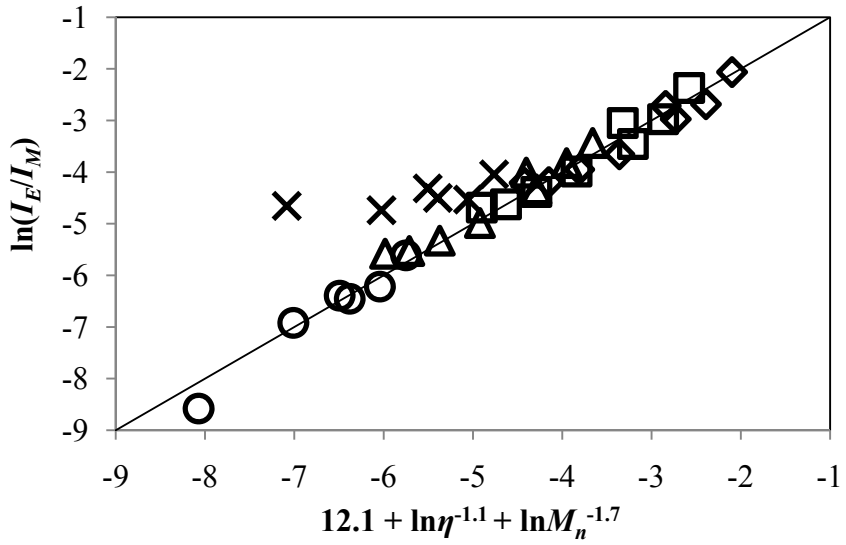

Figure 2.6: Plot of $\ln(I_E/I_M)$ as a function of viscosity and chain length according to Equation 2.42 for the Py_2-PNIPAM-6K (◇), Py_2-PNIPAM-8K (□), Py_2-PNIPAM-14K (△), Py_2-PNIPAM-25K (×), and Py_2-PNIPAM-45K (○) samples.

Next, the fluorescence decays of the Py_2-PNIPAM-Y and Py-PNIPAM-X% samples were acquired using the Time-Correlated Single Photon Counting (TC-SPC) technique (Section 2.2.8). Sample monomer and excimer decays for the Py_2-PNIPAM-6K and Py-PNIPAM-3% samples in the alcohols studied are shown in Figure 2.8. The decays of the Py_2-PNIPAM-6K, 8K, and 14K samples were analyzed with the Birks Scheme (Section 2.3.1). The results of the fits are presented in Tables A1 – A6 of Appendix A. Except for the Py_2-PNIPAM-14K sample run in viscous hexanol that yielded little excimer, all fits were excellent with residuals and autocorrelation function of the residuals randomly distributed around zero and χ^2 values smaller than 1.2.

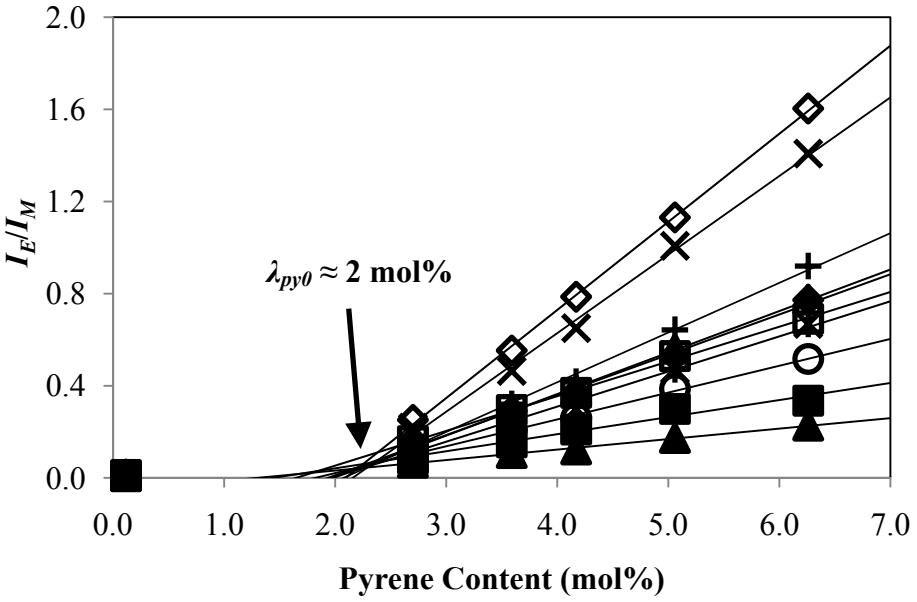

Figure 2.7: Plot of I_E/I_M as a function of pyrene content for the Py-PNIPAM-X% samples in acetonitrile (◇), 2-butanone (□), ethyl acetate (△), tetrahydrofuran (O), methanol (×), 80% methanol/hexanol (+), 60% methanol/hexanol (∗), ethanol (◆), 30% methanol/hexanol (■), and hexanol (▲).

The trends obtained so far are well described by a relationship between I_E/I_M and k_{cy} established 30 years ago by Cuniberti and Perico. They showed that, at temperatures less than 30 ºC where excimer dissociation can be neglected, the I_E/I_M ratio is given by Equation 2.43

$$\frac{I_E}{I_M} = \kappa \frac{\varphi_E^0}{\varphi_M^0} \tau_M k_1 [Py]_{loc} \tag{2.43}$$

κ, and the solvent viscosity, φ_M^0 and φ_E^0 are the fluorescence quantum yields of, respectively, the pyrene monomer and excimer, τ_M is the natural lifetime of the monomer, and $[Py]_{loc}$

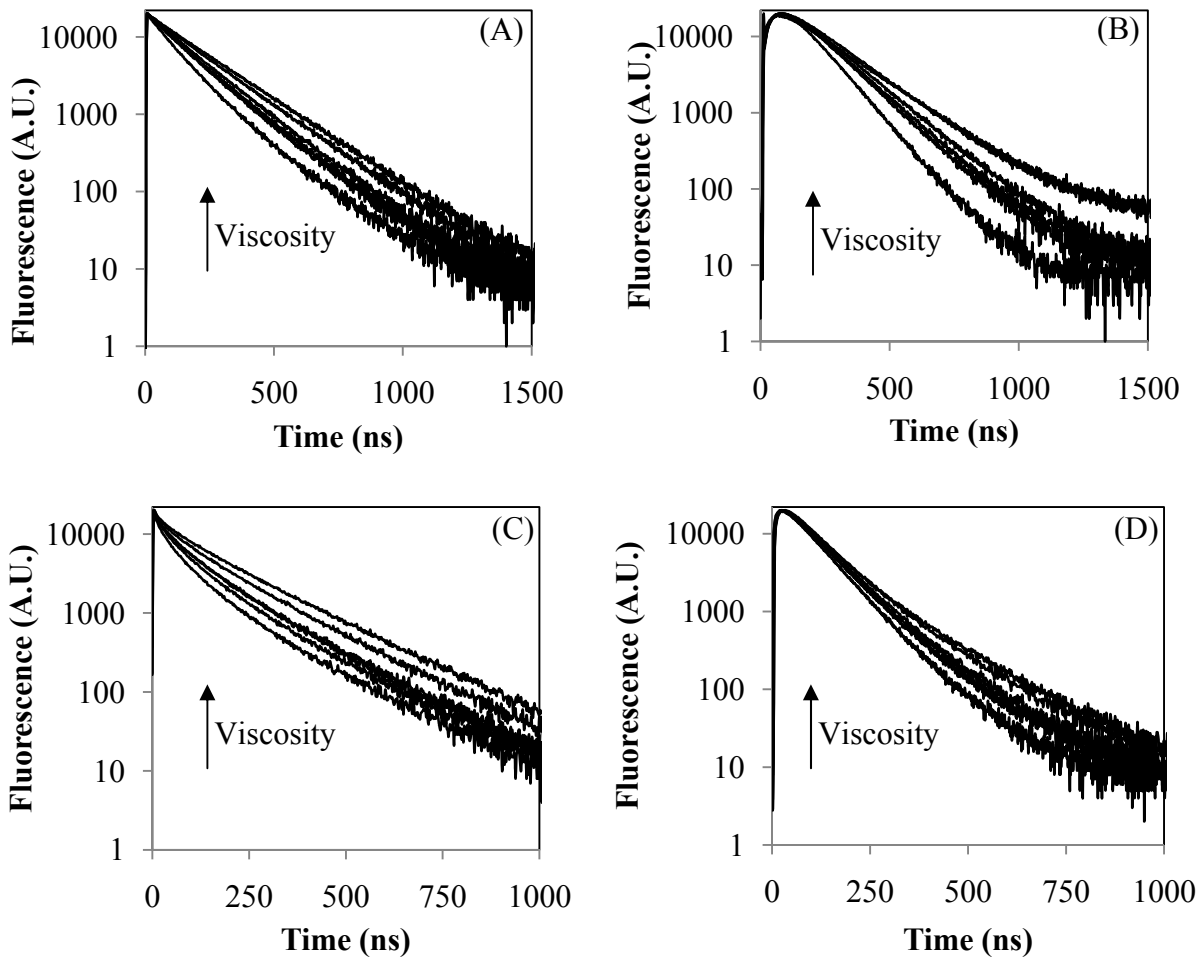

Figure 2.8: Fluorescence decays of pyrene end-labelled and randomly labelled PNIPAM, λ_{ex} = 344 nm. A) Py_2-PNIPAM-6K, λ_{em} = 375 nm. B) Py_2-PNIPAM-6K, λ_{em} = 510 nm. C) Py-PNIPAM-3%, λ_{em} = 375 nm. D) Py-PNIPAM-3%, λ_{em} = 510 nm. Top to bottom: Hexanol (η = 4.6 mPa·s), 30% methanol/hexanol (η = 1.7 mPa·s), ethanol (η = 1.1 mPa·s), 60% methanol/hexanol (η = 0.97 mPa·s), 80% methanol/hexanol (η = 0.71 mPa·s) and methanol (η = 0.55 mPa·s)

represents the local concentration of ground-state pyrene units in the polymer coil.[2] It is worth recalling that the parameter k_{cy} obtained from the Birks Scheme analysis of the fluorescence decays of the Py_2-PNIPAM-Y samples represents a pseudo-unimolecular rate constant describing cyclization which is equivalent to $k_1[Py]_{loc}$ in Equation 2.43. Therefore, the I_E/I_M ratios obtained from the steady-state spectra and the k_{cy} values obtained from the

Birks Scheme analysis of the fluorescence decays of the Py_2-PNIPAM-6K, 8K, and 14K polymers are proportional and should show similar trends. These values are plotted in Figure 2.5 as a function of viscosity for each chain length. A remarkable correlation is seen between I_E/I_M and k_{cy} for each end-labelled polymer except for Py_2-PNIPAM-14K in high viscosity solvents where the small amount of excimer formed complicated the analysis of the decays. In particular, it can be seen from Figure 2.5 that as viscosity increases, I_E/I_M and k_{cy} both decrease linearly in the alcohol solvents and mixtures. Increasing viscosity reduces the ability of the polymer chain ends to diffuse in the solution, resulting in a decrease in the frequency of cyclization events and consequently a decrease in I_E/I_M and k_{cy}.

In addition to comparing k_{cy} with the I_E/I_M ratios obtained for each Py_2-PNIPAM-Y polymer, the k_{cy} values obtained for each chain length in a specific solvent can also be compared with each other. Since k_{cy} is inversely proportional to the chain length, *N*, taking the product $k_{cy} \times N$ should eliminate the dependency of k_{cy} on chain length, and the resulting products for each polymer should be the same for a given solvent. Figure 2.9 shows a plot of $k_{cy} \times N$ as a function of η^{-1} for the end-labelled polymers. Ignoring the points for the Py_2-PNIPAM-25K polymer in hexanol and in the 30% methanol/hexanol mixture whose fluorescence decays could not be analyzed using the Birks Scheme due to minimal excimer signal, the 3 sets of data remain equivalent within experimental error. Taking the average of all k_{cy} values for a given solvent yields $< k_{cy} \times N >$, the average rate constant of cyclization of pyrene end-labelled PNIPAM in that solvent with chain length dependencies eliminated.

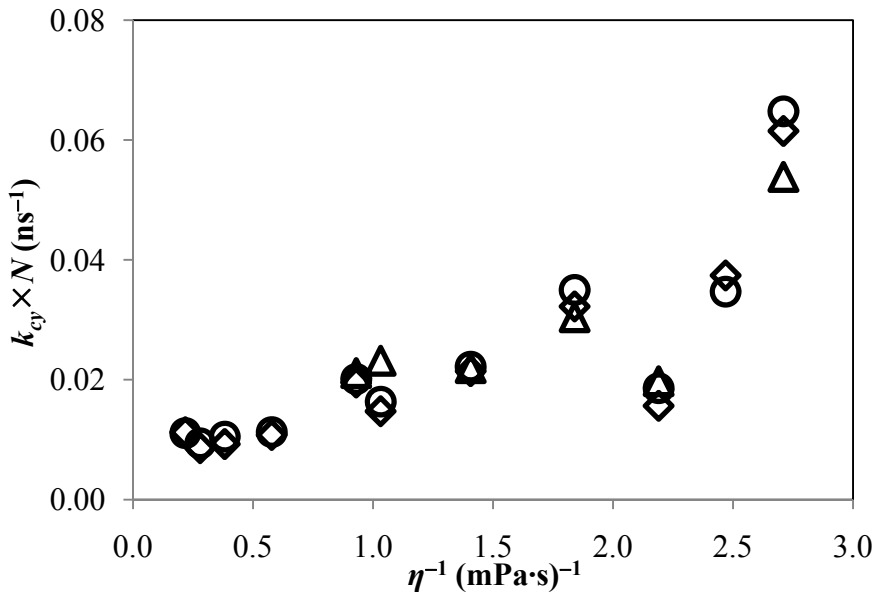

Figure 2.9: Plot of $k_{cy} \times N$ as a function of η^{-1} for the Py2-PNIPAM-Y samples.

A previous study on pyrene end-labelled poly(ethylene oxide) (PEO) demonstrated that , at high viscosity and molecular weight, k_{cy} remained constant. After a certain point, k_{cy} obeyed a scaling law similar to that observed for I_E / I_M . This scaling law is expressed in Equation 2.44.

$$\ln\left(k_{cy}\right) = \ln A + \alpha \ln \eta + \beta \ln \overline{M}_n \tag{2.44}$$

For a series of pyrene end-labelled PEO, α and β were found to equal −1.0 and −1.3, respectively.[29] As shown in Figure 2.10, the exact same behaviour was observed for the Py_2-PNIPAM-Y samples. Before the observed break point, $\ln\left(k_{cy}\right)$ remained constant within experimental error. After the breakpoint, $\ln\left(k_{cy}\right)$ obeyed Equation 2.44 where $\ln A$, α , and

β were found to equal 3 ± 1, –0.8 ± 0.1 and –1.0 ± 0.2, respectively. These exponents are smaller than those obtained for PEO.

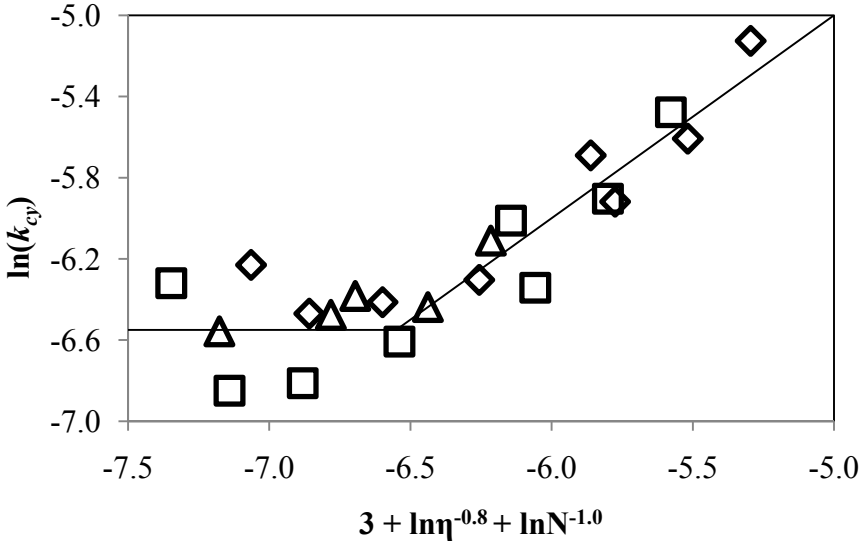

Figure 2.10: Plot of ln(k_{cy}) as a function of viscosity and chain length according to Equation 2.44 for the Py_2-PNIPAM-6K (◇), Py_2-PNIPAM-8K, (□), and Py_2-PNIPAM-14K (△) polymers.

The Py_2-PNIPAM-25K and 45K samples did not generate enough excimer signal in order to acquire the excimer decays. For these samples, only monomer decays were acquired and these were fit using a sum of two exponentials. The results of these fits are listed in Tables A7 and A8 of Appendix A. The monomer decays consisted of a shorter lifetime with a contribution of 3 – 14% of the overall decays as well as a longer lifetime with a contribution between 86 and 97% of the overall decays. In most cases, the longer lifetime matched the natural lifetime of the monomer, implying that the majority of the fluorescence signal was due to pyrene units which do not form excimer.

Finally, the fluorescence decays of the Py-PNIPAM-X% samples were fit using the Fluorescence Blob Model (FBM, see Section 2.3.3). In the analysis, the monomer lifetime

τ_M was fixed and was determined by acquiring the fluorescence decays of the Py-PNIPAM-0.1% sample, fitting the decay using a sum of two exponentials, and taking the long decaytime as the monomer lifetime. The short lifetime τ_S was determined by letting it float in a first analysis, averaging the values obtained for each pyrene content, and then fixing τ_S to its average value in a subsequent analysis.

The results of the FBM analysis are listed in Tables B1- B20 of Appendix B. Figures 2.11 – 2.14 represent plots of the parameters $k_e[blob]$, k_{blob}, N_{blob}, and $k_{blob} \times N_{blob}$ as functions of the corrected pyrene content, $\lambda_{Py} / (1 - f_{Mfree})$. The factor $(1 - f_{Mfree})$ serves as a correction factor to account for those pyrene units which are isolated, do not form excimer, and do not follow the FBM.[26] All of the parameters plotted in Figure 2.11 show substantial scatter. The scatter is believed to be a result of the long and flexible butyl linker used to label pyrene onto the polymer. Its main effect is to de-correlate the motion of the pyrene label from that of the backbone which requires the introduction of the additional parameter k_2 in the analysis of the decay. This was not the case with pyrenemethyl derivatives used in earlier work whose shorter linker ensures that their motion is more tightly correlated to that of the backbone.[13-16]

Despite this complication, the product $k_{blob} \times N_{blob}$ appears to take advantage of a cancellation of errors between the individual parameters k_{blob} and N_{blob} that results from the analysis and yields usually trends that show much less scatter.[27] This is indeed observed in Figure 2.14 where, except for the data obtained with Py-PNIPAM-2% which are close to the

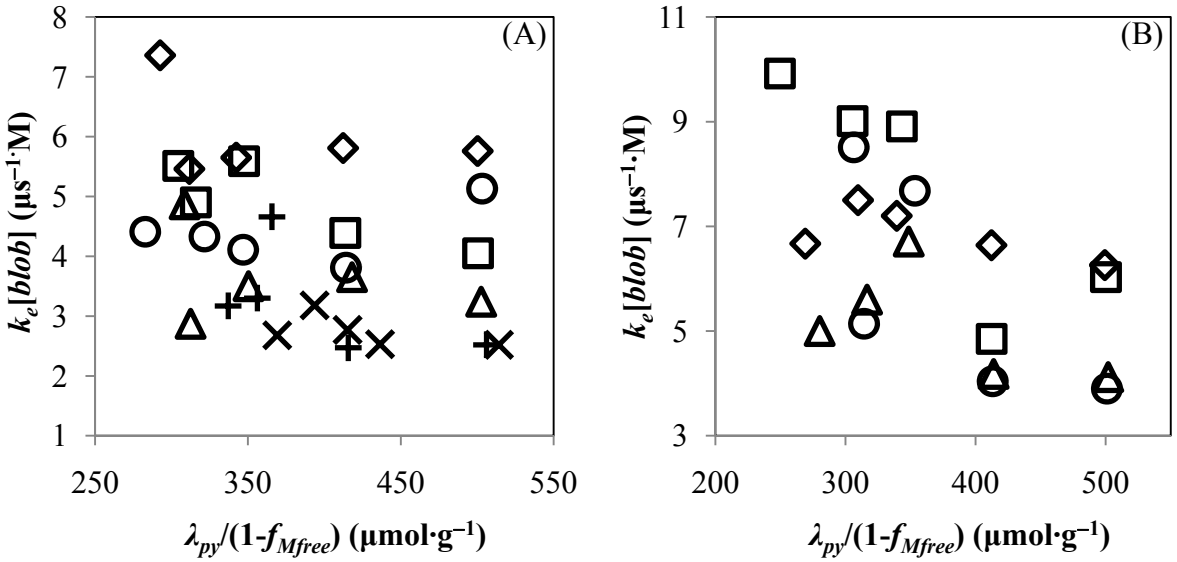

Figure 2.11: Plot of $k_e[blob]$ as a function of corrected pyrene content. A) Alcohols, methanol (◇), 80% methanol in hexanol (□), 60% methanol in hexanol (△), ethanol (○), 30% methanol in hexanol (+), and hexanol (×). B) Aprotic solvents, acetonitrile (◇), 2-butanone (□), ethyl acetate (△), tetrahydrofuran (○).

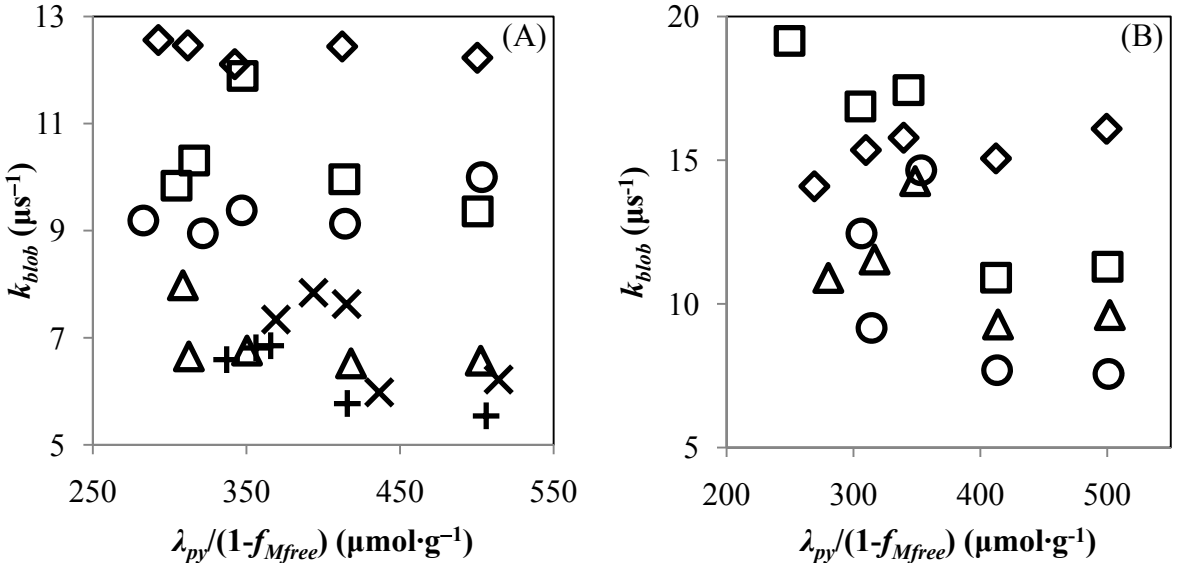

Figure 2.12: Plot of k_{blob} as a function of corrected pyrene content. A) Alcohols, methanol (◇), 80% methanol in hexanol (□), 60% methanol in hexanol (△), ethanol (○), 30% methanol in hexanol (+), and hexanol (×). B) Aprotic solvents, acetonitrile (◇), 2-butanone (□), ethyl acetate (△), tetrahydrofuran (○).

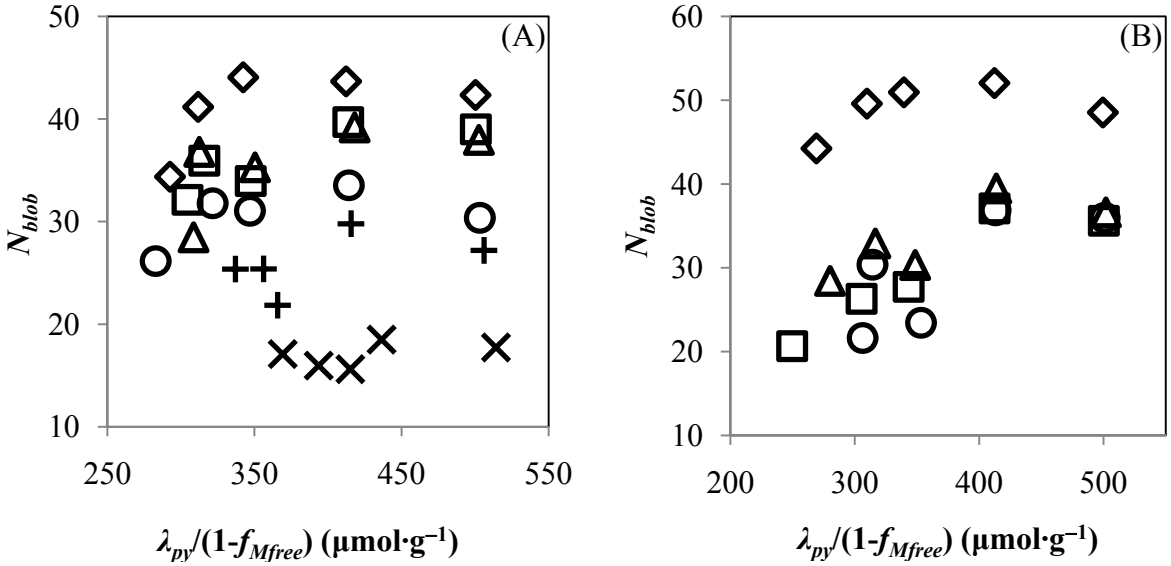

Figure 2.13: Plot of N_{blob} as a function of corrected pyrene content. A) Alcohols, methanol (◇), 80% methanol in hexanol (□), 60% methanol in hexanol (△), ethanol (○), 30% methanol in hexanol (+), and hexanol (×). B) Aprotic solvents, acetonitrile (◇), 2-butanone (□), ethyl acetate (△), tetrahydrofuran (○).

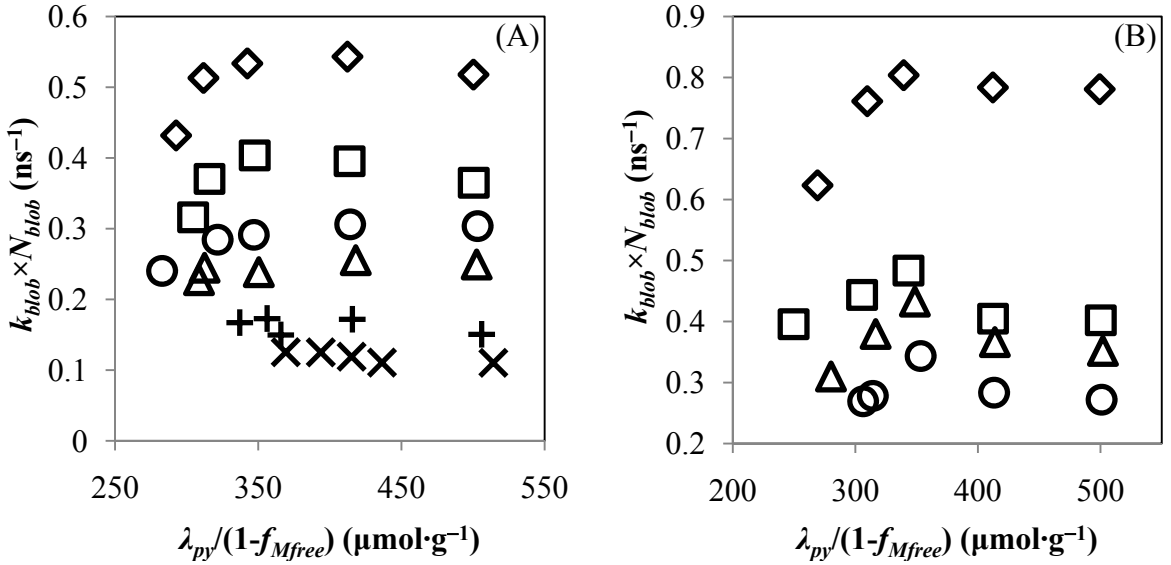

Figure 2.14: Plot of $k_{blob}\times N_{blob}$ as a function of corrected pyrene content. A) Alcohols, methanol (◇), 80% methanol in hexanol (□), 60% methanol in hexanol (△), ethanol (○), 30% methanol in hexanol (+), and hexanol (×). B) Aprotic solvents, acetonitrile (◇), 2-butanone (□), ethyl acetate (△), tetrahydrofuran (○).

transition point found in Figure 2.7, constant trends of $k_{blob} \times N_{blob}$ are obtained as a function of pyrene content in both protic and aprotic solvents. Ignoring the values retrieved for the Py-PNIPAM-2% sample, the remaining values were averaged to yield the average exchange rate constant, $<k_e[blob]>$, blob size, $< N_{blob} >$, and product, $< k_{blob} \times N_{blob} >$.

Figure 2.15 illustrates plots of $<k_e[blob]>$ and $< N_{blob} >$ as functions of η^{-1}, illustrating the dependence of these two parameters on viscosity. The exchange rate constant is found to increase with decreasing viscosity. At a lower viscosity, diffusional motion is enhanced, resulting in greater exchange of ground-state pyrene units between blobs. $< N_{blob} >$ is also observed to increase with decreasing viscosity since a lower viscosity allows for a greater volume being probed during the lifetime of pyrene.

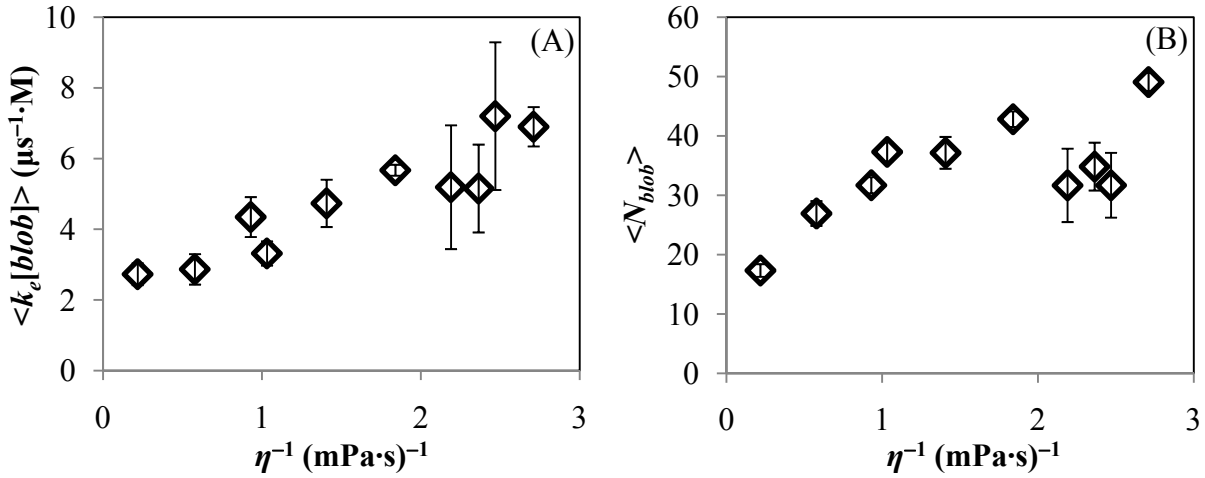

Figure 2.15: Plots of (A) $<k_e[blob]>$ and (B) $<N_{blob}>$ as functions of η^{-1}.

The product $< k_{blob} \times N_{blob} >$ is plotted in Figure 2.16 as a function of η^{-1} together with the normalized $< k_{cy} \times N >$ values obtained for the end-labelled polymers. When the data obtained in the aprotic solvents and for Py_2-PNIPAM-14K in the two most viscous

solvents are eliminated, Figure 2.16 shows that both $< k_{blob} \times N_{blob} >$ and $< k_{cy} \times N >$ increase linearly with η^{-1} in the alcohols. The deviation observed for I_E / I_M and $< k_{cy} \times N >$ in the remaining aprotic solvents (ignoring acetonitrile as a possible outlier) is once again observed for $< k_{blob} \times N_{blob} >$ whose values are significantly lower than the $< k_{blob} \times N_{blob} >$ values measured in the alcohols. A linear relationship between $< k_{blob} \times N_{blob} >$ and η^{-1} is expected once more viscous aprotic solvents are included in the study. Ignoring these differences, it is obvious from Figure 2.16 that both $< k_{blob} \times N_{blob} >$ and $< k_{cy} \times N >$ show similar trends, even when specific solvent effects are encountered.[27,28] This result confirms that the two parameters provide the same quantitative information regarding the chain dynamics of PNIPAM in organic solvents extending a conclusion that was previously limited to polystyrene only.[16]

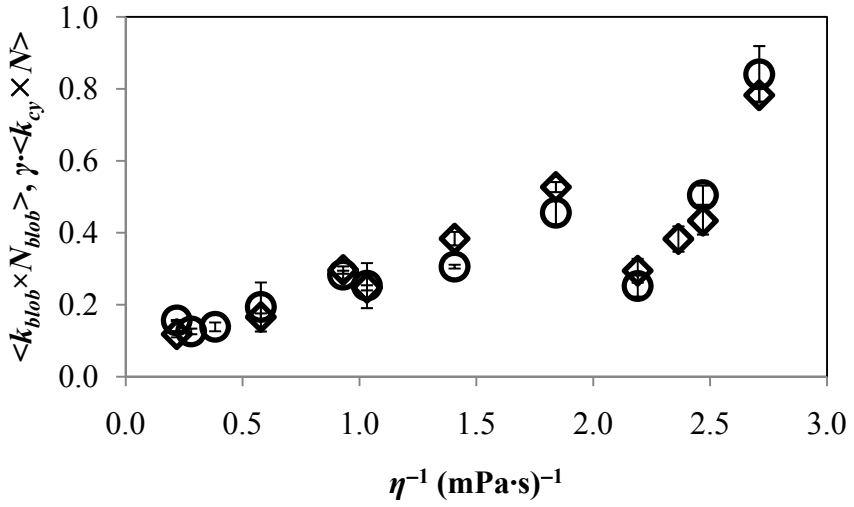

Figure 2.16: Plot of $<k_{blob} \times N_{blob}>$ (◇) and $\gamma \cdot <k_{cy} \times N>$ (○) as functions of η^{-1} where γ equals 14.

The results obtained for PNIPAM can also be compared with values previously obtained for PS.[26] $< N_{blob} >$ and $< k_{blob} \times N_{blob} >$ are plotted in Figure 2.17 for both PNIPAM and PS as a function of η^{-1}. According to Figure 2.16, both $< N_{blob} >$ and $< k_{blob} \times N_{blob} >$ are quite similar for PS and PNIPAM, although they take slightly larger values for PS than for PNIPAM. These results suggest that the PS backbone is slightly more flexible than that of PNIPAM. This conclusion can be drawn since a more flexible backbone would result in a larger volume probed by pyrene during its natural lifetime as well as a larger average rate constant of excimer formation, as observed for PS. Another quantity that can be used to measure the flexibility of a polymer chain is the characteristic ratio, C_∞.[30] C_∞ for PS in cyclohexane at 34.5 ºC and PNIPAM in THF at 25 ºC have been reported to be 10.2 and 10.6, respectively.[31] The comparable C_∞ values found for PS and PNIPAM is reflected by the results obtained for N_{blob}^0 and $< k_{blob} \times N_{blob} >$, as shown in Figure 2.17.

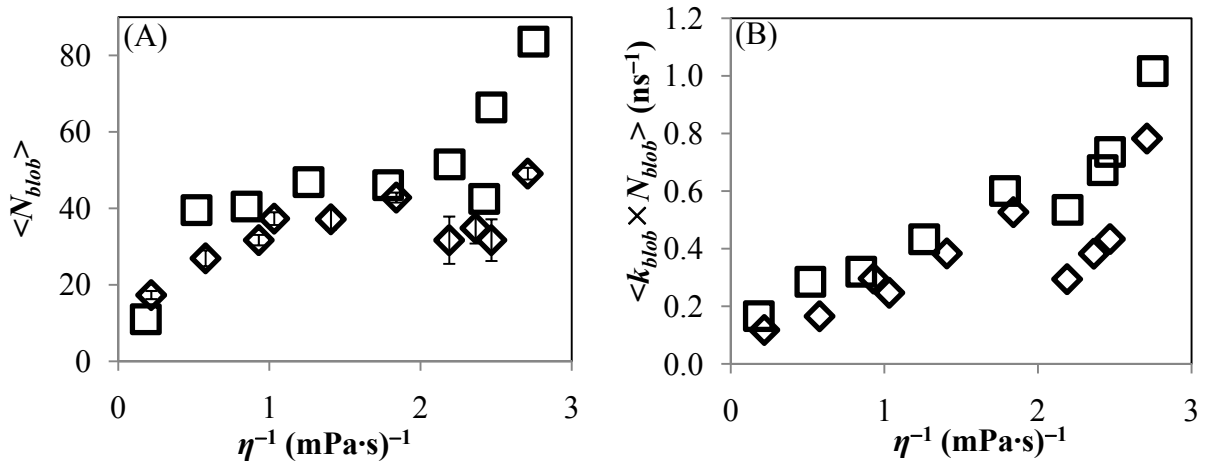

Figure 2.17: Plot of (A) $<N_{blob}>$ and (B) $<k_{blob} \times N_{blob}>$ versus η^{-1} for PNIPAM (◇) and PS (□).

2.5 Conclusions

The fluorescence results obtained thus far for the Py_2-PNIPAM-6K, 8K, and 14K polymers are in good agreement with those previously obtained for other pyrene end-labelled polymers.[3,8,13-17,26,29] Excimer formation was observed to be enhanced with decreasing viscosity and decreasing chain length. For the Py_2-PNIPAM-6K, 8K, and 14K samples, I_E/I_M and k_{cy} were found to scale as $\eta^{-1.1}\overline{M}_n^{-1.7}$ (Figure 2.6) and $\eta^{-0.8}\overline{M}_n^{-1.0}$ (Figure 2.10), respectively, which are in good agreement with previously reported values.[3,8,29] These experiments agree with the relationship derived by Cuniberti and Perico given by Equation 2.43.[2] Furthermore, the quantity $< k_{cy} \times N >$ was found to increase linearly with decreasing viscosity (Figure 2.9).

For the Py-PNIPAM-X% samples, the I_E/I_M ratios were also found to increase with decreasing viscosity and increasing pyrene content. Analysis of the fluorescence decays of the Py-PNIPAM-X% samples yielded the parameters k_{blob} and N_{blob}. Except for the Py-PNIPAM-2% sample, k_{blob}, N_{blob}, and $k_{blob} \times N_{blob}$ remained relatively constant with increasing pyrene content. Excluding the Py-PNIPAM-2% sample, the N_{blob} and $k_{blob} \times N_{blob}$ values were averaged over the various pyrene contents to yield $< N_{blob} >$ and $< k_{blob} \times N_{blob} >$, the average blob size and rate constant of excimer formation, respectively. Both $< N_{blob} >$ and $< k_{blob} \times N_{blob} >$ were found to increase linearly with η^{-1} (Figures 2.15B and 2.16), reflecting that, as the viscosity decreased, an excited pyrene probed a larger volume of space and that excimer formation was enhanced, respectively. When compared with the results obtained for pyrene-labelled polystyrene (PS, Figure 2.17), $< N_{blob} >$ and

$< k_{blob} \times N_{blob} >$ obtained for PNIPAM were found to be similar to the values found for PS, suggesting that both polymers exhibit a similar flexibility, as suggested from their C_∞ ratios.

Finally, the products $< k_{blob} \times N_{blob} >$ and $< k_{cy} \times N >$ obtained by analysing the fluorescence decays of Py-PNIPAM-X% with the FBM and those of Py_2-PNIPAM-Y with the Birks Scheme showed very similar trends (Figure 2.16). Both $< k_{blob} \times N_{blob} >$ and $< k_{cy} \times N >$ increase linearly with η^{-1}, with both parameters showing similar differences between the alcohols and the aprotic solvents studied. It can be concluded that the information obtained from the FBM analysis of the fluorescence decays of randomly labelled PNIPAM provides the same quantitative information describing the polymer chain dynamics as that obtained from the Birks Scheme analysis of the fluorescence decays of end-labelled PNIPAM.

Chapter 3: Fluorescence Studies of a Series of Monodisperse Telechelic α,ω-Dipyrenyl-Poly(*N*-isopropylacrylamide)s in Ethanol and in Water

3.1 Introduction

Some 35 years ago, studies of the end-to-end cyclization of polymer chains were of considerable interest, since they shed light onto fundamental aspects of processes such as the synthesis of cyclic polymers, the cyclization of DNA, and the dynamics of chains in solution. An important breakthrough was achieved in the early 1980's when theoretical predictions[1,2] and experimental observations[3,4] indicated that the end-to-end cyclization process can be probed by two pyrenyl moieties covalently attached onto the ends of a monodisperse polymer and is described under these conditions by a single rate constant (k_{cy}). The experiment is straightforward: one pyrene chromophore is excited and its emission is monitored as it encounters a ground-state pyrene to form an excimer.[5] The extreme sensitivity of fluorescence allows one to conduct such experiments with solutions of concentrations usually low enough to ensure that no intermolecular interactions take place, so that the fluorescence signal being detected reports solely on processes that occur intramolecularly.[6-18] The rate constant of excimer formation is a measure of k_{cy}, which in turn provides information about the long-range polymer chain dynamics and as such, is a measure of the flexibility of a given chain.

The most complete set of information about the rate constant k_{cy} has been obtained for a series of pyrene-labelled monodisperse polystyrenes which were synthesized by anionic polymerization.[6] Other backbones which have been investigated include

polytetrahydrofuran,[7] polydimethylsiloxane,[8-10] poly(ε–caprolactone),[11] polycarbonates,[12,133] and poly(ethylene oxide) (PEO).[14-18] The latter studies stand out as PEO is the only polymer in the list that is soluble in organic solvents and also in water. Since the pyrene label is soluble in organic solvents, its presence at the ends of the chain does not affect significantly the properties of the polymer in organic solvents, and, consequently, Py_2-PEO displays the typical kinetics expected for excimer formation via the diffusive encounters of two pyrenyl moieties in organic solvents.[14-18] Pyrene groups, however, are poorly soluble in water and their incorporation on PEO chain ends has profound effects on the properties of the polymer and on the kinetics of end-to-end cyclization. The photophysical properties of pyrene are also affected by its confinement in an aqueous environment.[16, 18-22] For instance; a substantial fraction of the excimer is formed instantaneously through direct excitation of ground-state pyrene aggregates, which are stabilized by the water-soluble PEO backbone. Nonetheless, given that end-to-end cyclization is described by a single rate constant, it has been possible to derive kinetic models that follow relatively well the process of excimer formation in aqueous solutions of Py_2-PEO and also account for the presence of pyrene ground-state dimers.[16,18-23]

Our research interests have focused on poly(*N*-isopropylacrylamide) (PNIPAM), which, like PEO, is a non-ionic polymer soluble in organic solvents and in water at room temperature. The two polymers share a number of properties, and have often been compared with regard to their interactions with surfactants[24,25] and with proteins.[25] But, in some important thermal and conformational properties, they markedly differ from each other. For instance, the lower critical solution temperatures (LCST) of aqueous PEO solutions shows a strong molecular-weight dependence, while that of PNIPAM is almost independent of the molecular weight, exhibiting very flat cloud point lines. Also, PEO chains are inferred to

adopt a loose helical form (11/2 helix) from MD simulation,[26] and the size of each turn is such that it can accommodate one water molecule linked to the chain via hydrogen bonds. In contrast, PNIPAM chains in water are partially collapsed by the association of hydrophobic isopropyl groups. One may expect, therefore, differences in the end-to-end cyclization dynamics of PNIPAM and PEO in water and in organic solvents. The objective of the work reported here was to investigate the fluorescence properties of α,ω-dipyrenyl-PNIPAM in ethanol and in water in order to assess the cyclization dynamics of PNIPAM in the two solvents and to compare them to those of PEO in the same solvents, using data reported previously for Py_2-PEO.

Recent advances in controlled radical polymerization have led to the development of synthetic protocols for the preparation of monodisperse polymers bearing reactive groups at their ends,[27] creating entries into families of polymers soluble in water and/or organic solvents carrying a fluorescent tag at one chain end, or both. Several examples can be found in the literature where PNIPAM prepared by living radical polymerization has been labelled with a pyrenyl groups at one [28-31] or both chain ends.[32] Using a procedure similar to previously reported syntheses, Py_2-PNIPAMs ranging in molecular weight ($\overline{M}_n$) from 6,000 to 45,000 g/mol were synthesized and the steady-state and time-resolved fluorescence properties of the polymers were studied in ethanol and in water. This study of the kinetics of excimer formation of monodisperse dipyrenyl end-labelled PNIPAM is the first new example, in addition to studies of Py_2-PEO that provides the opportunity to compare the photophysics of identical pyrene-tethered chains in water and an organic solvent. Conversely, it allows one to gain further insight into the properties of amphiphilic telechelic

PEOs and PNIPAMs, which have been compared and contrasted on the basis of scattering and rheology measurements that probe different length scales than the pyrene excimer.

3.2 Experimental Section

3.2.1 Materials

All chemicals were purchased from Sigma-Aldrich chemicals Co. unless otherwise specified. *N*-Isopropylacrylamide (NIPAM, 99%) was obtained from Acros Organics and recrystallized from an acetone/hexanes (4/6, v/v) mixture. Acryloyl chloride (97%), sodium bicarbonate ($NaHCO_3$, 99.5%), anhydrous sodium sulfate (Na_2SO_4, 99.0%), and triethylamine (99.5%) were used as received. Dimethyl sulfoxide (DMSO, 99.9%) was used without purification. 1,4-Dioxane and tetrahydrofuran (THF) were purified by a solvent purification system with two packed columns of activated alumina provided by Innovative Technology Inc. 4-(1-Pyrenyl)butyl iodide was synthesized as described earlier.[27] All other solvents were of reagent grade and used as received. Water was deionized (DI) using a Millipore MilliQ system. Ethanol (Fisher Scientific, HPLC grade reagent) was used as received.

3.2.2 Preparation of α,ω-Dipyrenyl Poly(*N*-isopropylacrylamide)

The polymer was prepared by a two-step end group transformation procedure, starting from a precursor telechelic polymer, α,ω-diisobutylsulfanylthiocarbonylsulfanyl poly(*N*-isopropylacrylamide) (iBS_2-PNIPAM)[27] prepared according to a previously reported procedure (Figure 3.1).[32] In a first step, the precursor polymer, iBS_2-PNIPAM was aminolysed by n-butylamine (10-fold molar excess with respect to the thiocarbonylthio

moiety) in THF to generate α,ω-dimercapto PNIPAM (HS_2-PNIPAM). In a second step, HS_2-PNIPAM was reacted with 4-(1-pyrenyl)butyl iodide (1.5-fold molar excess with respect to the mercapto (SH) groups) in DMF to yield the targeted polymer. This nucleophilic substitution reaction was catalyzed with potassium carbonate (K_2CO_3) and a small amount of the reducing agent triphenylphosphine (TPP) was added to prevent the formation of disulfide linkages between polymer chain ends. The polymer in DMF was first recovered by precipitation in diethyl ether. It was purified by two consecutive precipitations from THF to diethyl ether.

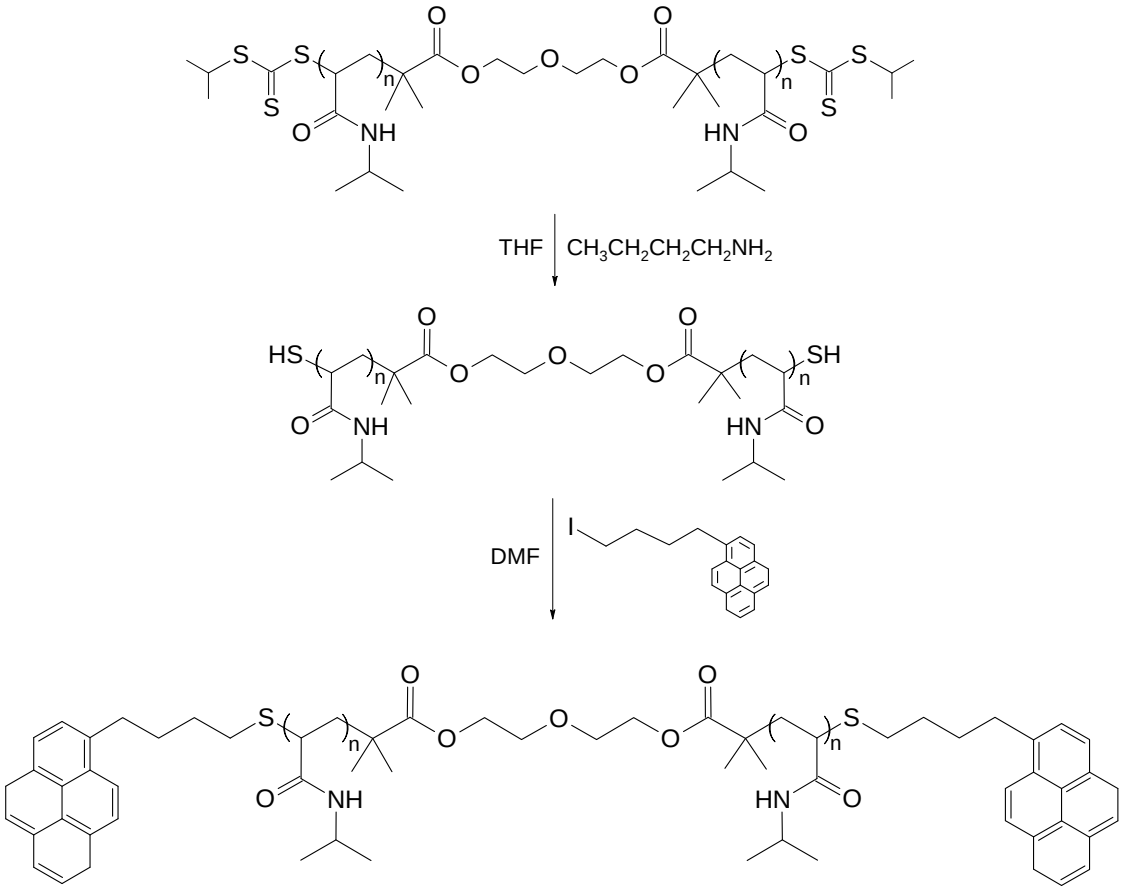

Figure 3.1: Synthetic scheme of telechelic α, ω-dipyrene poly(*N*-isopropylacrylamide).

3.2.3 Determination of Pyrene End-Functionality

The pyrene end-functionality was evaluated by UV−visible absorption spectroscopy. First, the isobutylsulfanylthiocarbonylsulfanyl moiety (iBS) content of the corresponding precursor polymers (iBS-PNIPAM) was determined for solutions of the polymer in chloroform, using the absorbance at 310 nm. A solution of diethylene glycol di(2-(1-isobutyl)sulfanylthiocarbonylsulfanyl-2-methyl propionate) in chloroform was used as the standard (ε_{310} = 28,600 $M^{-1}cm^{-1}$). Second, the pyrene content of Py_2-PNIPAM was determined for solutions of the polymer in methanol, using the absorbance of the pyrenyl chromophore at 342 nm where iBS moieties do not absorb. The molar extinction coefficient of the pyrenyl group in methanol was approximated by using that of 4-(1-pyrenyl)butanol (PyBuOH) in methanol (ε_{342} = 43,450 $M^{-1}cm^{-1}$). The molar extinction coefficient of PyBuOH was determined by preparing solutions of known concentration of PyBuOH in methanol and plotting their absorbance obtained with a 1 cm pathlength UV cell as a function of PyBuOH concentration. A straight line was obtained whose slope yielded the molar extinction coefficient of PyBuOH in methanol according to Beer-Lambert law. A comparison of the iBS concentration (end functionality assumed to be 100 %) and of the measured pyrene concentration gave the pyrene functionality values listed in Table 3.1.

3.2.4 Sample Preparation for Fluorescence Measurements

Since the pyrenyl pendants of the Py_2-PNIPAM samples form pyrene aggregates or dimers in aqueous solution, absorption measurements conducted in water must be carefully interpreted if they are to be used to determine polymer concentration. Indeed, it has been shown in one example that the molar absorption coefficient of a pyrenyl moiety is about 1.7 times larger when the pyrenyl unit exists as an isolated monomer compared to when it is part of a ground-

Table 3.1: Number-average molecular weights (M_n) and polydispersity indices (*PDI*) of the Py_2-PNIPAM samples.

Samples	$\overline{M}_n$ (kg·mol^{-1})	*PDI*	Py functionality
Py_2-PNIPAM-6K	5.9	1.05	85.4%
Py_2-PNIPAM-8K	7.6	1.08	82.6%
Py_2-PNIPAM-14K	13.7	1.10	87.4%
Py_2-PNIPAM-25K	25.4	1.07	75.5%
Py_2-PNIPAM-45K	44.5	1.10	74.8%

state pyrene aggregate.[33] Taking this fact into consideration, the Py_2-PNIPAM concentrations in water were determined as follows. First, the polymer was dissolved in ethanol where no pyrene aggregates are generated. The concentration of pyrenyl pendants was determined from the molar absorption coefficient of 4-(1-pyrene)butanol in ethanol (ε_{342} = 42,600 $M^{-1}cm^{-1}$) determined in the laboratory. The Py_2-PNIPAM solution was diluted to the desired concentration of pyrenyl groups in ethanol. Then, the ethanol was evaporated off and the same volume of water was added to the dried film of Py_2-PNIPAM. This solution was placed in the fridge for 30 minutes to enhance the dissolution of the polymer which is not soluble at high temperature. Finally, the solution was stirred vigorously and allowed to warm to room temperature (23 ± 1 ^oC). Following this protocol, the pyrene concentration of the Py_2-PNIPAM solutions in water was the same as the one determined for the Py_2-PNIPAM solutions in ethanol. A pyrene concentration of 2.4×10^{-6} mol.L^{-1} was used for the

fluorescence measurements done in ethanol. All Py_2-PNIPAM solutions in ethanol were degassed by bubbling a gentle flow of nitrogen through the solution for 30 minutes before steady-state or time-resolved fluorescence measurements were conducted. Aerated aqueous solutions of Py_2-PNIPAM were used for fluorescence measurements.

3.2.5 Size Exclusion Chromatography

The size exclusion chromatography (SEC) system consisted of an Agilent 1100 isocratic pump, a set of TSK-gel α-M (particle size 13 μm, exclusion limit 1×10^7 Da for polystyrene in DMF) and a TSK-gel α-3000 (particle size 7 μm, exclusion limit 1×10^5 Da for polystyrene in DMF) (Tosoh Biosep) columns, a Dawn EOS multi-angle laser light scattering detector λ = 690 nm (Wyatt Technology Co.) and an Optilab DSP interferometric refractometer λ = 690 nm (Wyatt Technology Co.) under the following conditions: injection volume, 100 μL; flow rate, 0.5 mL/min; eluent, DMF; temperature, 40 °C. The dn/dc value of PNIPAM was determined to be 0.0738 $mL\cdot g^{-1}$ at 690 nm in DMF at 40 °C using an Optilab DSP interferometric refractometer (Wyatt Technology Corp).

3.2.6 Steady-State Fluorescence

The fluorescence spectra of the Py_2-PNIPAM samples in ethanol and water were acquired on a Photon Technology International (PTI) LS-100 steady-state fluorometer. The fluorometer is equipped with an Ushio UXL-75Xe Xenon arc lamp and a PTI 814 photomultiplier detection system. Py_2-PNIPAM solutions in ethanol and water were respectively degassed and non-degassed. The solutions were excited at 344 nm. The monomer fluorescence intensity (I_M) was obtained by taking the integral under the fluorescence spectrum from 372 to 378 nm. The fluorescence intensity of the excimer (I_E)

was determined by first normalizing the fluorescence spectrum of 4-(1-pyrene)butanol at a concentration of 2.5×10^{-6} mol·L^{-1} in ethanol and 0.6×10^{-6} mol·L^{-1} in water to the peak at 375 nm of the fluorescence spectrum of the Py_2-PNIPAM solutions. At such low concentration, 4-(1-pyrene)butanol emits as the pyrene monomer. Second, the normalized spectrum of 4-(1-pyrene)butanol was subtracted from that of the Py_2-PNIPAM solution. Third, the fluorescence intensity of the subtracted spectrum was integrated from 500 to 530 nm to yield I_E.

3.2.7 Time-Resolved Fluorescence

The fluorescence decays of the pyrene monomer and excimer of the Py_2-PNIPAM solutions were acquired on an IBH time-resolved fluorometer equipped with a nano-LED light source. The Py_2-PNIPAM solutions were prepared with a pyrene concentration of 1.2×10^{-6} mol·L^{-1}. The solutions were excited at 344 nm and the fluorescence decays were monitored at 375 nm and 510 nm for the pyrene monomer and excimer using a cut-off filter at 370 and 495 nm, respectively. A Ludox solution was used at the excitation wavelength to determine the instrument response function which was convoluted with the desired theoretical function for the decay analysis.

3.2.8 Analysis of the Fluorescence Decays

All monomer and excimer fluorescence decays were first fitted with a sum of exponentials according to Equation 3.1.

$$f(t) = \sum_{i=1}^{N} a_{Xi} \times \exp(-t / \tau_{Xi}) \quad \text{with } X = \text{M (monomer) or E (excimer)} \tag{3.1}$$

The monomer and excimer fluorescence decays acquired for the Py_2-PNIPAM solutions in ethanol were also fitted with Equations 3.2 and 3.3 which are based on the Birks scheme given in Scheme 3.1.[5]

Scheme 3.1: The Birks scheme for the formation of excimer with a pyrene end-labelled monodisperse polymer

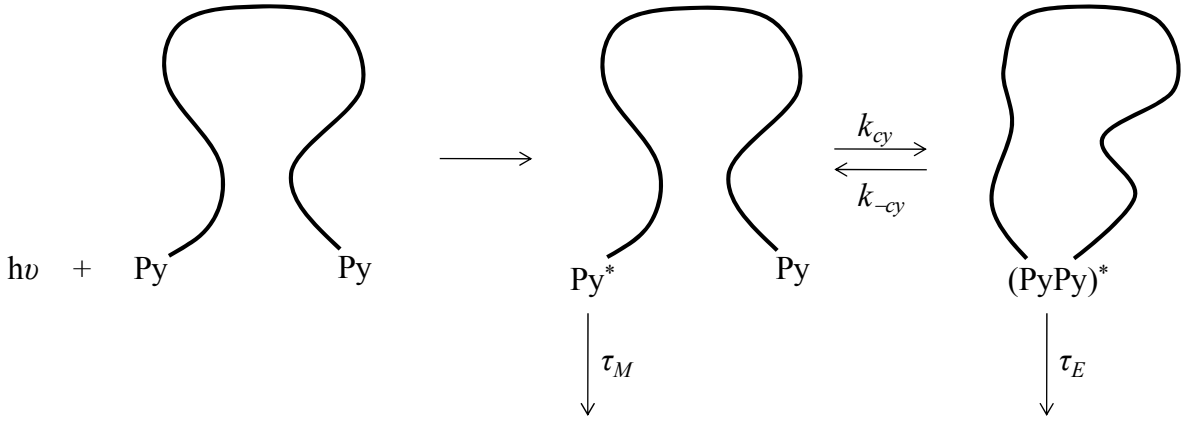

In Scheme 3.1, the parameters k_{cy}, k_{-cy}, τ_M, and τ_E represent the rate constant of excimer formation, the rate constant of excimer dissociation, the monomer lifetime, and the excimer lifetime, respectively.

$$[Py^*] = \frac{[Py^*_{diff}]_o}{\sqrt{(X-Y)^2 + 4k_{cy}k_{-cy}}} \left((X - \tau_2^{-1}) \times \exp(-t/\tau_1) - (X - \tau_1^{-1}) \times \exp(-t/\tau_2) \right) + [Py^*_{free}]_o \exp(-t/\tau_M) \tag{3.2}$$

$$[E^*]=\frac{k_{cy}[Py^*_{diff}]_o}{\sqrt{(X-Y)^2+4k_{cy}k_{-cy}}}\left(-\exp(-t/\tau_1)+\exp(-t/\tau_2)\right)+[Py^*_S]_o\exp(-t/\tau_S) \tag{3.3}$$

The parameters $X = k_{cy} + {\tau_M}^{-1}$ and $Y = k_{-cy} + {\tau_E}^{-1}$ are used in the expressions of the decay times τ_1 and τ_2 which are given in Equations 3.4 and 3.5. The initial concentrations of pyrene units that form excimers by diffusion or do not form excimers because they are attached onto monolabelled chains are represented by $[Py^*_{diff}]_o$ and $[Py^*_{free}]_o$, respectively, in Equations 3.2 and 3.3. Occasionally, a short-lived pyrene species with a decay time of 2 – 4 ns and denoted as Py^*_S is encountered when excimer formation occurs in restricted geometries such as when the pyrene pendants are confined onto a polymer.[18] The origin of this spike is discussed further in the Result and Discussion section. The monomer lifetime τ_M in ethanol was estimated to equal 220 ns by analyzing the monoexponential fluorescence decay of 4-(1-pyrene)butanol in ethanol.

$$\tau_1^{-1}=\frac{X+Y+\sqrt{(X-Y)^2+4k_{cy}k_{-cy}}}{2} \tag{3.4}$$

$$\tau_2^{-1}=\frac{X+Y-\sqrt{(X-Y)^2+4k_{cy}k_{-cy}}}{2} \tag{3.5}$$

The monomer and excimer fluorescence decays were fitted globally to ensure that the decaytimes τ_1 and τ_2 remained the same in the analysis of the monomer and excimer decays. The decay time τ_S was fixed to 2 ns in the analysis.

3.3 Results and Discussion

3.3.1 Preparation and Characterization of the Polymers

The synthesis of α,ω-dipyrenyl poly(*N*-isopropylacrylamide)s (Py_2-PNIPAM) is depicted in Figure 3.1. First, PNIPAMs of narrow size distribution bearing a trithiocarbonate group at each chain end were prepared by reversible addition-fragmentation chain transfer (RAFT) polymerization of NIPAM using a difunctional trithiocarbonate compound, i.e., diethylene glycol di(2-(1-isobutyl)sulfanylthiocarbonylsulfanyl-2-methyl propionate), as chain transfer agent.[27] The isobutyltrithiocarbonate groups were aminolyzed yielding thiol end groups, which were subjected to nucleophilic substitution using 4-(1-pyrenyl)butyl iodide in the presence of sodium carbonate. Evidence for the successful end-labelling was obtained by monitoring the UV absorption of the pyrenylbutyl pendants at 342 nm. The number average molecular weight ($\overline{M}_n$) and polydispersity index (PDI) of the polymers shown in Table 3.1 were determined by GPC analysis in DMF, a good solvent for PNIPAM and its hydrophobically-modified analogues.[32] The extent of pyrene incorporation onto the polymer chain ends (end functionality of the polymers, Table 3.1) was determined from the absorbance of the pyrenyl groups for solutions of the polymers in methanol.

3.3.2 Overview of the Solution Properties of the Polymers in Ethanol and in Water

The two solvents selected for the study have similar viscosities at 25 ^{o}C (ethanol: η = 1.07 mPa·s and water: η = 0.89 mPa·s). The intrinsic viscosity ([η]) of a commercial PNIPAM sample was determined to be 48.5 ± 0.5 and 46.6 ± 0.6 mL·g^{-1} in ethanol and water at 25 ^{o}C indicating that the dimensions (radius of gyration or end-to-end distance) of the PNIPAM polymer coil should be similar in water and ethanol. All Py_2-PNIPAM samples were soluble in ethanol, but only the Py_2-PNIPAM samples with $\overline{M}_n$ values of 14,000 g/mol or higher were soluble in water at 23 ^{o}C, the temperature of the fluorescence measurements reported here. Samples of lower molecular weight (5,900 and 7,600 g/mol), which were reluctant to dissolve in water, were used only for the studies of Py_2-PNIPAM in ethanol. Fluorescence spectra, normalized at 375 nm, of Py_2-PNIPAM samples in ethanol and in water are shown in Figures 2A and 2B, respectively. The spectra present a strong contribution from the pyrene monomer emission, with bands at 376 nm to 396 nm, as well as a weak pyrene excimer emission, with its characteristic broad emission centered at 470 nm. The excimer emission intensity decreases with increasing chain length. The contribution of excimer emission was weaker for polymers dissolved in ethanol, indicating that in water hydrophobic interactions between the pyrene end-groups tend to overcome the natural tendency of the polymer to stretch due to excluded volume effects, bringing the pyrene pendants into close contact under the form of pyrene aggregates where excimer is generated efficiently.[16,18-21]

3.3.3 Solutions of Py_2-PNIPAM Samples in Ethanol

The experiments reported below aimed at characterizing intramolecular excimer formation. If excimer is generated intramolecularly, its emission intensity, relative to the pyrene monomer intensity, should be independent on polymer concentration. Sample fluorescence emission spectra for the Py2-PNIPAM polymers in ethanol and water are shown in Figure 3.2. We established that the ratio of pyrene excimer to monomer emission intensities, I_E/I_M, was constant (= 3.1×10^{-3}) for Py_2-PNIPAM-45K solutions in ethanol ranging in concentration from 23 to 530 mg/L equivalent to a pyrene concentration of 0.32 to 25 μmol/L. The fluorescence spectra of all Py_2-PNIPAM samples in ethanol were acquired at a pyrene concentration of 2.5×10^{-6} mol·L^{-1}, a value for which excimer formation occurs exclusively between pyrene units linked to the same chain. The effect of chain length on the I_E/I_M ratio is seen in Figure 3.3 where the I_E/I_M ratios are reported as a function of $\overline{M}_n$. The slope of the log-log plot shown in Figure 3.3 equals -1.4 ± 0.2 for solutions in ethanol. This exponent is smaller than that found in Chapter 2 where the I_E/I_M ratio was found to scale as $\overline{M}_n^{-1.7}$, and this discrepancy is believed to be due to the greater accuracy obtained in the calculations performed in Chapter 2 owing to the larger amount of data obtained.

The scaling relationship $I_E/I_M \propto \overline{M}_n^{-1.4}$ found in ethanol for the Py_2-PNIPAM samples is in agreement with values expected from theoretical work conducted by Cuniberti and Perico[34,35] who proposed Equation 3.6 to estimate the I_E/I_M ratio for pyrene-labelled polymers at temperatures < 30 °C where the rate constant for excimer dissociation can be neglected with respect to τ_E^{-1}.

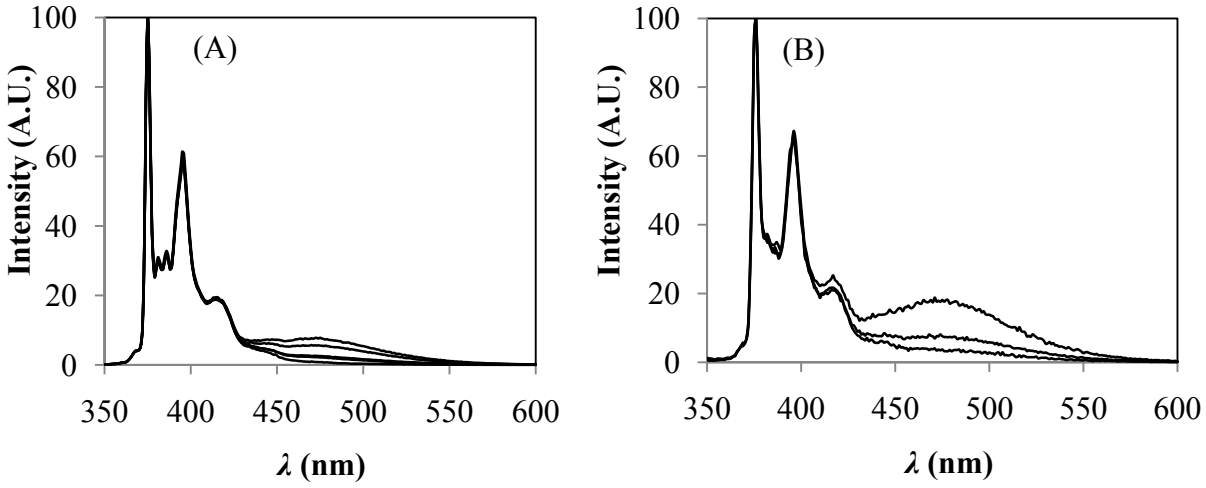

Figure 3.2: Fluorescence spectra of pyrene end-labelled PNIPAM normalized at 376 nm, λ_{ex} = 344 nm. A) [Py] = 2.5×10^{-6} mol.L^{-1} in ethanol, top to bottom: Py-PNIPAM-6k, Py-PNIPAM-8k, Py-PNIPAM-14k, Py-PNIPAM-25k, Py-PNIPAM-45k. B) [Py] = 1.25×10^{-6} mol.L^{-1} in water, top to bottom: Py-PNIPAM-14k, Py-PNIPAM-25k, Py-PNIPAM-45k.

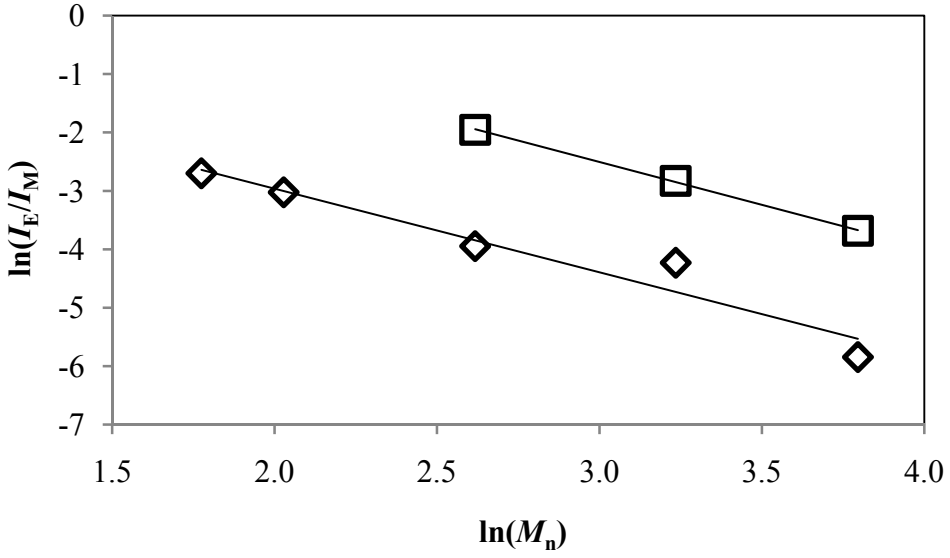

Figure 3.3: Plot of ln(I_E/I_M) versus ln(M_n) for pyrene end-labelled PNIPAM in water (□, [Py] = 1.25×10^{-6} mol·L^{-1}) and ethanol (◇, [Py] = 2.5×10^{-6} mol·L^{-1}). Ethanol: slope = −1.4 ± 0.2, Water: slope = −1.5 ± 0.1.

$$\frac{I_E}{I_M} = \kappa \frac{\phi_E^o}{\phi_M^o} \tau_M \, k_1 [Py]_{loc} \tag{3.6}$$

In Equation 3.6, κ is a constant that depends on the geometry and sensitivity of the spectrofluorometer used, k_1 is the bimolecular encounter rate constant, which for free pyrene units would equal $2\times RT/(3\times\eta)$ with R, T, and η being respectively the ideal gas constant, the absolute temperature in K, and the solvent viscosity, ϕ_M^o and ϕ_E^o are the fluorescence quantum yields of, respectively, the pyrene monomer and excimer, τ_M is the natural lifetime of the pyrene monomer, and $[Py]_{loc}$ represents the effective concentration of the unexcited chromophores in the neighborhood of the excited species. The end-to-end cyclization rate constant k_{cy} is taken as the product $k_1\times[Py]_{loc}$. Since the parameters ϕ_M^o, ϕ_E^o, κ, and τ_M are constants that do not depend on chain length, Equation 3.6 implies that the I_E/I_M ratio depends only on k_{cy} which has been shown theoretically[35,36] and experimentally[6,8,12,14] to scale with the number average degree of polymerization N as $N^{-\gamma}$, where γ has been found to take values between 0.9 and 1.9 depending on the polymer backbone and solvent. Based on the above, the I_E/I_M ratio found to scale as $N^{-1.4}$ (Figure 3.3) for the Py_2-PNIPAM samples in ethanol conforms to what is theoretically[35,36] and experimentally[6,8,12,14] expected for the intramolecular excimer formation of a pyrene end-labelled monodisperse polymer in an organic solvent.

Next, fluorescence decays for the pyrene monomer and excimer emissions were acquired for the Py_2-PNIPAM samples in ethanol in order to gain information about the dynamics of excimer formation. All time-resolved fluorescence experiments were carried out

with solutions where the pyrene concentration was 2.5×10^{-6} mol·L^{-1}. The decays recorded for the monomer and excimer emissions are shown in Figure 3.4A and 3.4B, respectively. The pyrene monomer decay rate increases with decreasing polymer chain length, reflecting the increasingly more facile excimer formation. In fact, measurable excimer formation takes place only in ethanolic solutions of Py_2-PNIPAM samples of $\overline{M}_n$ = 14,000 g/mol, or less (see Figure 3.2A), so that the excimer fluorescence decays of Py_2-PNIPAM-25K and Py_2-PNIPAM-45K in ethanol could not be acquired. The excimer fluorescence decays of the shorter chains exhibited a well-defined rise time (Figure 3.4B) confirming that excimer formation occurs by diffusive encounters of the chain ends. As the polymer chain length increases, the excimer decays more slowly in the same manner as the pyrene monomer, a consequence of the coupling that exists between the concomitant disappearance of the pyrene monomer and formation of the pyrene excimer.[5] A spike was found at the early times in the excimer decay of Py_2-PNIPAM-12K. The origin of this spike is debatable. Such a spike is usually observed for pyrene end-labelled polymers of high molecular weight or in viscous solvents when excimer formation by diffusion is not favored.[18,36] It can also be the result of some residual light scattering making its way through the detector and the monochromator despite the use of a 495 nm cut off filter, or possibly it could originate from an impurity that emits weakly and is observed only when little excimer is formed.

The monomer and excimer fluorescence decays were first fitted with a sum of exponentials (i.e. Equation 3.1) yielding the pre-exponential factors and decay times listed in Tables 3.2 and 3.3. As the chain length of the Py_2-PNIPAM sample increases, the number average lifetime ($<\tau>$) increases, eventually reaching a value close to 220 ns, the lifetime of 4-(1-pyrene)butanol in ethanol. The increase in $<\tau>$ reflects the decrease in efficiency for

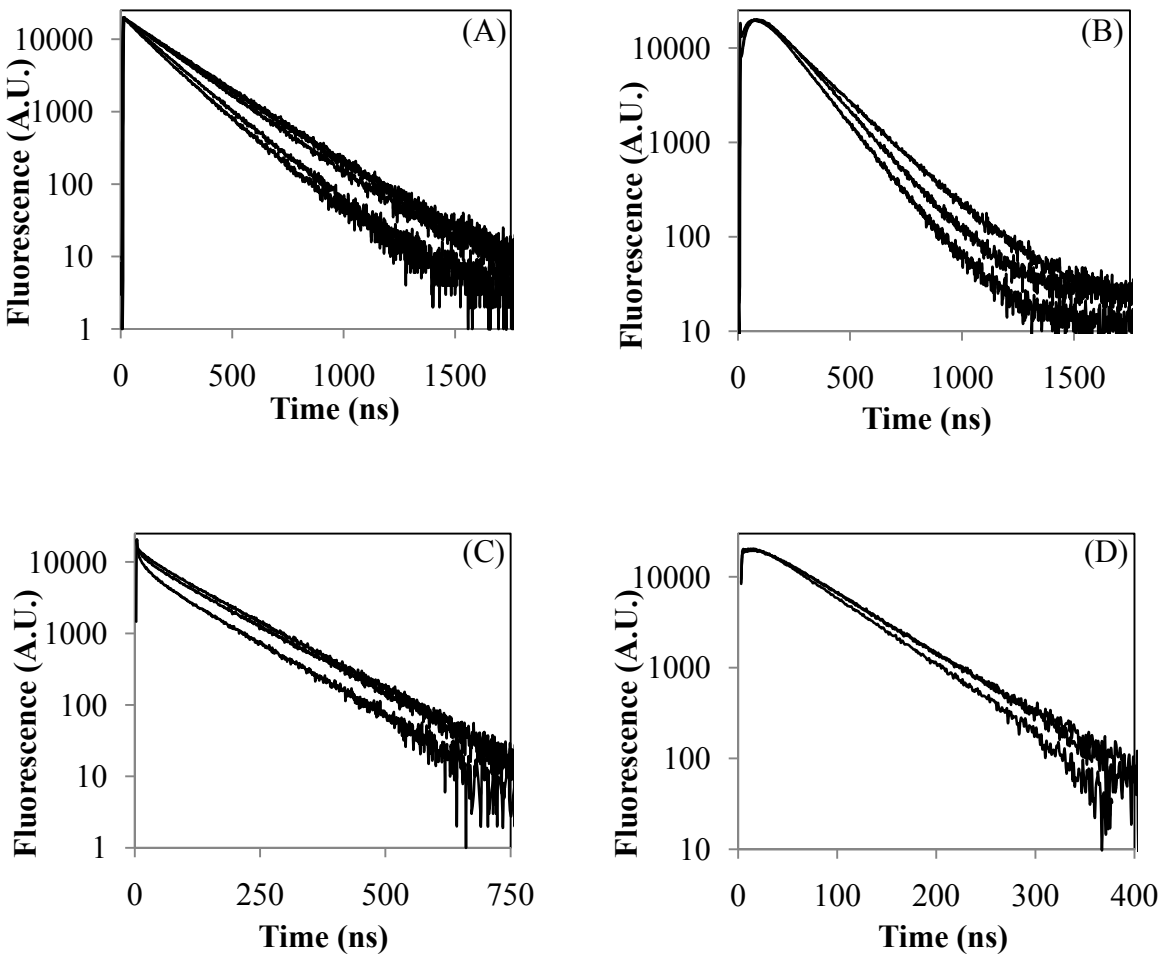

Figure 3.4: Fluorescence decays of pyrene end-labelled PNIPAM, λ_{ex} = 344 nm. A) Ethanol, [Py] = 2.5×10^{-6} mol.L^{-1}, λ_{em} = 375 nm, top to bottom: Py-PNIPAM-45k, Py-PNIPAM-25k, Py-PNIPAM-14k, Py-PNIPAM-8k, Py-PNIPAM-6k. B) Ethanol, [Py] = 2.5×10^{-6} mol.L^{-1}, λ_{em} = 510 nm, top to bottom: Py-PNIPAM-14k, Py-PNIPAM-8k, Py-PNIPAM-6k. C) Water, [Py] = 1.2×10^{-6} mol.L^{-1}, λ_{em} = 375 nm, top to bottom: Py-PNIPAM-45k, Py-PNIPAM-25k, Py-PNIPAM-14k. D) Water, [Py] = 1.2×10^{-6} mol.L^{-1}, λ_{em} = 510 nm, top to bottom: Py-PNIPAM-45k, Py-PNIPAM-25k, Py-PNIPAM-14k.

excimer formation as the pyrene end groups are separated by increasing chain length. For Py_2-PNIPAM-45K, the pyrene units are kept so far apart that they emit only as independent monomers and do not form excimers. The excimer decays have a short component whose origin could be light scattering, a trace of impurity, or ground-state dimers.[18,37] The ratio

Table 3.2: Pre-exponential factors and decay times obtained by fitting the monomer fluorescence decays of the Py_2-PNIPAM samples in ethanol with a sum of exponentials (Equation 3.1 with $N = 2$).

Sample	τ_{M1} (ns)	a_{M1}	τ_{M2} (ns)	a_{M2}	χ^2	$\langle\tau\rangle$ (ns)
Py_2-PNIPAM-6K	109 ± 3	0.42 ± 0.03	174 ± 2	0.58 ± 0.04	1.01	147 ± 10
Py_2-PNIPAM-8K	91 ± 6	0.15 ± 0.02	171.8 ± 0.8	0.85 ± 0.03	1.08	160 ± 8
Py_2-PNIPAM-14K	112 ± 13	0.10 ± 0.02	204 ± 1	0.90 ± 0.04	1.05	195 ± 12
Py_2-PNIPAM-25K	71 ± 8	0.07 ± 0.01	213.8 ± 0.5	0.93 ± 0.03	1.07	204 ± 9
Py_2-PNIPAM-45K	95 ± 27	0.04 ± 0.01	218.2 ± 0.8	0.96 ± 0.03	1.20	213 ± 10

Table 3.3: Pre-exponential factors and decay times obtained by fitting the excimer fluorescence decays of the Py_2-PNIPAM samples in ethanol with a sum of exponentials (Equation 3.1 with $N = 3$).

Sample	τ_{E1} (ns)	A_{E1}	τ_{E2} (ns)	A_{E2}	τ_{E3} (ns)	A_{E3}	χ^2	A_{E2}/A_{E3}
Py_2-PNIPAM-6K	1.2 ± 0.2	0.83 ± 0.04	47.2 ± 0.3	–1.6 ± 0.4	142.0 ± .2	1.8 ± 0.4	1.05	–0.9 ± 0.3
Py_2-PNIPAM-8K	1.9 ± 0.1	0.78 ± 0.02	48.6 ± 0.3	–2.1 ± 0.2	158.5 ± 0.2	2.3 ± 0.2	1.10	–0.9 ± 0.1
Py_2-PNIPAM-14K	1.5 ± 0.1	0.77 ± 0.02	42.5 ± 0.3	–0.59 ± 0.05	190.1 ± 0.2	0.82 ± 0.07	1.05	–0.72 ± 0.09

A_{E2} / A_{E3} is negative and equals –0.90 for Py_2-PNIPAM-6K and Py_2-PNIPAM-8K. This value is close to −1.0 which indicates that excimer formation is diffusion controlled as expected from the prominent rise time observed in the excimer decays shown in Figure 3.4B. As the chain length increases and excimer formation is less efficient, the A_{E2} / A_{E3} ratio becomes more positive and equals –0.72 for Py_2-PNIPAM-14K.

A global analysis of the monomer and excimer fluorescence decays of the Py_2-PNIPAM solutions in ethanol was performed according to the Birks scheme with Equations 3.2 and 3.3. The fits were excellent with χ^2 values smaller than 1.30 and residuals and autocorrelation function of the residuals being randomly distributed around zero. The parameters k_{cy}, k_{-cy}, τ_E, and f_{free} ($f_{free} = [Py^*_{free}]_o / ([Py^*_{free}]_o + [Py^*_{diff}]_o)$ retrieved from the analysis are listed in Table 3.4.

Table 3.4: Excimer formation rate constant (k_{cy}), excimer dissociation rate constant (k_{-cy}), excimer lifetime (τ_E), and molar fraction of pyrene monomer that do not form excimer (f_{free}).

Sample	k_{cy} (10^7 s^{-1})	k_{-cy} (10^7 s^{-1})	τ_E (ns)	f_{free}
Py_2-PNIPAM-6K	0.34 ± 0.05	0.4 ± 0.1	60 ± 6	0.097 ± 0.007
Py_2-PNIPAM-8K	0.26 ± 0.04	0.43 ± 0.08	64 ± 6	0.096 ± 0.008
Py_2-PNIPAM-14K	0.15 ± 0.08	0.9 ± 0.2	74 ± 25	0.24 ± 0.09

The rate constant for excimer formation decreases with increasing chain length as $k_{cy} \propto \overline{M}_n^{-\gamma}$ with γ = 0.91 ± 0.03. The γ-value is smaller than the values of 1.62 found for Py_2-

polystyrene in cyclohexane at 34.5 °C,[6] 1.52 found for Py_2-polytetrahydrofuran,[8] 1.9 and 1.7 found for Py_2-polycarbonate in acetonitrile and acetone, respectively,[12] but it is similar to the values of 1.1, 0.90, and 0.91 found for Py_2-poly(ethylene oxide) in diethyleneglycol diethyl ether at 50 °C, toluene at 45 °C, and tetrahydrofuran at 20 °C, respectively.[14] Although τ_E and k_{-cy} increase somewhat with increasing chain length (mostly for Py_2-PNIPAM-14K), this increase is believed to be an artifact because τ_E and k_{-cy} describe intrinsic properties of the pyrene excimer which should not depend on polymer chain length, as long as the chain is long enough as should be the case with the Py_2-PNIPAM samples. This artifact is due to limitations in the Birks' scheme analysis of fluorescence decays acquired with long pyrene end-labelled polymer constructs that do not generate much excimer. Indeed, as can be seen in Figure 3.2, excimer formation is strongly reduced for the Py_2-PNIPAM samples having an $\overline{M}_n$ greater than 14 K. This increase of τ_E and k_{-cy} with increasing polymer chain length has been observed in at least one instance.[37] If τ_E and k_{-cy} are averaged one finds that the excimer lifetime equals 66 ± 7 ns which is reasonable for a pyrene excimer in organic solvent.[5] The excimer dissociation rate constant is small and equals 6 ± 3 $\times 10^6$ s^{-1}. These results are typical for excimer formation of a pyrene end-labelled monodisperse polymer in organic solvents.[5]

3.3.4 Solutions of Py_2-PNIPAM Samples in Water at 23 °C

In Figure 3.5, the I_E/I_M ratio is plotted as a function of the molar pyrene concentration for solutions in water of Py_2-PNIPAM ($\overline{M}_n \geq 14{,}000$ g/L). The ratio I_E/I_M increases linearly with increasing polymer concentration, an indication that intermolecular

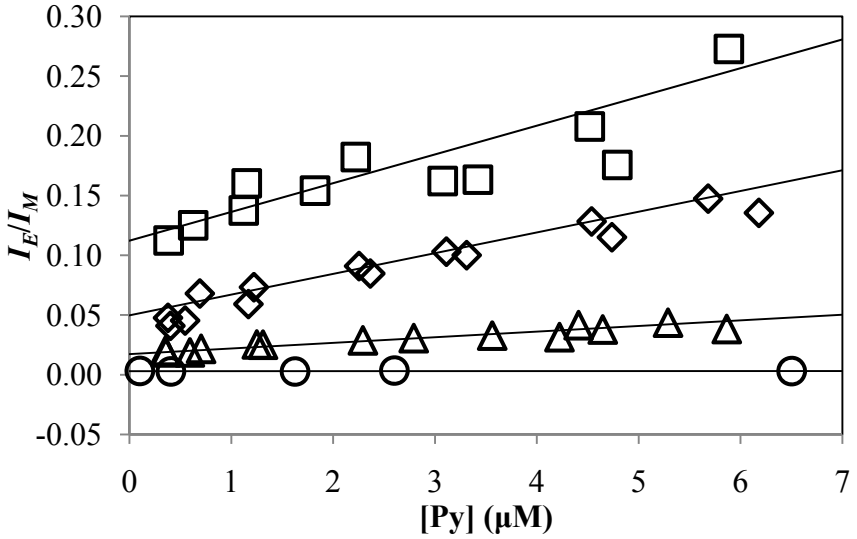

Figure 3.5: Plot of I_E/I_M versus [Py] for Py_2-PNIPAM-45k (△), Py_2-PNIPAM-25k (◇), and Py_2-PNIPAM-14k (□) in water and Py_2-PNIPAM-45k (○) in ethanol.

excimer formation is taking place in this concentration range ($1 < [Py] < 7\times10^{-6}$ mol/L).[9] For solutions of identical Py concentration, the I_E/I_M ratio decreases with increasing chain length, as was the case for Py_2-PNIPAM in ethanol. The I_E/I_M ratio of the Py_2-PNIPAM solutions having a pyrene concentration of 1.25 μM was plotted as a function of $\overline{M}_n$ in Figure 3.3 (symbol: square). For this pyrene concentration, the I_E/I_M ratio was found to scale as $\overline{M}_n^{-\gamma}$ where γ equals 1.5 ± 0.1, an exponent similar to the one of 1.4 ± 0.2 found in ethanol and within the range of exponents obtained for other Py_2-polymers in organic solvents.[6,8,12,14] Since the viscosities of water and ethanol are rather close to each other, viscosity is not expected to affect significantly the value of k_1 in Equation 3.6. Furthermore, the similarity of the intrinsic viscosity values of unmodified PNIPAM in water and in ethanol suggests that the dimensions of the polymer coil are the same in water and ethanol. Therefore, the enhancement of excimer formation observed in Figures 2 and 3 for Py_2-

PNIPAM in water is an indication that hydrophobic associations between pyrene pendants occurs, inducing a decrease of the average size of the polymer coil and an increase in $[Py]_{loc}$ in Equation 3.6.

Fluorescence decays of Py_2-PNIPAM solutions in water were acquired only for the longer chains. The excimer decays were not bi-exponential (see Tables 3.5 and 3.6) which rules out the possibility of using the typical Birks scheme to fit the fluorescence decays.[5] This departure from the traditional Birks scheme is attributed to the presence of ground-state pyrene aggregates which form excimer instantaneously upon direct excitation, as observed previously in studies of aqueous solutions of Py_2-PEO.[17-21] The presence of ground-state pyrene aggregates is supported by the values taken by the ratio, a_{E-}/a_{E+}, of the sum of the negative pre-exponential factors divided by the sum of the positive pre-exponential factors. For Py_2-PNIPAM-14K. the only polymer amenable to studies in both ethanol and water, the A_{E-}/A_{E+} ratio is more positive in water (–0.42) than in ethanol (–0.72). For aqueous solutions, the A_{E-}/A_{E+} ratio did not change much with $\overline{M}_n$, taking values of –0.40 and –0.43 for aqueoPy_2-PNIPAM-25K and Py_2-PNIPAM-45K, respectively. The presence of the ground-state pyrene aggregates complicates the quantitative analysis of the fluorescence decays. A detailed analysis of the decays is beyond the scope of this report.

Table 3.5: Pre-exponential factors and decay times obtained by fitting the monomer fluorescence decays of the Py_2-PNIPAM samples in water with a sum of exponentials (Equation 3.1 with $N = 3$).

Sample	τ_{M1} (ns)	a_{M1}	τ_{M2} (ns)	a_{M2}	τ_{M3} (ns)	a_{M3}	χ^2	$<\tau>$ (ns)
Py_2-PNIPAM-14K	4.5 ± 0.3	0.302 ± 0.006	28.0 ± 0.8	0.264 ± 0.005	109.1 ± 0.3	0.433 ± 0.005	1.10	56.0 ± 0.8
Py_2-PNIPAM-25K	6.8 ± 0.5	0.198 ± 0.006	44 ± 2	0.195 ± 0.006	118.4 ± 0.4	0.607 ± 0.007	1.05	82 ± 1
Py_2-PNIPAM-45K	4.9 ± 0.7	0.133 ± 0.009	38 ± 2	0.182 ± 0.006	117.7 ± 0.3	0.685 ± 0.008	1.09	88 ± 2

Table 3.6: Pre-exponential factors and decay times obtained by fitting the excimer fluorescence decays of the Py_2-PNIPAM samples in water with a sum of exponentials (Equation 3.1 with $N = 3$).

Sample	τ_{E1} (ns)	A_{E1}	τ_{E2} (ns)	A_{E2}	τ_{E3} (ns)	A_{E3}	χ^2	A_{E-} / A_{E+}
Py_2-PNIPAM-14K	10.8 ± 0.2	–0.74 ± 0.01	57.8 ± 0.7	1.66 ± 0.03	106 ± 13	0.08 ± 0.03	1.01	–0.43 ± .03
Py_2-PNIPAM-25K	17.6 ± 0.4	–0.66 ± 0.02	56 ± 2	1.40 ± 0.04	96 ± 6	0.25 ± 0.06	1.18	–0.40 ± 0.05
Py_2-PNIPAM-45K	16.2 ± 0.3	–0.76 ± 0.02	60 ± 1	1.57 ± 0.06	99 ± 9	0.19 ± 0.07	1.12	–0.43 ± 0.06

3.4 Conclusions

Five pyrene end-labelled PNIPAM samples of narrow molecular weight distribution ranging in size from $\overline{M}_n \sim$ 6,000 to 45,000 g/mol (Figure 3.1 and Table 3.1) were prepared and their solutions in ethanol and in water were studied by fluorescence spectroscopy. All polymers were soluble in ethanol, but only samples of $\overline{M}_n \geq$ 14,000 g/mol were water-soluble. In the case of the polymers of $\overline{M}_n$ 14,000, 25,000 and 45,000 g/mol, the excimer emission was enhanced for polymers in water, compared to solutions in ethanol, an effect attributed to the presence of pyrene aggregates via intra- and inter-chain association. This association process is triggered by the hydrophobicity of the pyrene end groups and bears similarity to the process of flower micelle formation in aqueous solutions of di-(*n*-octadecyl)-PNIPAM.[38] It is also akin to the micellization induced by Py in aqueous solutions of semi-telechelic Py-PNIPAM reported previously.[39] Time-resolved fluorescence measurements, which revealed a diminished rise time in the excimer profiles of the Py_2-PNIPAM samples in water (Figure 3.4), confirmed the presence of pyrene ground state aggregates. The ratio I_E/I_M, taken as a measure of the rate of excimer formation, was found to scale as $\overline{M}_n^{-\gamma}$ where γ equals 1.4 ± 0.2 and 1.5 ± 0.1 in ethanol and water, respectively. These exponents are within the range of exponents typically obtained with pyrene end-labelled monodisperse polymers.[6,8,12,14] All parameters retrieved from the analysis of the fluorescence decays of polymers in ethanol were reasonable, and the rate of excimer formation k_{cy} was found to scale as $\overline{M}_n^{-0.9}$, an exponent which is smaller than the one obtained by analysis of steady state data (I_E/I_M ratio). The discrepancy may be a consequence of the smaller set of data points available for k_{cy}, since it was possible to determine k_{cy} accurately for only three

polymers (Py_2-PNIPAM-6K, Py_2-PNIPAM-8K, and Py_2-PNIPAM-14K) (see Table 4) whereas all five Py_2-PNIPAM samples yielded accurate I_E/I_M ratios (Figure 3.3). The photophysical properties of Py_2-PNIPAM in ethanol are similar to those of Py_2-PEO of similar size in organic solvents, forming excimer according to the Birks scheme. As observed for solutions of Py_2-PEO in water, excimer formation kinetics are complex for aqueous solutions of Py_2-PNIPAM, due to the presence of aggregates of ground-state pyrene units and they need to be subjected to a detailed data treatment in order to compare the properties of the two families of polymers in water. Work towards this goal is ongoing, as it is expected to unveil how differences in the hydration of the PEO and PNIPAM main chains[40] can impact the association of their amphiphilic derivatives in water monitored on the time and distance scales of pyrene excimer formation.

Chapter 4: A Study of the Dynamics of the Branch Ends of a Series of Pyrene-Labelled Dendrimers Based on Pyrene Excimer Formation

4.1 Overview

A series of pyrene-labeled dendrimers were prepared from generation $n = 1$ to $n = 4$ where the pyrenes were attached to the end groups of the dendrimers. Pyrene excimer formation was monitored by steady-state and time-resolved fluorescence spectroscopy as a function of generation number and in terms of the I_E/I_M ratio and the average rate constant of excimer formation $\langle k \rangle$. To account for the unconventional distribution of pyrene labels which were neither randomly distributed throughout the macromolecule nor limited to just two units which are the only two pyrene-labeling schemes that can be dealt with in a straightforward manner, a Model Free (MF) analysis was applied to the global analysis of the fluorescence decays. Within experimental error, the I_E/I_M ratios and $\langle k \rangle$ obtained from, respectively, the steady-state fluorescence spectra and the time-resolved fluorescence decays were found to increase linearly with increasing generation number. This result is inconsistent with the fact that both the I_E/I_M ratio and $\langle k \rangle$ are proportional to the local concentration of pyrene inside the dendrimer ($[Py]_{loc}$) which is not expected to increase with generation number if the excited pyrene is assumed to diffuse freely throughout the dendrimer interior. Since the core-dense model predicts that the dendrimer terminal ends can occupy any position throughout the dendrimer interior, these results suggest that excimer formation between the pyrene-labeled ends is enhanced due to the branched nature of the dendrimer.

4.2 Link to Original Content

Chapter 4 has been published in the *Journal of Physical Chemistry B*. The original content can be found at the DOI, online link, or citation provided.

DOI:

10.1021/jp9102228

Online Link:

http://pubs.acs.org/doi/abs/10.1021/jp9102228

Full Citation:

Yip, J.; Duhamel, J; Bahun, G. J.; Adronov, A. A Study of the Dynamics of the Branch Ends of a Series of Pyrene-Labelled Dendrimers Based on Pyrene Excimer Formation *J. Phys. Chem. B*. **2010**, *114*, 10254-10265.

Chapter 5: Conclusions

This thesis presents a series of experiments that demonstrates how pyrene can be used to probe the intramolecular encounters between two positions of a macromolecule. Two different macromolecules were studied. The first macromolecule, poly(*N*-isopropylacrylamide) (PNIPAM), was labelled with pyrene both randomly and at the chain ends. The synthesis of both the randomly and end-labelled PNIPAM samples was conducted in the Laboratory of Prof. Françoise Winnik at the Université de Montréal.[1-3] The second macromolecule, a dendrimer built from a bis(hydroxymethyl)propionic acid backbone, was labelled at the chain terminals with pyrene. The synthesis of the dendrimer molecules was conducted in the Laboratory of Prof. Alex Adronov at McMaster University.[4] Steady-state fluorescence spectra and time-resolved fluorescence decays of the pyrene-labelled macromolecules were then acquired in suitable solvents. From the steady-state fluorescence spectra, the I_E/I_M ratio was calculated as a first measure of the extent of excimer formation. The time-resolved fluorescence decays were then analyzed with the appropriate model in order to gain information about the time-scale over which excimer formation took place.

In Chapter 2, two PNIPAM series were studied. The first was a series of polymers randomly labelled with pyrene and was referred to as Py-PNIPAM-X%, where X represents the pyrene content and equals 0.1, 2, 3, 4, 5, and 6 mol%. The second was a series of monodisperse polymers that were labelled with pyrene only at the end positions and was referred to as Py_2-PNIPAM-Y, where Y represents the molecular weight and equals 6, 8, 14, 26, and 45 kDa. Steady-state fluorescence spectra and time-resolved fluorescence decays

were acquired in solvents of varying viscosity to determine the effect of viscosity on the kinetics of excimer formation. These solvents included methanol, ethanol, hexanol, binary mixtures of methanol and hexanol where the methanol content was 6%, 15%, 30%, 60%, and 80% by mass, acetonitrile, 2-butanone, ethyl acetate, and tetrahydrofuran. The fluorescence decays of the monomer and excimer for the Py-PNIPAM-X% and Py_2-PNIPAM-Y polymers were analyzed using the Fluorescence Blob Model (FBM)[5] and the Birks Scheme,[6] respectively.

The I_E/I_M ratios obtained were found to increase with decreasing viscosity, increasing pyrene content (for the Py-PNIPAM-X% polymers), and decreasing chain length (for the Py_2-PNIPAM-Y polymers). These observations could be rationalized as follows. A decrease in viscosity enhances the diffusional motion of the polymer, resulting in increased excimer formation. As the pyrene content increases for a randomly labelled polymer, the local pyrene concentration increases, resulting in increased excimer formation. Finally, a decrease in the chain length of an end-labelled polymer brings the pyrene-labelled ends closer together, resulting in an increase in the I_E/I_M ratio. The I_E/I_M ratios for the Py_2-PNIPAM-Y polymers were also found to scale as $\eta^{\alpha} \times N^{\beta}$ where η and N represent the solvent viscosity and the polymer chain length, respectively. The exponents α and β were found to equal -1.1 and -1.7, respectively (Figure 2.6), and are in good agreement with values obtained for other polymers.[7-10] For the Py-PNIPAM-X% polymers, an onset pyrene content of ~2 mol% was observed (Figure 2.7). Below this onset pyrene content, very little excimer was formed. Above this pyrene content, the I_E/I_M ratio increased linearly with increasing pyrene content.

The Birks Scheme analysis of the monomer and excimer decays of the Py_2-PNIPAM-Y polymers yielded k_{cy}, the rate constant of cyclization of the polymer chain.[6] In high viscosity solvents and for long chain lengths, k_{cy} was observed to reach a plateau (Figure 2.10). After a certain break point, k_{cy} scaled as $\eta^{\alpha} \times N^{\beta}$, where the exponents α and β were found to equal -1.09 ± 0.06, and -1.72 ± 0.05, respectively. These values agree well with those obtained for a series of poly(ethylene oxides) (PEO) end-labelled with pyrene, where α and β were found to equal -1.0 and -1.3, respectively.[11] The rate constant k_{cy} also correlated well with the corresponding I_E / I_M ratios at small chain length and low solution viscosity (Figure 2.5). This is expected since theoretical work done by Cuniberti and Perico predicts that the two quantities should be proportional (Equation 2.43).[12] Finally, taking the product $k_{cy} \times N$ eliminated the dependence of the cyclization rate constant on chain length, and, within experimental error, the product was found to be the same for each end-labelled polymer in each solvent (Figure 2.9).

Analysis of the monomer and excimer decays of the Py-PNIPAM-X% polymers yielded the parameters $k_e[blob]$, k_{blob}, and N_{blob}.[5] Within experimental error, the three parameters remained constant with increasing pyrene content and increased with decreasing viscosity (Figures 2.11 – 2.13 and 2.15). Ignoring the data obtained with the Py-PNIPAM-2% sample which corresponded to the pyrene content above which excimer was formed (Figure 2.7), the product $k_{blob} \times N_{blob}$ also remained constant with pyrene content within experimental error (Figure 2.14) and averaging $k_{blob} \times N_{blob}$ for the remaining polymers in a given solvent yielded $< k_{blob} \times N_{blob} >$, the average rate constant of excimer formation in that

solvent. For the alcohols, $< k_{blob} \times N_{blob} >$ was found to increase linearly with decreasing viscosity (Figure 2.16). A notable difference was observed in the aprotic solvents studied, where $< k_{blob} \times N_{blob} >$ was found to be significantly lower than expected, except in acetonitrile which may be an outlier. Differences in pyrene fluorescence have already been observed between alcohols and aprotic solvents, and the reasons for these differences are not fully understood.[13,14]

Finally, $k_{cy} \times N$ was compared with $< k_{blob} \times N_{blob} >$ to determine if the two rate constants describe polymer chain flexibility in a similar manner. Within experimental error, both quantities showed similar trends in both the alcohols and the aprotic solvents (Figure 2.16), demonstrating that the same information on polymer chain dynamics is obtained, regardless of the manner in which the pyrene label is incorporated into the polymer, either randomly or specifically at the ends.

In Chapter 3, the Py_2-PNIPAM-Y samples were studied in ethanol and in water to investigate the effect that pyrene solubility which is good in ethanol and poor in water has on excimer formation. Monomer and excimer decays were acquired for the Py_2-PNIPAM-6K, 8K, and 14K polymers in ethanol. For the Py_2-PNIPAM-25K and 45K polymers in ethanol, not enough excimer signal was present and only the monomer decays were acquired. In water, only the Py_2-PNIPAM-14K, 26K, and 45K polymers were soluble, and monomer and excimer decays were acquired only for these samples.

The I_E / I_M ratio was found to scale as $\overline{M}_n^{-1.4}$ in ethanol (Figure 3.3), which agrees with previous theoretical and experimental work.[7-11] The exponent of –1.4 is smaller than that observed in Chapter 2, and this discrepancy is believed to be due to the greater accuracy

obtained in Chapter 2 owing to the greater number of data points included in the optimization. In water, I_E/I_M scaled as $\overline{M}_n{}^{-1.5}$. This exponent is similar to that observed in ethanol. The I_E/I_M ratio was also measured as a function of polymer concentration in Figure 3.5. In water, I_E/I_M decreased with decreasing pyrene concentration down to very low pyrene concentrations, suggesting the presence of intermolecular ground-state pyrene aggregates in aqueous solution, even at concentrations as low as 0.5 μM. In ethanol, I_E/I_M remained constant over the entire pyrene concentration range studied, implying that excimer formation was due only to intramolecular interactions in this solvent.

The fluorescence decays of the monomer and excimer for the Py_2-PNIPAM-6K, 8K, and 14K polymers in ethanol were analyzed globally using the Birks Scheme[6] to yield k_{cy}, the rate constant of cyclization. k_{cy} was found to scale as $\overline{M}_n{}^{-0.9}$ (Table 3.4). This exponent is smaller than that observed for the I_E/I_M ratio, but is similar to values previously obtained for other polymers[11,13] and for Py_2-PNIPAM samples obtained in a broader range of organic solvents in Chapter 2. For the Py_2-PNIPAM-26K and 45K polymers in ethanol, the number average lifetime ($<\tau>$) was found to approach 220 ns, the lifetime of 1-pyrenebutanol in ethanol. This increase in $<\tau>$ with increasing chain length reflects the decrease in excimer formation observed for the longer polymers since the pyrene-labelled ends are held further apart. The a_{E2}/a_{E3} ratio was also calculated by fitting the excimer decays of the Py2-PNIPAM-6K, 8K, and 14K polymers with a sum of exponentials (Table 3.2). The ratio was close to –1, indicating that very little ground-state pyrene aggregates were present.

In water, $< \tau >$ for the pyrene monomer also increased with increasing chain length, reflecting the decrease in excimer formation for longer chains (Table 3.5). Analysis of the excimer decays with a sum of exponentials yielded the a_{E-} / a_{E+} ratio which was found to remain constant at around –0.4, a value which is significantly more positive than –1 (Table 3.6). This result confirms the earlier conclusion that ground-state pyrene aggregates are present in water. The difference in the level of ground-state pyrene aggregates in ethanol and in water is due solely to the difference in pyrene solubility between the two solvents. Ethanol is a good solvent for pyrene, minimizing the presence of ground-state aggregates, whereas water is a poor solvent for pyrene, causing the pyrene units to aggregate. The presence of intermolecular ground-state pyrene aggregates greatly complicates the analysis of the fluorescence decays and no further analysis was conducted.

In Chapter 4, four generations of dendrimers were synthesized with a bis(hydroxymethyl)propionic acid backbone and terminal sites that were covalently labelled with pyrene, as well as a dendrimer-polystyrene hybrid where each dendrimer was covalently attached to one end of a linear polystyrene. The pyrene-labelled dendrimers were referred to as Py_x-GY-COOH where x represents the number of pyrene units per dendrimer and equals 2, 4, 8, and 16, and Y represents the generation number and equals 1, 2, 3, and 4 (Figure 4.1). The pyrene-labelled dendrimer hybrids were referred to as Py_x-GY-PS (Figure 4.2). Since these pyrene-labelled macromolecules are neither end-labelled polymers nor randomly labelled macromolecules, which are currently the only two types of pyrene-labelled macromolecules whose fluorescence decays can be dealt with in a quantitative manner, a new model was derived in order to analyze the fluorescence decays. This model, termed the Model-Free (MF) model, uses a sum-of-exponentials to model the function $f(t)$ which

describes the distribution of rate constants of excimer formation which results in the complex fluorescence decays.

Steady-state fluorescence spectra and time-resolved fluorescence decays were acquired in tetrahydrofuran (THF), a good solvent for both the dendrimer and the pyrene groups attached at its periphery. Initial results showed a linear increase in the $(I_E/I_M)^{SS}$ ratio with increasing generation number from generations 1 to 3, followed by a decrease from generation 3 to 4 for the Py_x-GY-COOH dendrimers. The superscript *SS* serves as a reminder that this ratio was calculated from the steady-state fluorescence spectra (Figure 4.3). However, the $(I_E/I_M)^{SS}$ ratio for the Pyx-GY-PS hybrids did not follow this trend, and instead, increased linearly with generation number. The results obtained from the MF analysis of the fluorescence decays also contradicted this trend. According to the MF analysis, the average rate constant of excimer formation, $< k >$, was found to increase linearly with increasing generation number. Analysis of the fluorescence decays of the monomer also showed a contribution from a species that fluoresced with a lifetime close to 210 ns, the lifetime of 1-pyrenebutyric acid in THF, suggesting the presence of unattached pyrene impurities. According to the MF analysis, this impurity represented 3 mol% of all pyrene species in solution for the G4 dendron. After purification of the G4 dendron, both the $(I_E/I_M)^{SS}$ ratio and $< k >$ increased linearly with generation number (Figure 4.4). This finding reflects the effect that even minute amounts of pyrene impurities can have on steady-state fluorescence results.

In addition to measuring the average rate constant of excimer formation, the MF model also gave the $(I_E/I_M)^{SPC}$ ratio, calculated based on the time-resolved fluorescence

decays. The superscript *SPC* reminds us that this ratio was derived from the time-resolved fluorescence decays acquired with the single photon counting technique. The $(I_E/I_M)^{SPC}$ ratio is an absolute quantity, which implies that measurements of the $(I_E/I_M)^{SPC}$ ratio performed in different laboratories can be compared. In addition, the $(I_E/I_M)^{SPC}$ ratio was used to predict how changing the fractions of the different pyrene species in solution would affect the I_E/I_M ratio. Setting the fraction of free pyrene units, f_{free}, equal to zero for the G4 dendron, the trends observed for $(I_E/I_M)^{SPC}$ before and after setting f_{free} equal to zero matched exactly the trends observed for $(I_E/I_M)^{SS}$ before and after purification of the Py_{32}-G4-COOH dendrimer, respectively. The similar trends led to the conclusion that the odd behavior found for the $(I_E/I_M)^{SS}$ ratio of the G4 dendron was due to the presence of a minute amount of unattached pyrene label.

The linear increase in $< k >$ with generation number suggested that the volume probed by pyrene scales as $n^{0.9}$, where n represents the generation number of the dendrimer. However, previous experimental work has shown that, on average, the volume of a dendrimer molecule scales as $n^{1.9}$.[16-27] This difference implies that the volume of a dendrimer grows much more quickly than the volume probed by the pyrene units attached to the terminal sites. This does not, however, imply that the terminal sites do not probe the entire volume of the dendrimer, as is predicted by the shell-dense model,[28] but rather that the pyreneyl pendants undergo excimer formation before having had the time to probe the entire volume of the dendrimer. The branched nature of the dendrimer holds the pyrene units close together, forcing excimer formation between the nearby pyrene units, and decreasing the volume that can be probed by an excited pyrene during its lifetime.

Pyrene is a very useful probe that provides significant information about various properties of a macromolecule; the difficulty lies in finding the appropriate model to analyze and interpret the complex fluorescence decays obtained, in order to successfully extract that information. This thesis gives three examples where analysis of the fluorescence decays acquired for three types of fluorescently labelled macromolecules was successfully conducted to deliver information on the internal dynamics of the macromolecules.

References

Chapter 1

1. Lakowicz, J. R. *Principles of Fluorescence Spectroscopy*. Plenum Press: New York, 1983; a) p1-18. b) p257-259. c)p303-305.
2. Duhamel, J. *Molecular Interfacial Phenomena of Polymers and Biopolymers*. Woodhead Publishing Limited: Cambridge, England, 2005; p216-222.
3. Winnik, F. M. *Chem. Rev.* **1993**, *93*, 587-614.
4. Berlman, I. B. *Handbook of Fluorescence Spectra of Aromatic Molecules*. Academic Press, Inc.: New York, 1971; p383.
5. Birks, J. B. *Photophysics of Aromatic Molecules*. Wiley: New York, 1970; p 301.
6. Hagen, S. J. *J. Mol. Biol.* **2000**, *301*, 1019-1027.
7. de Gennes, P. G. *J. Phys. Lett.* **1985**, *46*, L-639-L-642.
8. Annabale, T.; Buscall, R.; Eettelaie, R.; Whittlestone, D. *J. Rheol.* **1995**, *47*, 83-229.
9. Cuniberti, C.; Perico, A. *Eur. Polym. J.* **1977**, *13*, 369-374.
10. Redpath, A. E. C.; Winnik, M. A. *J. Am. Chem. Soc.* **1980**, *102*, 6869-6871.
11. Cuniberti, C.; Perico, A. *Eur. Polym. J.* **1980**, *16*, 887-893.
12. Winnik, M. A.; Redpath, T.; Richards, D. H. *Macromolecules* **1980**, *13*, 328-335.
13. Redpath, A. E. C.; Winnik, M. A. *J. Am. Chem. Soc.* **1982**, *104*, 5604-5607.
14. Winnik, M. A. *Acc. Chem. Res.* **1985**, *18*, 73-79.
15. Martinho, J. M. G.; Winnik, M. A. *Macromolecules* **1986**, *19*, 2281-2284.

16. Boileau, S.; Méchin, F.; Martinho, J. M. G.; Winnik, M. A. *Macromolecules* **1989**, *22*, 215-220.

17. Martinho, J. M. G.; Sousa, A. T. R.; Winnik, M. A. *Macromolecules* **1993**, *26*, 4484-4488.

18. Mathew, A. K.; Siu, H.; Duhamel, J. *Macromolecules* **1999**, *32*, 7100-7108.

19. Tachiya, M. *Chem. Phys. Lett.* **1975**, *33*, 289-292.

20. Ingratta, M.; Duhamel, J. *Macromolecules* **2009**, *42*, 1244-1251.

21. Ingratta, M.; Hollinger, J.; Duhamel, J. *J. Am. Chem. Soc.* **2008**, *130*, 9420-9428.

22. Duhamel, J.; Kanagalingam, S.; O`Brien, T.; Ingratta, M. *J. Am. Chem. Soc.* **2003**, *125*, 12810-12822.

23. Ingratta, M.; Duhamel, J. *J. Phys. Chem. B* **2008**, *112*, 9209-9218.

24. Teerstra, J. S.; Lin, W. Y.; Gauthier, M.; Ingratta, M.; Duhamel, J. *Polymer* **2009**, *50*, 5456-5466.

25. Kanagalingam, S.; Spartalis, J.; Cao, T. M.; Duhamel, J. *Macromolecules* **2002**, *35*, 8571-8577.

26. Irondi, K.; Zhang, M.; Duhamel, J. *J. Phys. Chem. B* **2006**, *110*, 2628-2637.

27. Siu, H.; Duhamel, J. *J. Phys. Chem. B* 2005, 109, 1770-1780.

28. Winnik, M. A.; Egan, L. S.; Tencer, M.; Croucher, M. D. *Polymer* **1987**, *28*, 1553-1560.

29. Dong, D. C.; Winnik, M. A. *Photochem. and Photobiol.* **1982**, *35*, 17-21.

30. Dong, D. C.; Winnik, M. A. *Can. J. Chem.* **1984**, *62*, 2560-2565

31. Kalyanasundaram, K.; Thomas, J. K. *J. Am. Chem. Soc.* **1977**, *99*, 2039-2044.

32. Lianos, P.; Georghiou, S. *Photochem. Photobiol.* **1979**, *30*, 355-362.

33. Zachariasse, K. A.; Vaz, W. L. C.; Sotomayor, C.; Kühnle, W. *Biochim. Biophys. Acta* **1982**, *688*, 323-332.

34. Siu, H.; Duhamel, J. *Macromolecules* **2006**, *39*, 1144-1155.

Chapter 2

1. Cuniberti, C.; Perico, A. *Eur. Polym. J.* **1977**, *13*, 369-374.
2. Cuniberti, C.; Perico, A. *Eur. Polym. J.* **1980**, *16*, 887-893.
3. Redpath, A. E. C.; Winnik, M. A. *J. Am. Chem. Soc.* **1980**, *102*, 6869-6871.
4. Winnik, M. A.; Redpath, T.; Richards, D. H. *Macromolecules* **1980**, *13*, 328-335.
5. Redpath, A. E. C.; Winnik, M. A. *J. Am. Chem. Soc.* **1982**, *104*, 5604-5607.
6. Winnik, M. A. *Acc. Chem. Res.* **1985**, *18*, 73-79.
7. Martinho, J. M. G.; Winnik, M. A. *Macromolecules* **1986**, *19*, 2281-2284.
8. Boileau, S.; Méchin, F.; Martinho, J. M. G.; Winnik, M. A. *Macromolecules* **1989**, *22*, 215-220.
9. Martinho, J. M. G.; Sousa, A. T. R.; Winnik, M. A. *Macromolecules* **1993**, *26*, 4484-4488.
10. Birks, J. B. *Photophysics of Aromatic Molecules*. Wiley: New York, 1970; p 301.
11. Winnik, F. M. *Chem. Rev.* **1993**, *93*, 587-614.
12. Berlman, I. B. *Handbook of Fluorescence Spectra of Aromatic Molecules*. Academic Press, Inc.: New York, 1971; p383.
13. Mathew, A. K.; Siu, H.; Duhamel, J. *Macromolecules* **1999**, *32*, 7100-7108.
14. Ingratta, M.; Duhamel, J. *Macromolecules* **2009**, *42*, 1244-1251.
15. Ingratta, M.; Hollinger, J.; Duhamel, J. *J. Am. Chem. Soc.* **2008**, *130*, 9420-9428.

16. Kanagalingam, S.; Spartalis, J.; Cao, T. M.; Duhamel, J. *Macromolecules* **2002**, *35*, 8571-8577.
17. Irondi, K.; Zhang, M.; Duhamel, J. *J. Phys. Chem. B* **2006**, *110*, 2628-2637.
18. Teertstra, S. J.; Lin, W. Y.; Gauthier, M.; Ingratta, M.; Duhamel, J. *Polymer* **2009**, *50*, 5456-5466.
19. Duhamel, J.; Kanagalingam, S.; O`Brien, T.; Ingratta, M. *J. Am. Chem. Soc.* **2003**, *125*, 12810-12822.
20. Ingratta, M.; Duhamel, J. *J. Phys. Chem. B* **2008**, *112*, 9209-9218.
21. Heskins, M.; Guillet, J. E. *J. Macromol. Sci. Chem.* **1968**, *A2*, 1441-1455.
22. Winnik, F. M. *Macromolecules* **1990**, *23*, 233-242.
23. Qiu, X. P.; Winnik, F. M. *Macromolecules* **2007**, *40*, 872-878.
24. Sequi, F.; Qiu, X. P.; Winnik, F. M. *J. Polym. Sci. A* **2008**, *46*, 314-326.
25. Tachiya, M. *Chem. Phys. Lett.* **1975**, *33*, 289-292.
26. Ingratta, M.; Mathew, M.; Duhamel, J. *Can. J. Chem.* **2010**, *88*, 217-227.
27. Dong, D. C.; Winnik, M. A. *Photochem. and Photobiol.* **1982**, *35*, 17-21.
28. Dong, D. C.; Winnik, M. A. *Can. J. Chem.* **1984**, *62*, 2560-2565.
29. Chen, S.; Duhamel, J.; Winnik, M. A. Submitted to *J. Phys. Chem. B*. **2010**.
30. Bicerano, J. *Prediction of Polymer Propeties, 2nd Ed*. Marcel Dekker: New York, 1996; p338-339.
31. Fang, Z.; Zhen, T.; Sato, T. *Science in China B* **1999**, *42*, 290-297.

Chapter 3

1. Wilemski, G.; Fixman, M. *J. Chem. Phys.* **1974**, *60*, 866-877.

2. Wilemski, G.; Fixman, M. *J. Chem. Phys.* **1974**, *60*, 878-890.

3. Cuniberti, C.; Perico, A. *Eur. Polym. J.* **1977**, *13*, 369-374.

4. Winnik, M. A.; Redpath, T.; Richards, D. H. *Macromolecules* **1980**, *13*, 328-335.

5. Birks, J. B. *Photophysics of Aromatic Molecules*. Wiley: New York, 1970; p 301.

6. Winnik, M. A. *Acc. Chem. Res.* **1985**, *18*, 73-79.

7. Slomkowski, S.; Winnik, M. A. *Macromolecules* **1986**, *19*, 500-501.

8. Svirskaya, P.; Danhelka, J.; Redpath, A. E. C.; Winnik, M. A. *Polymer* **1983**, *24*, 319-322.

9. Kim, S. D.; Torkelson, J. M. *Macromolecules* **2002**, *35*, 5943-5952.

10. Gardinier, W. E.; Bright, F. V. *J. Phys. Chem. B* **2005**, *109*, 14824-14829.

11. Piçarra, S.; Gomes, P. T.; Martinho, J. M. G. *Macromolecules* **2000**, *33*, 3947-3950.

12. Boileau, S.; Méchin, F.; Martinho, J. M. G.; Winnik, M. A. *Macromolecules***1989**, *22*, 215-220.

13. Duhamel, J.; Khayakin, Y.; Hu, Y. Z.; Winnik, M. A.; Boileau, S.; Méchin, F. *Eur. Polymer. J*. **1994**, *30*, 129-134.

14. Ghiggino, K. P.; Snare, M. J.; Thistlethwaite, P. J. *Eur. Polym. J.* **1985**, *21*, 265-272.

15. Lee, S.; Winnik, M. A. *Macromolecules* **1997**, *30*, 2633-2641.

16. Lee, S.; Duhamel, J. *Macromolecules* **1998**, *31*, 9193-9200.

17. Farinha, J. P. S.; Piçarra, S.; Miesel, K.; Martinho, J. M. G. *J. Phys. Chem. B* **2001**, *105*, 10536-10545.

18. Costa, T.; Seixas de Melo, J.; Burrows, H. D. *J. Phys. Chem. B* **2009**, *113*, 618-626.

19. Cheung, S.-T.; Winnik, M. A.; Redpath, A. E. C. *Makromol. Chem.* **1982**, *183*, 1815-1824.

20. Char, K.; Frank, C. W.; Gast, A. P. *Macromolecules* **1989**, *22*, 3177-3180.

21. Duhamel, J.; Yekta, A.; Hu, Y.; Winnik, M. A. *Macromolecules* **1992**, *25*, 7024-7030.

22. Winnik, F. M. *Chem. Rev.* **1993**, *93*, 587-614.

23. Farinha, J. P. S.; Martinho, J. M. G.; Xu, H.; Winnik, M. A.; Quirk, R. P. *J. Polym. Sci. B Polym. Phys.* **1994**, *32*, 1635-1642.

24. Walter, R. ; Rička, J.; Quellet, C. ; Nyffenegger, R. ; Binkert, T. *Macromolecules* **1996,** *29*, 4019-4028.

25. Gan, D.; Lyon A.L. *Macromolecule*s **2002,** *35*, 9634-9639.

26. Tasaki, K. *J. Am. Chem. Soc*. **1996,** *118*, 8459-8469.

27. Qiu, X.-P.; Winnik, F. M. *Macromolecules* **2007**, 40, 872-878.

28. Duan, Q.; Miura, Y.; Narumi, A.; Shen, X.; Sato, S.-I.; Satoh, T.; Kakuchi, T. *J. Polym. Sci. A Polym. Chem.* **2006**, *44*, 1117-1124.

29. Scales, C. W.; Convertine, A. J.; McCormick, C. L. *Biomacromolecules* **2006**, *7*, 1389-1392.

30. Rao, J.; Xu, J.; Luo, S.; Liu, S. *Langmuir* **2007**, *23*, 11857-11865.

31. Rao, J.; Zhang, J.; Xu, J.; Liu, S. *J. Coll. Interface Sci.* **2008**, *328*, 196-202.

32. Segui, F.; Qiu, X.-P.; Winnik, F. M. *J. Polym. Sci. A Polym. Chem.* **2008**, *46*, 314-326.

33. Siu, H.; Duhamel, J. *J. Phys. Chem. B* **2008**, *112*, 15301-15312.

34. Cuniberti, C.; Perico, A. *Eur. Polym. J.* **1980**, *16*, 887-893.

35. Cuniberto, C.; Perico, A. *Prog. Polym. Sci.* **1984**, *10*, 271-316.

36. Siu, H.; Duhamel, J. *Langmuir* **2010**, *26*, 10985-10994.

37. Ingratta, M.; Hollinger, J.; Duhamel, J. *J. Am. Chem. Soc.* **2008,** *130*, 9420-9428.

38. Koga, T. ; Tanaka, F. ; Motokawa, R. ; Koizumi, S. ; Winnik, F. M. *Macromolecules* **2008,** *41*, 9413-9422.

39. Winnik, F. M. ; Adronov, A.; Kitano, H. *Can. J. Chem.* **1995**, 73, 2030-2040.

40. Okada, Y. ; Tanaka, F. *Macromolecules* **2005** *38,* 4465-4471.

Chapter 4

Please refer to original document.

Chapter 5

1. Winnik, F. M. *Macromolecules* **1990**, *23*, 233-242.
2. Qiu, X. P.; Winnik, F. M. *Macromolecules* **2007**, *40*, 872-878
3. Sequi, F.; Qiu, X. P.; Winnik, F. M. *J. Polym. Sci. A* **2008**, *46*, 314-326
4. Bahun, G. J.; Adronov, A. *J. Polym. Sci. A*: *Polym. Chem.* **2010**, *48*, 1016-1028.
5. Mathew, A. K.; Siu, H.; Duhamel, J. *Macromolecules* **1999**, *32*, 7100-7108.
6. Birks, J. B. *Photophysics of Aromatic Molecules*. Wiley: New York, 1970; p 301.
7. Winnik, M. A. *Acc. Chem. Res.* **1985**, *18*, 73-79.
8. Svirskaya, P.; Danhelka, J.; Redpath, A. E. C.; Winnik, M. A. *Polymer* **1983**, *24*, 319-322.
9. Boileau, S.; Méchin, F.; Martinho, J. M. G.; Winnik, M. A. *Macromolecules***1989**, *22*, 215-220.
10. Ghiggino, K. P.; Snare, M. J.; Thistlethwaite, P. J. *Eur. Polym. J.* **1985**, *21*, 265-272.
11. Chen, S.; Duhamel, J.; winnik, M. A. Submitted to *J. Phys. Chem. B.* **2010**.
12. Cuniberti, C.; Perico, A. *Eur. Polym. J.* **1980**, *16*, 887-893.

13. Dong, D. C.; Winnik, M. A. *Photochem. and Photobiol.* **1982**, *35*, 17-21.

14. Dong, D. C.; Winnik, M. A. *Can. J. Chem.* **1984**, *62*, 2560-2565.

15. Ghiggino, K. P.; Snare, M. J.; Thistlethwaite, P. J. *Eur. Polym. J.* **1985**, *21*, 265-272.

16. Pavlov, G. M.; Korneeva, E. V.; Meijer, E. W. *Colloid Polym. Sci.* **2002**, *280*, 416-423.

17. Scherrenberg, R.; Coussens, B.; Vliet, P. V.; Edouard, G.; Brackman, J.; Brabander, E. D. *Macromolecules* **1998**, *31*, 456–461.

18. Mansfield, M. L. *Macromolecules* **2000**, *33*, 8043–8049.

19. Mansfield, M. L.; Jeong, M. *Macromolecules* **2002**, *35*, 9794–9798.

20. Rathgeber, S.; Monkenbusch, M.; Kreitschmann, M.; Urban, V.; Brulet, A. *J. Chem. Phys.* **2002**, *117*, 4047–4062.

21. Rathgeber, S.; Pakula, T.; Urban, V. *J. Chem. Phys.* **2004**, *121*, 3840–3853.

22. Mansfield, M. L.; Klushin, L. *Macromolecules* **1993**, *26*, 4262–4268.

23. Murat, M.; Grest, G. S. *Macromolecules* **1996**, *29*, 1278–1285.

24. Cavallo, L.; Fraternali, F. *Chem. Eur. J.* **1998**, *4*, 927–934.

25. Giupponi, G.; Buzza, D. M. A. *Macromolecules* **2002**, *35*, 9799–9812.

26. Uppuluri, S.; Keinath, S. E.; Tomalia, D. A.; Dvornic, P. R. *Macromolecules* **1998**, *31*, 4498–4510.

27. Maiti, P. K.; Çağin, T.; Wang, G.; Goddard, W. A., III *Macrolecules* **2004**, *37*, 6236–6254.

28. De Gennes, P. G.; Hervet, H. *J. Phys. Lett.* **1983**, *44*, L-351–L-360.

Appendix A: Fluorescence Data for the Py_2-PNIPAM-Y Samples

Table A1: Decay times and pre-exponential factors retrieved from the Birks Scheme analysis of the monomer decays of the Py_2-PNIPAM-6K sample.

Solvent	τ_1 (ns)	A_1	τ_2 (ns)	A_2	τ_M (ns)	A_M	τ_s (ns)	A_s	χ^2
Acetonitrile	41	0.26	78	0.63	190	0.10	2	0.02	1.10
2-Butanone	35	0.08	72	0.72	105	0.04	2	0.16	1.07
Tetrahydrofuran	43	0.07	140	0.81	190	0.10	2	0.02	1.06
Methanol	47	0.07	108	0.64	220	0.08	2	0.20	1.09
80%	49	0.06	135	0.78	220	0.12	2	0.05	1.12
60%	48	0.04	152	0.74	220	0.10	2	0.12	1.10
Ethanol	47	0.05	142	0.66	220	0.10	2	0.19	1.05
30%	46	0.04	175	0.80	220	0.14	2	0.02	1.14
Hexanol	36	0.04	191	0.76	220	0.17	2	0.02	1.12

Table A2: : Decay times and pre-exponential factors retrieved from the Birks Scheme analysis of the excimer decays of the Py_2-PNIPAM-6K sample.

Solvent	τ_1 (ns)	A_1	τ_2 (ns)	A_2	τ_E (ns)	A	τ_s (ns)	A_s	k_{cy} (μs^{-1})	k_{-cy} (μs^{-1})	χ^2
Acetonitrile	41	–2.82	78	2.94	54	2	2	0.05	11	2.6	1.10
2-Butanone	35	–2.60	72	2.76	43	9	2	0.39	5.9	3.3	1.07
Tetrahydrofuran	43	–0.57	140	0.61	63	11	2	0.18	3.2	6.0	1.06
Methanol	47	–0.82	108	0.86	56	9	2	0.08	5.9	2.2	1.09
80%	49	–0.66	135	0.72	59	14	2	0.06	3.8	2.9	1.12
60%	48	–0.59	152	0.66	61	18	2	0.14	2.8	3.7	1.10
Ethanol	47	–0.59	142	0.65	60	14	2	0.14	3.4	3.6	1.05
30%	46	–0.44	175	0.52	66	21	2	0.16	1.9	6.0	1.14
Hexanol	36	–0.30	191	0.42	77	18	2	0.25	1.9	14	1.12

Table A3: Decay times and pre-exponential factors retrieved from the Birks Scheme analysis of the monomer decays of the Py_2-PNIPAM-8K sample.

Solvent	τ_1 (ns)	A_1	τ_2 (ns)	A_2	τ_M (ns)	A_M	τ_s (ns)	A_s	χ^2
Acetonitrile	43	0.16	89	0.67	190	0.06	2	0.12	1.02
2-Butanone	37	0.09	77	0.80	105	0.04	2	0.08	1.06
Tetrahydrofuran	44	0.04	152	0.77	190	0.10	2	0.09	1.04
Methanol	49	0.05	126	0.72	220	0.08	2	0.15	1.15
80%	50	0.05	151	0.82	220	0.13	2	0.01	1.11
60%	49	0.04	171	0.84	220	0.12	2	0.00	1.15
Ethanol	48	0.05	159	0.82	220	0.10	2	0.04	1.10
30%	47	0.03	187	0.77	220	0.07	2	0.12	1.10
Hexanol	41	0.04	199	0.70	220	0.20	2	0.06	1.08

Table A4: Decay times and pre-exponential factors retrieved from the Birks Scheme analysis of the excimer decays of the Py_2-PNIPAM-8K sample.

Solvent	τ_1 (ns)	A_1	τ_2 (ns)	A_2	τ_E (ns)	A	τ_s (ns)	A_s	k_{cy} (μs^{-1})	k_{-cy} (μs^{-1})	χ^2
Acetonitrile	43	–0.90	89	0.93	54	5	2	0.06	8.1	2.6	1.02
2-Butanone	37	–2.44	77	2.59	45	9	2	0.58	4.9	3.5	1.06
Tetrahydrofuran	44	–0.55	152	0.58	61	21	2	0.27	2.1	5.5	1.04
Methanol	49	–0.69	126	0.73	58	14	2	0.13	4.2	2.4	1.15
80%	50	–0.63	151	0.68	62	17	2	0.14	2.8	3.3	1.11
60%	49	–0.55	171	0.60	66	22	2	0.23	1.9	4.6	1.15
Ethanol	48	–0.51	159	0.56	64	17	2	0.17	2.6	4.3	1.10
30%	47	–0.45	187	0.52	72	24	2	0.34	1.4	6.8	1.10
Hexanol	41	–0.20	199	0.28	93	18	2	0.41	1.5	12.4	1.08

Table A5: Decay times and pre-exponential factors retrieved from the Birks Scheme analysis of the monomer decays of the Py_2-PNIPAM-14K sample.

Solvent	τ_1 (ns)	A_1	τ_2 (ns)	A_2	τ_M (ns)	A_M	τ_s (ns)	A_s	χ^2
Acetonitrile	44	0.06	124	0.67	190	0.13	2	0.14	1.08
Tetrahydrofuran	40	0.03	172	0.61	190	0.26	2	0.11	1.01
Methanol	47	0.04	167	0.77	220	0.19	2	0.00	1.11
80%	45	0.03	185	0.65	220	0.20	2	0.12	1.08
60%	41	0.03	195	0.56	220	0.29	2	0.12	1.04
Ethanol	42	0.03	190	0.61	220	0.24	2	0.13	1.11
30%	36	0.02	200	0.49	220	0.34	2	0.14	1.15
Hexanol[a]	--	--	--	--	--	--	--	--	--

[a]Decays could not be fit using the Birks Scheme

Table A6: Decay times and pre-exponential factors retrieved from the Birks Scheme analysis of the excimer decays of the Py_2-PNIPAM-14K sample.

Solvent	τ_1 (ns)	A_1	τ_2 (ns)	A_2	τ_E (ns)	A	τ_s (ns)	A_s	k_{cy} (μs^{-1})	k_{-cy} (μs^{-1})	χ^2
Acetonitrile	44	–0.63	124	0.69	57	12	2	0.13	3.9	4.0	1.08
Tetrahydrofuran	40	–0.44	172	0.52	78	20	2	0.55	1.4	11.3	1.01
Methanol	47	–0.49	167	0.59	64	19	2	0.21	2.2	5.1	1.11
80%	45	–0.41	185	0.51	71	22	2	0.34	1.6	7.5	1.08
60%	41	–0.34	195	0.47	87	16	2	0.37	1.7	11.6	1.04
Ethanol	42	–0.35	190	0.48	74	21	2	0.31	1.5	9.4	1.11
30%	36	–0.20	200	0.30	84	23	2	0.49	1.4	15.2	1.15
Hexanol[a]	--	--	--	--	--	--	--	--	--	--	--

[a]Decays could not be fit using the Birks Scheme

Table A7: Pre-exponential factors and decay times obtained by fitting the monomer fluorescence decays of the Py_2-PNIPAM-25K sample with a sum of two exponentials.

Solvent	τ_1 (ns)	A_1	τ_2 (ns)	A_2	$<\tau>$ (ns)	χ^2
Acetonitrile	76	0.136	174	0.864	160	1.09
Methanol	82	0.097	209	0.903	197	1.09
80%	76	0.077	216	0.923	206	1.14
60%	89	0.082	217	0.918	206	0.97
Ethanol	81	0.083	215	0.917	204	1.08
30%	86	0.070	217	0.930	208	1.06
Hexanol	49	0.056	212	0.944	203	1.23

Table A8: Pre-exponential factors and decay times obtained by fitting the monomer fluorescence decays of the Py_2-PNIPAM-45K sample with a sum of two exponentials.

Solvent	τ_1 (ns)	A_1	τ_2 (ns)	A_2	$<\tau>$ (ns)	χ^2
Acetonitrile	58	0.060	185	0.94	177	1.05
Methanol	87	0.057	220	0.94	212	1.22
80%	100	0.063	222	0.94	214	1.13
60%	71	0.043	219	0.96	213	1.06
Ethanol	105	0.060	219	0.94	212	1.20
30%	88	0.049	219	0.95	213	0.99
Hexanol	69	0.035	216	0.97	210	1.08

Appendix B: Fluorescence Data for the Py-PNIPAM-X% Samples

Table B1: Parameters retrieved from the FBM analysis of the monomer decays of the Py-PNIPAM-X% samples in acetonitrile.

Sample	$k_e[blob]$ ($\mu s^{-1}\cdot M$)	k_{blob} ($\times 10^7\ s^{-1}$)	$< n >$	f_{Mdiff}	k_2 (ns^{-1})	$f_{M_{k_2}}$	τ_M (ns)	$f_{M_{free}}$	χ^2
Py-PNIPAM-2%	6.7	1.4	1.4	0.60	0.26	0.25	190	0.15	1.14
Py-PNIPAM-3%	7.5	1.5	1.9	0.60	0.26	0.34	190	0.05	1.08
Py-PNIPAM-4%	7.5	1.6	2.1	0.62	0.26	0.36	190	0.02	1.19
Py-PNIPAM-5%	6.6	1.5	2.7	0.53	0.26	0.46	190	0.01	1.23
Py-PNIPAM-6%	6.3	1.6	3.1	0.47	0.26	0.53	190	0.01	1.18

Table B2: Parameters retrieved from the FBM analysis of the excimer decays of the Py-PNIPAM-X% samples in acetonitrile.

Sample	$f_{E_{diff}}$	τ_{E_0} (ns)	$f_{E_{diff}}$	τ_{E_L} (ns)	f_{E_L}	k_2 (ns^{-1})	$f_{E_{k_2}}$	χ^2
Py-PNIPAM-2%	0.56	51	0.00	81	0.20	0.26	0.23	1.14
Py-PNIPAM-3%	0.50	52	0.03	75	0.19	0.26	0.28	1.08
Py-PNIPAM-4%	0.49	52	0.00	70	0.23	0.26	0.28	1.19
Py-PNIPAM-5%	0.43	50	0.00	72	0.20	0.26	0.37	1.23
Py-PNIPAM-6%	0.36	50	0.00	70	0.24	0.26	0.40	1.15

Table B3: Parameters retrieved from the FBM analysis of the monomer decays of the Py-PNIPAM-X% samples in 2-butanone.

Sample	$k_e[blob]$ ($\mu s^{-1} \cdot M$)	k_{blob} ($\times 10^7\ s^{-1}$)	$< n >$	f_{Mdiff}	k_2 (ns^{-1})	$f_{M_{k_2}}$	τ_M (ns)	$f_{M_{free}}$	χ^2
Py-PNIPAM-2%	9.9	1.9	0.6	0.69	0.17	0.22	105	0.08	1.14
Py-PNIPAM-3%	9.0	1.7	1.0	0.67	0.17	0.29	105	0.04	1.07
Py-PNIPAM-4%	8.9	1.7	1.2	0.69	0.17	0.28	105	0.03	1.2
Py-PNIPAM-5%	4.9	1.1	1.9	0.57	0.17	0.42	105	0.01	1.2
Py-PNIPAM-6%	6.0	1.1	2.3	0.53	0.17	0.46	105	0.01	1.2

Table B4: Parameters retrieved from the FBM analysis of the excimer decays of the Py-PNIPAM-X% samples in 2-butanone.

Sample	$f_{E_{diff}}$	τ_{E_0} (ns)	$f_{E_{diff}}$	τ_{E_L} (ns)	f_{E_L}	k_2 (ns^{-1})	$f_{E_{k_2}}$	χ^2
Py-PNIPAM-2%	0.65	49	0.03	71	0.11	0.17	0.21	1.14
Py-PNIPAM-3%	0.59	44	0.00	63	0.16	0.17	0.25	1.07
Py-PNIPAM-4%	0.56	43	0.01	62	0.19	0.17	0.23	1.16
Py-PNIPAM-5%	0.51	44	0.00	63	0.11	0.17	0.37	1.2
Py-PNIPAM-6%	0.47	43	0.00	63	0.13	0.17	0.41	1.15

Table B5: Parameters retrieved from the FBM analysis of the monomer decays of the Py-PNIPAM-X% samples in ethyl acetate.

Sample	$k_e[blob]$ ($\mu s^{-1}\cdot M$)	k_{blob} ($\times 10^7\ s^{-1}$)	$< n >$	f_{Mdiff}	k_2 (ns^{-1})	$f_{M_{k_2}}$	τ_M (ns)	$f_{M_{free}}$	χ^2
Py-PNIPAM-2%	5.0	1.1	0.9	0.58	0.15	0.24	200	0.18	1.14
Py-PNIPAM-3%	5.6	1.1	1.3	0.61	0.15	0.31	200	0.07	1.12
Py-PNIPAM-4%	6.7	1.4	1.3	0.63	0.15	0.32	200	0.04	1.23
Py-PNIPAM-5%	4.2	0.9	2.0	0.53	0.15	0.45	200	0.01	1.10
Py-PNIPAM-6%	4.1	01.0	2.3	0.48	0.15	0.51	200	0.01	1.19

Table B6: Parameters retrieved from the FBM analysis of the excimer decays of the Py-PNIPAM-X% samples in ethyl acetate.

Sample	$f_{E_{diff}}$	τ_{E_0} (ns)	$f_{E_{diff}}$	τ_{E_L} (ns)	f_{E_L}	k_2 (ns^{-1})	$f_{E_{k_2}}$	χ^2
Py-PNIPAM-2%	0.59	47	0.00	103	0.16	0.15	0.24	1.14
Py-PNIPAM-3%	0.54	49	0.00	93	0.18	0.15	0.28	1.12
Py-PNIPAM-4%	0.50	50	0.01	86	0.23	0.15	0.26	1.23
Py-PNIPAM-5%	0.46	51	0.00	82	0.15	0.15	0.39	1.10
Py-PNIPAM-6%	0.41	51	0.00	83	0.16	0.15	0.43	1.19

Table B7: Parameters retrieved from the FBM analysis of the monomer decays of the Py-PNIPAM-X% samples in tetrahydrofuran.

Sample	$k_e[blob]$ ($\mu s^{-1}\cdot M$)	k_{blob} ($\times 10^7\ s^{-1}$)	$< n >$	f_{Mdiff}	k_2 (ns^{-1})	$f_{M_{k_2}}$	τ_M (ns)	$f_{M_{free}}$	χ^2
Py-PNIPAM-2%	8.5	1.2	0.8	0.54	0.12	0.21	190	0.25	1.13
Py-PNIPAM-3%	5.1	0.9	1.2	0.66	0.12	0.27	190	0.06	1.06
Py-PNIPAM-4%	7.7	1.5	1.0	0.70	0.12	0.24	190	0.06	1.16
Py-PNIPAM-5%	4.0	0.8	1.9	0.59	0.12	0.39	190	0.01	1.15
Py-PNIPAM-6%	3.9	0.8	1.3	0.56	0.12	0.43	190	0.01	1.15

Table B8: Parameters retrieved from the FBM analysis of the excimer decays of the Py-PNIPAM-X% samples in tetrahydrofuran.

Sample	$f_{E_{diff}}$	τ_{E_0} (ns)	$f_{E_{diff}}$	τ_{E_L} (ns)	f_{E_L}	k_2 (ns^{-1})	$f_{E_{k_2}}$	χ^2
Py-PNIPAM-2%	0.63	55	0.11	172	0.02	0.12	0.24	1.13
Py-PNIPAM-3%	0.63	52	0.05	108	0.07	0.12	0.26	1.06
Py-PNIPAM-4%	0.60	54	0.14	100	0.06	0.12	0.21	1.16
Py-PNIPAM-5%	0.53	52	0.00	87	0.11	0.12	0.35	1.15
Py-PNIPAM-6%	0.50	50	0.00	86	0.11	0.12	0.39	1.15

Table B9: Parameters retrieved from the FBM analysis of the monomer decays of the Py-PNIPAM-X% samples in methanol.

Sample	$k_e[blob]$ ($\mu s^{-1}\cdot M$)	k_{blob} ($\times 10^7\ s^{-1}$)	$< n >$	f_{Mdiff}	k_2 (ns^{-1})	$f_{M_{k_2}}$	τ_M (ns)	$f_{M_{free}}$	χ^2
Py-PNIPAM-2%	7.4	1.3	1.2	0.56	0.21	0.22	210	0.22	1.16
Py-PNIPAM-3%	5.5	1.2	1.5	0.65	0.21	0.29	210	0.06	1.13
Py-PNIPAM-4%	5.7	1.2	1.8	0.64	0.21	0.33	210	0.03	1.25
Py-PNIPAM-5%	5.8	1.2	2.2	0.55	0.21	0.44	210	0.01	1.19
Py-PNIPAM-6%	5.8	1.2	2.7	0.49	0.21	0.50	210	0.01	1.09

Table B10: Parameters retrieved from the FBM analysis of the excimer decays of the Py-PNIPAM-X% samples in methanol.

Sample	$f_{E_{diff}}$	τ_{E_0} (ns)	$f_{E_{diff}}$	τ_{E_L} (ns)	f_{E_L}	k_2 (ns^{-1})	$f_{E_{k_2}}$	χ^2
Py-PNIPAM-2%	0.58	57	0.13	116	0.07	0.21	0.23	1.16
Py-PNIPAM-3%	0.53	52	0.00	83	0.24	0.21	0.24	1.13
Py-PNIPAM-4%	0.50	52	0.00	79	0.25	0.21	0.26	1.25
Py-PNIPAM-5%	0.43	54	0.00	72	0.23	0.21	0.34	1.19
Py-PNIPAM-6%	0.37	53	0.04	72	0.23	0.21	0.37	1.09

Table B11: Parameters retrieved from the FBM analysis of the monomer decays of the Py-PNIPAM-X% samples in 80% methanol in hexanol.

Sample	$k_e[blob]$ ($\mu s^{-1}\cdot M$)	k_{blob} ($\times 10^7\ s^{-1}$)	$< n >$	f_{Mdiff}	k_2 (ns^{-1})	$f_{M_{k_2}}$	τ_M (ns)	$f_{M_{free}}$	χ^2
Py-PNIPAM-2%	5.5	1.0	1.2	0.54	0.17	0.21	210	0.25	1.18
Py-PNIPAM-3%	4.9	1.0	1.4	0.65	0.17	0.28	210	0.07	1.09
Py-PNIPAM-4%	5.6	1.2	1.4	0.66	0.17	0.30	210	0.04	1.08
Py-PNIPAM-5%	4.4	1.0	2.0	0.59	0.17	0.40	210	0.01	1.14
Py-PNIPAM-6%	4.1	0.9	2.5	0.53	0.17	0.46	210	0.01	1.21

Table B12: Parameters retrieved from the FBM analysis of the excimer decays of the Py-PNIPAM-X% samples in 80% methanol in hexanol.

Sample	$f_{E_{diff}}$	τ_{E_0} (ns)	$f_{E_{diff}}$	τ_{E_L} (ns)	f_{E_L}	k_2 (ns^{-1})	$f_{E_{k_2}}$	χ^2
Py-PNIPAM-2%	0.60	52	0.03	117	0.13	0.17	0.24	1.18
Py-PNIPAM-3%	0.58	51	0.00	96	0.17	0.17	0.25	1.09
Py-PNIPAM-4%	0.55	52	0.00	87	0.21	0.17	0.25	1.08
Py-PNIPAM-5%	0.49	54	0.03	83	0.14	0.17	0.33	1.14
Py-PNIPAM-6%	0.43	53	0.01	76	0.18	0.17	0.38	1.21

Table B13: Parameters retrieved from the FBM analysis of the monomer decays of the Py-PNIPAM-X% samples in 60% methanol in hexanol.

Sample	$k_e[blob]$ ($\mu s^{-1}\cdot M$)	k_{blob} ($\times 10^7\ s^{-1}$)	$< n >$	f_{Mdiff}	k_2 (ns^{-1})	$f_{M_{k_2}}$	τ_M (ns)	$f_{M_{free}}$	χ^2
Py-PNIPAM-2%	4.9	0.80	1.0	0.52	0.11	0.22	210	0.26	1.05
Py-PNIPAM-3%	2.9	0.67	1.4	0.66	0.11	0.28	210	0.06	1.12
Py-PNIPAM-4%	3.5	0.68	1.5	0.64	0.11	0.31	210	0.05	1.01
Py-PNIPAM-5%	3.7	0.65	2.0	0.58	0.11	0.39	210	0.02	1.08
Py-PNIPAM-6%	3.2	0.66	2.4	0.54	0.11	0.45	210	0.01	1.06

Table B14: Parameters retrieved from the FBM analysis of the excimer decays of the Py-PNIPAM-X% samples in 60% methanol in hexanol.

Sample	$f_{E_{diff}}$	τ_{E_0} (ns)	$f_{E_{diff}}$	τ_{E_L} (ns)	f_{E_L}	k_2 (ns^{-1})	$f_{E_{k_2}}$	χ^2
Py-PNIPAM-2%	0.58	57	0.13	154	0.05	0.11	0.24	1.05
Py-PNIPAM-3%	0.59	47	0.00	103	0.15	0.11	0.25	1.12
Py-PNIPAM-4%	0.55	55	0.13	111	0.05	0.11	0.27	1.01
Py-PNIPAM-5%	0.50	54	0.11	101	0.05	0.11	0.34	1.08
Py-PNIPAM-6%	0.43	51	0.02	81	0.19	0.11	0.36	1.06

Table B15: Parameters retrieved from the FBM analysis of the monomer decays of the Py-PNIPAM-X% samples in ethanol.

Sample	$k_e[blob]$ ($\mu s^{-1}\cdot M$)	k_{blob} ($\times 10^7\ s^{-1}$)	$< n >$	f_{Mdiff}	k_2 (ns^{-1})	$f_{M_{k_2}}$	τ_M (ns)	$f_{M_{free}}$	χ^2
Py-PNIPAM-2%	4.4	0.92	0.9	0.60	0.15	0.21	210	0.19	1.12
Py-PNIPAM-3%	4.3	0.90	1.2	0.64	0.15	0.28	210	0.09	1.10
Py-PNIPAM-4%	4.1	0.94	1.3	0.66	0.15	0.30	210	0.04	1.23
Py-PNIPAM-5%	3.8	0.91	1.7	0.61	0.15	0.38	210	0.01	1.10
Py-PNIPAM-6%	5.1	1.00	1.9	0.55	0.15	0.43	210	0.01	1.05

Table B16: Parameters retrieved from the FBM analysis of the excimer decays of the Py-PNIPAM-X% samples in ethanol.

Sample	$f_{E_{diff}}$	τ_{E_0} (ns)	$f_{E_{diff}}$	τ_{E_L} (ns)	f_{E_L}	k_2 (ns^{-1})	$f_{E_{k_2}}$	χ^2
Py-PNIPAM-2%	0.61	52	0.10	118	0.09	0.15	0.21	1.12
Py-PNIPAM-3%	0.56	51	0.08	106	0.13	0.15	0.24	1.10
Py-PNIPAM-4%	0.52	52	0.04	94	0.17	0.15	0.25	1.23
Py-PNIPAM-5%	0.50	51	0.00	87	0.19	0.15	0.31	1.10
Py-PNIPAM-6%	0.34	51	0.01	80	0.22	0.15	0.34	1.05

Table B17: Parameters retrieved from the FBM analysis of the monomer decays of the Py-PNIPAM-X% samples in 30% methanol in hexanol.

Sample	$k_e[blob]$ ($\mu s^{-1}\cdot M$)	k_{blob} ($\times 10^7\ s^{-1}$)	$< n >$	f_{Mdiff}	k_2 (ns^{-1})	$f_{M_{k_2}}$	τ_M (ns)	$f_{M_{free}}$	χ^2
Py-PNIPAM-2%	4.7	0.69	0.9	0.43	0.086	0.20	210	0.37	1.06
Py-PNIPAM-3%	3.2	0.66	1.0	0.61	0.086	0.26	210	0.13	1.04
Py-PNIPAM-4%	3.3	0.68	1.1	0.66	0.086	0.28	210	0.06	0.98
Py-PNIPAM-5%	2.5	0.58	1.5	0.64	0.086	0.34	210	0.02	1.15
Py-PNIPAM-6%	2.5	0.55	1.7	0.60	0.086	0.38	210	0.02	1.02

Table B18: Parameters retrieved from the FBM analysis of the excimer decays of the Py-PNIPAM-X% samples in 30% methanol in hexanol.

Sample	$f_{E_{diff}}$	τ_{E_0} (ns)	$f_{E_{diff}}$	τ_{E_L} (ns)	f_{E_L}	k_2 (ns^{-1})	$f_{E_{k_2}}$	χ^2
Py-PNIPAM-2%	0.58	55	0.12	169	0.04	0.086	0.26	1.06
Py-PNIPAM-3%	0.59	52	0.08	128	0.07	0.086	0.26	1.04
Py-PNIPAM-4%	0.59	50	0.05	113	0.11	0.086	0.25	0.98
Py-PNIPAM-5%	0.56	52	0.06	103	0.09	0.86	0.30	1.15
Py-PNIPAM-6%	0.52	54	0.11	118	0.03	0.086	0.36	1.02

Table B19: Parameters retrieved from the FBM analysis of the monomer decays of the Py-PNIPAM-X% samples in hexanol.

Sample	$k_e[blob]$ ($\mu s^{-1}\cdot M$)	k_{blob} ($\times 10^7\ s^{-1}$)	$< n >$	f_{Mdiff}	k_2 (ns^{-1})	$f_{M_{k_2}}$	τ_M (ns)	$f_{M_{free}}$	χ^2
Py-PNIPAM-2%	2.8	0.76	0.77	0.39	0.072	0.16	210	0.45	0.99
Py-PNIPAM-3%	2.7	0.73	0.76	0.59	0.072	0.21	210	0.20	1.07
Py-PNIPAM-4%	3.2	0.78	0.77	0.63	0.072	0.21	210	0.15	1.02
Py-PNIPAM-5%	2.5	0.60	1.00	0.66	0.072	0.28	210	0.07	1.24
Py-PNIPAM-6%	2.5	0.62	1.15	0.65	0.072	0.32	210	0.03	1.06

Table B20: Parameters retrieved from the FBM analysis of the excimer decays of the Py-PNIPAM-X% samples in hexanol.

Sample	$f_{E_{diff}}$	τ_{E_0} (ns)	$f_{E_{diff}}$	τ_{E_L} (ns)	f_{E_L}	k_2 (ns^{-1})	$f_{E_{k_2}}$	χ^2
Py-PNIPAM-2%	0.60	52	0.11	169	0.04	0.072	0.25	0.99
Py-PNIPAM-3%	0.64	51	0.08	145	0.05	0.072	0.23	1.07
Py-PNIPAM-4%	0.64	50	0.07	127	0.07	0.072	0.21	1.02
Py-PNIPAM-5%	0.63	53	0.05	127	0.05	0.072	0.26	1.24
Py-PNIPAM-6%	0.59	53	0.07	118	0.06	0.072	0.29	1.06